Order Number 1346736

Modeling and simulation of one-link flexible manipulators

Guan, Guoguang, M.S.

The University of Arizona, 1991

U·M·I
300 N. Zeeb Rd.
Ann Arbor, MI 48106

MODELING AND SIMULATION OF ONE-LINK FLEXIBLE MANIPULATORS

by

Guoguang Guan

A Thesis Submitted to the Faculty of the

DEPARTMENT OF SYSTEMS AND INDUSTRIAL ENGINEERING

In Partial Fulfillment of the Requirements
For the Degree of

MASTER OF SCIENCE

WITH A MAJOR IN INDUSTRIAL ENGINEERING

In the Graduate College

THE UNIVERSITY OF ARIZONA

1 9 9 1

STATEMENT OF AUTHOR

This thesis has been submitted in partial fulfillment of requirements for an advanced degree at the University of Arizona and is deposited in the University Library to be made available to borrowers under rules of the library.

Brief quotations from this thesis are allowable without special permission, provided that accurate acknowledgment of source is made. Requests for permission for extended quotation from or reproduction of this manuscript in whole or in part may be granted by the head of the major department or the Dean of the Graduate College when in his or her judgment the proposed use of the material is in the interests of scholarship. In all other instances, however, permission must be obtained from the author.

SIGNED: 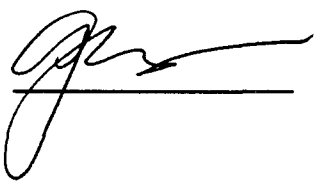

APPROVAL BY THESIS DIRECTOR

This thesis has been approved on the date showed below:

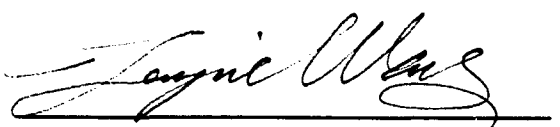

Wang, Fei-Yue
Assistant Professor of Systems and
Industrial Engineering Department

12/11/1991

Date

ACKNOWLEDGEMENTS

The author would like to express the grateful appreciation to Dr. Fei-Yue Wang for his extensive encouragement, time and valuable assistance in the development of this thesis. The author is also grateful to Dr. Sidney J. Yakowitz and Dr. Ferenc Szidarovszky for their time devoted to reviewing this thesis and their willingness to serve on my thesis committee.

The author greatly appreciates his parents' constant support, love and understanding to make this education possible.

Contents

List of Figures

List of Tables

Abstract

First, this thesis presents four types of dynamic models for one-link flexible manipulators: Euler-Bernoulli model, Euler-Bernoulli model with rotatory inertia, Timoshenko model, and Euler-Bernoulli model with tip mass through *Hamilton Principle*, and exact modal frequencies and vibration modes are derived through Laplace transformation and eigenanalysis. The numerical analysis is conducted to verify the established models and investigate the influences of rotatory inertia, shear deformation and tip mass. Second, this thesis presents the exact dynamic solutions of Euler-Bernoulli model for the step torque input and design of a dynamics simulator for one-link flexible manipulators based on the exact dynamic solutions. Several types of sensor models have been specified in the designed simulator to provide various sensory data sets required for feedback controls. A simulation study is performed to verify the designed simulator and to demonstrate the usage of the dynamics simulator for controller design and evaluations.

Chapter 1 Introduction

1.1 Research Motivation

The industrial robots have emerged as a primary means of contemporary automation due to their potentials for productivity increases and product quality improvements. The last decade has seen robots and manipulators beginning to contribute significantly toward this automation. Additionally, this trend has been accelerated by the current space exploration projects and applications. For last 10 years, a lot of researchers have been attracted to develop the more effective methods to design, model, control and identify the robot systems and significant contributions have been achieved for the manufacture applications of the conventional robots and manipulators. But there still are several obstacles of expanding further applications of the new generation flexible robots and manipulators.

The main drawback of the conventional robots and manipulators is the assumption that robot arms are rigid. There are two severe limitations to this present-generation procedure for the controlling robots: First, there is always some flexibility in the structure and drive trains of the robots, and it is therefore impossible to achieve truly high precision; Second, in order to get some degree of precision, it is necessary to make robot members and drive trains very stiff, and therefore limits the robot to slow speeds and requires high levels of drive power. When the performance demands is not that severe, we can afford this luxury. But sometimes we can not afford to keep the robot rigid. Obviously, this problem is especially critical for the space exploration and operation. Conversely, the flexible robots and manipulators can provide the following advantages :

- higher speed
- smaller actuators
- lower energy consumption

- safer operation due to reduced inertia
- lower overall cost
- enhanced back-drive ability due to elimination of gearing
- lower overall mass to be transported
  (useful for both space and earthly applications)
- lowered mounting strength and rigid requirements

The successful material industries have allowed us to reduce the excessive weight by employing the nonconventional materials such as aluminum alloys and composite materials. The resulting slender lightweight links would be strong in compression, but comparatively weaker in bending. This elastic flexibility of the robots and manipulators will make the conventional *collocated controller* that the sensors collocated with the actuators invalid. The design of noncollocated controller, while the sensors are located exactly at the end-effector which is controlled, has become the main obstacle of the flexible robots study.

All the efforts toward the modeling and control of the flexible robots and manipulators are going to be paid back as the advantages of flexible robots and manipulators. These research results have paved the way for the more effective flexible robots and manipulators to be applied on manufacture and space exploration in the real world.

1.2 Research Issues of Flexible Robots and Manipulators

The new generation robots and manipulators have introduced the flexibilities to the study of modeling and control of the flexible arms. These flexibilities will couple with the rigid characteristics of the robots and manipulators and complicate the responses of the robots and manipulators. The classical control algorithms no longer insure the stability and satisfied accuracy for these flexible arms. So, there is a critical need of the effective controllers which achieve the same motion objective as the controller for rigid manipulators, and also stabilize the vibrations with a

limited number of actuators.

1.2.1 Introduction

Conventional industrial manipulators use the links and drives made still to minimize vibrations at the expense of lower speed and higher actuator power. Also, the reason of today's robots are controlled by the collocated controller, is that the collocation guarantees stable control. The improved control is one of the critical needs for the new generation robots, since the flexible arms have much complex dynamics due to the flexibilities distributed along the mechanical structure. Obviously, accuracy in the positioning the end-point of flexible manipulators and avoidance of its oscillations is the major open problem facing the new generation of very fast, light and high precision robots. Till today, the technique of the achieving stable control using the *noncollocated* sensors and actuators has not well-developed.

To achieve the above goals, many researchers have been investigating the available methods for effective modeling and control of the flexible robots and manipulators for last ten years. The strategies of the modeling and control methods are several and diverse. All these efforts have broaded the horizon of study issues of modeling and control of the flexible robots and manipulators. Also, some special approaches to deal with the flexible robots and manipulators are also presented. For example, in [Park 90], the author redesigned the flexible robots structures and changed the position of actuator to make the model stable by the simple controller.

Most of the current researches deal with the simulation study only. Some of the mechanical models are setup for the experiments investigation. All these experiments have demonstrated the effectiveness of the relative simple algorithm for the flexible manipulator modeling and control, while most of the experiment studies have focused on single link manipulator or multi-link with one flexible link. Such setups have servered as valuable test-beds for the modeling, system

identification, and controller design and evaluation. Some mechanical models are:

1. MIT FLEXBOT, Dept. of Mechanical Engineering, MIT
2. ARMA, Dept. of Electrical Engineering, Ohio State University.
3. RALF, Dept. of Electrical Engineering, Georgia Institute of Technology.
4. Stanford, Dept. of Aeronautics and Astronautics, Stanford.
5. CIRSSE, NASA Center for Intelligent Robotic System for Space Exploration, Rensselaer Polytechnic Institute.

In following sections, some important issues of modeling and control of the flexible robots and manipulators are introduced.

1.2.2 Modeling of Flexible Robots and Manipulators

The principal application of the modeling of flexible robots and manipulators is controller design. The accuracy of the model have the significant influence on the controller performance. Also, the format of the model determines the strategy of controller design. As in [Cann 84], the author emphasized the accuracy of the model has more weight than the complicated control algorithms in the flexible problems. The rigid body dynamic analysis will no longer be accurate and controller based on rigid model will not perform satisfactorily. So, the flexibilities, which deteriorates the accuracy, stability and repeatability, should be provided to design the effective controller for the flexible robots.

The basic strategy of modeling of flexible robots and manipulators is to treat the flexibility as an added degree of freedom. There are two very popular methods of modeling of flexible arms: *Energy Assumed Modes* method, which combine the energy method, such as *Hamilton's Principle* and *Lagrangian Principle*, and assumed vibration modes technique, and Finite Element Method (FEM). How-

ever, the *Kane's* method (*Lagrangian's* form of *D'Alembert's Principle*) which is not based on the energy method, was used by a few researchers.

Hamilton's Principle : Every elastic mechanical system is characterized by a specificed function dependent on the position of the system, generalized velocities and time. This function is the *Hamilton Function* and can be expressed as :

$$\begin{aligned} L &= L(q^1, q^2, q^3, \cdots, q^r, \dot{q}^1, \dot{q}^2, \dot{q}^3, \cdots, \dot{q}^r, t) \\ &= T - P + W \qquad\qquad i = 1, 2, 3, \cdots, r \end{aligned}$$

Here, the q^i is the ith degree of freedom; the $\dot{q}^i$ the velocity of ith degree of freedom; T the system Kinetic energy; P the system Potential energy; W the total work done by the input force within the system.

If the system moves from the position A to position B over time period (t_A, t_B), the *Hamilton* function L exhibits the property that the integration of the L over A and B assumes a stationary value. It can be written as:

$$\delta \int_{t_A}^{t_B} L dt = 0$$

The motion *integro-partial differential equation* (IPDE) of the flexible robots can be derived by employed the *Hamilton's Principle*. Usually, this IPDE may not be utilized for the controller design directly due to the complications and high nonlinear characteristics until the further simplifications are conducted. The IPDE can be simplified to the *partial differential equation* (PDE) based on the appropriate assumptions.

Assumed Vibration Mode Technique : This technique is an effective tool to discretize the PDE in case of the unavailability of the exact vibrational modes. The simplified dynamic models of the flexible manipulators are still the high order differential equations with the boundary conditions, and the motion variables are

dependent on both the position and time. The common way to investigate these systems is to conduct the variable discretization along the vibration modes. Most of the time, the exact vibration modes can not be found. So, many kinds of assumed vibration modes, e.g. cantilever beam vibration modes, are employed to achieve the approximation. This approximation can make the controller design feasible at the price of more complicated target dynamic systems and less positioning accuracy.

Different from the assumed vibration modes, the exact vibration modes display the main characteristics and the insights of the corresponding physical systems. These vibration modes do not dependent on the mode order and the orthogonality conditions, and are the representatives of the true physics properties. The exact vibration mode can simplify the calculation of the orthogonality conditions and the final target dynamic systems. But till now, the exact vibration modes can only be obtained for the single link problems, .

The number of the vibration modes, which should remain in the model to insure the approximation, need to be determined for the assumed modes method. So, the infinite number of modes are required for accurate purpose. This make the feedback control impossible to be conducted in practice. The effective method to simplify the complicated dynamic equations of the multi-link robots and manipulators is the order reduction.

Finite Element Method : The inverse and forward dynamics are the main tools of the finite element method. The inverse problem is the calculation from the force/torque to motions; while the forward problem is the opposite. This is the more general method to deal with the multi-link flexible robots and manipulators. Due to the complicated situation, the FEM requires a lot computation time. Although the new algorithm has been developed to conduct the calculation in the frequency domain, it still need heavy computational efforts, which prevents the real-time solution. Now, in most numerical simulations, the FEM model em-

ploys the forward Fourier transform, inverse Fourier transform and linear complex system numerical calculations.

The assumed modes can be close to the exact vibration modes when the simple one-link flexible manipulator is under study. This method need the orthogonality condition to generate the dynamic equations of the modal amplitude function. The calculation effort of the orthogonality condition will increase dramatically with the configuration of the flexible structure. So, the assumed modes methods are more related to the simple problems, such as the one-link flexible manipulators. For the multi-link flexible robots and manipulators, which usually have the complicated configures, the FEM is more applicable then the energy assumed method. However, the main drawback of the FEM is that it provides less physical insights of the flexible robots and manipulators systems. Although inverse and forward techniques with the finite element method can be applied to any complicated systems theoretically, but the controller designs for these models are very difficult.

Multi-Link Robots and Manipulators : For the multi-link and flexibility distributed case, more dynamics details should be provided not only to the controller design, but also to the trajectory planning. Different from the one-link case, which need little dynamics to conduct the trajectory planning, the piecewise dynamic boundaries may not keep constant and they are the function of position, payload mass and even the payload shape. Due to the couplings among the links, large configuration changes and high speeds, the system can not be presented accurately by the simple beam equations. The coupling between the links make the transformation matrix very complicated and its size turns to be very big. This may gave the excuse that the today's researches are more concentrated on the one-link flexible manipulators than the multi-link robots.

Many existing models are simplified to the linear system. The single-link

case may be acceptably represented as a linear system, however the multi-link problem is strongly nonlinear, neglecting the nonlinear terms may lead to substantial errors in the response. The difficulties involved in dealing with the nonlinearities and the fact that the vibration mode of a linearization vary with the configuration of the nonlinear system.

Many models of the flexible robots and manipulators have been developed through the above strategies and methods. Some experiments are conducted based on these models and many excellent results are presented. The drawback of the existing formulating method is the procedure is tedious and complex, and the errors are almost inevitable. Thus there is still a need of an effective way for analysis of the flexible robots and manipulators systems.

1.2.3 Control of Flexible Robots and Manipulators

The control of the flexible robots and manipulators can be divided into two level. The lower level is called *control* or *path tracking*, while the upper level is called the *path* or *trajectory planning*. In fact, upper stage is the optimal programming problem subject to the trajectory constraints which can be obtained through the dynamic model. The *path tracking* attempts to track the desired path which is design by the trajectory planning. Both these two level controls turn to complicated when the flexibility of robots is involved. Accuracy in the positioning of the end-point of flexible manipulators and avoidance of its oscillations is one of the major open problems in the new generation robots. The classical control algorithms are no longer effective for the flexible robots and manipulators due to the introduction of the *noncollocated* problems.

Uncollocated Problems : The conventional robots equipped by the *collocated* sensors and actuators can be solved easily through the classical control algorithms. The position is converted by the real-time kinematic computation based on the

rigid assumption. When the flexibility is taken into account, the joint variables are no longer necessary for the end effector position. Consequently, the classical control algorithms will cause the unstability or big position errors for the flexible robots and manipulators. The *noncollocated* issue was first addressed by Cannon and Schmitz in [Cann 84]. The previous researches have well verified that the classic PD or PID control of noncollocated problem turn out to be either nonstable or large error at the end of trajectory for flexible robots and manipulators. Furthermore, [Eppi 88] showed by using the servo control developed for the rigid arms, the control performance of the flexible arms is severely limited by the phase nature.

It is appealing to try to find the analogue for flexible arms of the so-called computed torque or inverse control method for the rigid body, while the extension of these nonlinear techniques to joint level control of flexible arms seems to be quite straightforward. Problems arise for the end-effector trajectory control due to the *noncollocated* sensors, when the computed torque method is used. Even when considering approximated linear models for flexible arms, the nonminimum phase nature of the end-effector control problem makes the exact reproduction of trajectory a hard task.

So, the new control algorithms should be developed for these flexible robots and manipulators which take the flexibility into account. Several new methods of the controller design were proposed to be applied on the flexible manipulators. Currently, the mostly used are the adaptive control, perturbation control and optimal control in the linear or nonlinear fashion. All these strategies can be applied to both upper and lower level control.

Adaptive Control: Adaptive approach provides an intelligent means of control for one-link or multi-link flexible structure whose model is not known exactly, or may changes in time. The common adaptive control used in real world is the model reference adaptive control (MRAC). This strategy use the mathematically

defined reference model to follow the real manipulators operation. The parameters of the mathematical reference model are the estimated values of the exact system. Therefore the adaptive control is the effective way to implement the difference between the exact systems and models due to accuracy of the dynamic model, especially when the dynamics model of the real systems may not known exactly or change with time.

Perturbation Control : Perturbation techniques have showed to be the promising method in deal with flexible manipulators. The attractive feature of this strategy is that the slow control can be designed on the basis of well-established control scheme for the rigid manipulators, such as the decoupling control, resolved acceleration control and adaptive control. On the other hand, the fast control can be synthesized as a linear state feedback control with the slow state variables acting as parameters. The combination of the reduced order model and the perturbation has been presented as the successful means for the multi-link flexible robots and manipulators control. In fact, if the fast subsystem is stabilizable for any joint trajectory of interest, the orbits of the overall system will approach in the limit those derived via the two subsystems.

Optimal Control : The application of the optimal control is very intuitional. Some factors like control time and energy consumption play the important role financially. The usual strategy of the optimal control is to employ *Pontryagin's Optimal Principle*. Alternative approach is to transfer This may need more computational efforts. This problem became more complicated when the multi-link flexible manipulators are subjected to be studied. Most of the trajectory planning algorithms presented today assume very little about the robotics dynamics. although the upper-bounds of the velocity and acceleration vary with the joint position. Some time the optimal control should combine with other control algorithms to average the merits the control.

Although many control algorithms have been proposed, the tracking control for the multi-link problems are still very difficult due to the nonlinearation. The vibration modes vary with the configuration of the nonlinear system. And in fact, the multi-link cases have not been investigated very much till today.

Identification Problem : The above controls are assumed the parameters of the system keep constant. However, the payload of the flexible manipulator changes when the robot pick or place a item. Also, during the robots operation, the payload parameter should be estimated whenever the payload is changed. To make the control procedure complete and effective, the vary load or system identification problem at the task site should be investigated. The varying payload have influence on the model pattern, control algorithm, exact vibration modes and controller computation. Within the same model pattern, the model need to be adjusted to meet the exact systems parameter for control torque computation. The whole identification procedure need the prior experiment to establish appropriate prefilter parameters, sampling time and weight of control law.

Both frequency domain and on-link identification technique have been developed through the efforts of W. J. Book and D. M. Rovner. The combination of the state space and frequency domain techniques was proposed for the effective justification in term of speed motion in [Book 83]. In [Rovn 87], the author has proposed the on-line identification technique and given a good result for the one-link flexible manipulator subjected to payloads which were less than ten present of the beam weight.

1.3 Transfer Function and Stability

The main fact of the controller design is the stability of the robot system. For the linear system, the transfer function is the most common tool to investigate the stability of the flexible manipulators. Currently, many researchers use the

finite assumed modes approach to model the flexible manipulators. When the number of modes is increased for more accurate modeling, the relative degree of the transfer function may become ill-defined. Some researches recommend to redefine the motion variable to keep the relative degree well-defined.

Questions of finite stabilizability have already been studied in the control theory literature, the general result governing this question is given in the control system synthesis by Vidyasagar. A necessary condition for a given system with a transfer function $p(s)$ to be stabilizable using a finite dimensional controller is that $p(s)$ should have a *stable coprime factorization*: that is, one should be able to factor the function $p(s)$ as a ratio $n(s)/d(s)$, where $n(s)$ and $d(s)$ are the transfer functions of stable distributed systems, and moreover, the zeroes of the $n(s)$ and $d(s)$ in the closed right half plane do not accumulate at a common point.

For the multi-link robots and manipulators, the transfer functions are not necessary to be linear and may not be obtained easily. So, the alternative approach to investigate the stability of flexible arms is to assure that the system energy will approach zero after finite amount of time by *Lyapunov* energy analysis. This approach is almost the only effective tool for the complicated robots systems, however, it requires tedious and complicated calculations.

1.4 Other Strategies

There are two basic strategies to improve the solutions of modeling and control of flexible robots and manipulator problem. One is to design and modify the control algorithm for the existing dynamic model, while the other is to remodel the flexible robots and manipulators for well-developed control laws. The first approach has been discussed a lot in the previous sections. If the first approach is used, the non-minimum phase nature can not be modified and the control of the end-point remains a difficult problem. The second strategy provides the chance of redesigning the structure of the flexible arms to insure the effectiveness of control.

In [Park 90], the author presented a new concept of design the one-link flexible manipulators. He presented that the position where the torque is applied has the important influence on the stability of the flexible manipulators. The concept is to change the position of the actuator and the distance between the sensors and actuators to keep the system stable. Also, it is possible to make the 'collocated' manipulator by fixing the sensor and actuators somewhere except the hub to ensure the stability.

1.5 Contributions of the Thesis

Among all the varied issues of the modeling and control of the flexible robots and manipulators, this thesis aims to improve the strategy of modeling and control of one-link flexible manipulators. The main contributions of this thesis are the followings:

1. One Euler-Bernoulli dynamic model of the one-link flexible manipulator and the other three dynamic models, which take into account the influences of the rotatory inertia, shear deformation and the tip mass, are derivated by employing the *Hamilton's Principle*. Opposite to the previous conventional models, e.g. [Cann 84], the developed models are well-constrainted.

2. The exact modal frequency equations and the vibration modes of the four models are derivated through the Laplace transformation and eigenanalysis.

3. The influences of the rotatory inertia, shear deformation, hub inertia and tip mass on the vibration behaviors of the flexible manipulators are presented through the numerical analysis.

4. The exact dynamic solution of the Euler-Bernoulli model for step torque input is obtained. Also, the finite pulse and impulse responses of Euler-Bernoulli dynamic model are presented as the verification tool for exact dynamic solution.

5. A dynamics simulator is designed based on the exact dynamic solution of Euler-Bernoulli model for step torque input. It provides multi-pattern outputs for specified control algorithm and ideal tool for evaluation of control algorithms.

6. The design of dynamics simulator is verified by a simulation study. Also, three simple control algorithms are evaluated through the simulation study.

1.6 Organization of the Thesis

In Chapter 2, the previous research efforts toward the modeling and control of the flexible robots and manipulators are outlined. The Chapter 3 presents the derivations of four dynamic models, which considers the influence of the rotatory inertia, shear deformation and tip mass. In Chapter 4, the exact modal frequency equations and the vibration modes are derivated for four established models, and the influences of the rotatory inertia, shear deformation, hub inertia and the tip mass on the vibration behaviors of the flexible manipulators are presented through the numerical analysis. The Chapter 5 demonstrates the derivations of the exact dynamic solution of Euler-Bernoulli model for step torque input. In Chapter 6, a dynamics simulator is designed based on the exact dynamic solution of Euler-Bernoulli model. The Chapter 7 presents a simulation case study for verification of designed dynamics simulator and evaluations of three simple control algorithms through the designed dynamics simulator. The conclusion of this thesis and further study are addressed in the Chapter 8.

Chapter 2 Literature Review

2.1 Introduction

The development of the industries has stimulated the employments of the robots and manipulators for last 30 years. However, the researches of modeling and control flexible robots and manipulators turn to be conspicuous only after the first systematic study [Cann 84] of the precise control of the one-link flexible manipulator was introduced in 1984. After that, the intensive efforts towards the modeling and control of the flexible robots and manipulators have broaden the research horizon. During recent years, varieties of strategies and methods have been introduced to improve the preformences of the flexible robots and manipulators. Many successful simulation and experiment works have been presented for modeling, control and stability analysis of the flexible robots and manipulators.

The subjects and strategies of the research of flexible robots are diverse and cover a broad range of the research fields. The following sections in this chapter are going to outline the previous efforts toward the flexible robot research, which includes modeling, control, identification, and stability analysis.

2.2 Modeling of Flexible Robots and Manipulators

Modeling of the flexible robots and manipulators has been investigated through many works, e.g. [Barb 88], [Bayo 88], [Bayo 89], [Bell 90], [Bisw 88], [Brem 87], [Book 82], [Cann 84], [Dado 86], [Fuku 85], [Hast 86], [Kris 88], [Oakl 89], [Wang 89], [Wang 90], [Wang 91a], [Wang 91b] and [Wang 91c]. Among these models, the most common methods for the modeling of the flexible robots and manipulators are the *Assumed Modes Method* and *Finite Element Method.* But, the applications of these two methods are diverse.

2.2.1 Assumed Mode Method

Back in the 1984, the first systematic dynamic model of the flexible manipulator developed by Cannon [Cann 84] is underconstrained. Many dynamic models developed laster are still understrained, especially for the multi-link flexible robots. The exact vibration modes of the flexible systems are not available in presence of the underconstrained motion equations. So, the assumed mode method become the main tool for the investigations of the flexible robots and manipulators.

Assumed Mode Shapes

To assure the accuracy of the model by the assumed modes method, different approximated vibration modes, e.g. cantilever beam and polynomials vibration mode, have been proposed by some researchers. But, the exact vibration modes related closely to simple problem, e.g. Bernoulli beam, usually close to the the assumed modes. In [Barb 88], the author conducted an interesting comparison between the results obtained using the vibration modes of an Euler beam with a clamped and pinned end. The conclusion indicated that the real behaviors of the flexible slewing beam is in between those two approaches, dependent on the hub/beam inertia ratio.

Applications of the Assumed Modes Method

The first systematic study of the one-link flexible manipulators by the assumed modes methods is [Cann 84], which is recognized as the classical study of the one-link flexible manipulator. Also, this is the first time that the importance and effectiveness of the flexible robots and manipulators are addressed. The author presented a dynamic model of a single link flexible manipulator which was developed through the energy method. This model mistreated the boundary conditions and failed to derivate the exact vibration modes of the physics systems.

The other example of the application of the assumed mode method can be found in [Hast 86]. The author developed the linear state-space model for a single

link flexible manipulator. The method employed to generate the model utilizes a separable formation of assumed modes to represent the transverse displacement due to bending. The performance of the model is investigated for different model orders and assumed modes. The experiment results showed the choice of the assumed modes and the number of the modes can have the obvious influences on the performances of flexible manipulators.

Exact Vibration Modes

Based on the studies of assumed modes model, the assumed mode shapes have the obvious drawback for the positioning purpose. Comparatively, the exact vibration modes naturally represent the physical insights of the systems, and can simplify the controller design algorithms and enhance the positioning accuracy. Due to the different derivations of the motion equations, most models are underconstrained and can not provide the necessary conditions for the derivations of the exact vibration modes. In [Wang 90], [Wang 91a] and [Wang 91b] the exact vibration modes of one-link flexible manipulators is derivated based on the well-constrained dynamic models. Also, in [Bell 90], the exact vibration modes of the slewing link were found. Till today, the exactness of the vibration modes is still limited to a linearized description of the single link.

2.2.2 Modeling Technique of Assumed Modes Method

The format of the final dynamic model also can provide some convenience for the controller design. The order of the dynamic model, the formats of the energy principles, even the coordinate frames and the selection of the motion variables will determine the final format of the dynamic model. The issues about the modeling techniques are presented as the followings:

The infinite dimensions are intented to be used to obtain the acceptable

accuracy. Many researchers have used the dynamics models consisting of infinite number of modes to increase the accuracy. However, the number of modes that should retain is still unknown for the specific flexible manipulator system. If using the full order modes to describe the motion and design the controller, the high order of the controller may not feasible for implement in practice. Hence, H. Krishnan and M. Vidyasagar constructed a low order model for the flexible manipulator system by using *Hankel-Norm Minimization* method in [Kris 88]. The experiment showed that the controller based on the reduced order model guarantees effective vibration control of the flexible arm.

The comparisons of all the variety of *Lagrangian Principle* can be found in [Brem 87]. The author conducted a comparisons between several formats of the *Lagranginan Principle*, which is used to describe the flexible manipulators. Finally, it was presented that the very first but essential task of the modeling of flexible arms is to select an efficient mathematical description for development of systems equations.

The other interest of modeling is the choose of motion variables. In the [Wang 89], the result showed that when number of the mode increased for more accurate modeling, the relative degree of the transfer function become ill-defined. This can greatly affect the performance of a controller designed using this model. The alternate approach is proposed the rigid body deformations *minus* the elastic deformation as the output to ensure the well-defined transfer function.

In [Bell 90], the authors derivated two dynamic models of one-link flexible manipulator from two equivalent formations (pseudo-clamped and pseudo-pinned). The exactness of the mode shapes allows to prove the equivalence of these two approaches, which are different on the choice of the non inertial rotating frame. In

the pseudo-pinned case, these is no coupling between the flexibility and rigid body, the flexible modes is exacted by the input torque, while in pseudo-clamped case, the final dynamic model shows the complicated coupling.

2.2.3 Finite Element Method

In the complicate manipulator environment system, realistic simulation of the motion of manipulator in its environment is necessary. Also, many control schemes require torque is calculated in the real time. To this end, the FEM is introduced as the general methods for modeling of the flexible robots and manipulators. The main applications of the FEM are based on the forward and inverse dynamics.

Applications of the FEM

In 1982, W. J. Book developed an recursive, *Lagrangian-assumed mode* model ([Book 82]) which introduced the straight forward dynamic modeling technique. This strategy can be applied on any multi-link flexible robots theoretically. However, this strategy requires the finite number of dimensions. Four years later, M. Dado and A. H. Soni addressed a general finite element method with the inverse and forward techniques in [Dado 86]. In the forward analysis, the inertial loads are determined by using the known acceleration, while in the inverse analysis, the accelerations of the driven coordinates are determined by solving the dynamic equation and equilibrium equations.

The other modelings of the flexible robots and manipulators by finite element method can be found in [Bayo 88] and [Bayo 89]. In [Bayo 88], a technique was presented for the solution of the inverse dynamics of open-chain flexible robots. The proposed method finds the joint torque is necessary to produce a specified end effector motion. The performance and capabilities of this technique are tested through a simulation analysis. Additionally, the result shows the new strategy is

not only for the feed-forward control, but also for incorporation in feed-back control strategies. In [Bayo 89], E. Bayo showed the successful application of the modified inverse dynamics techniques to model the flexible manipulators. The advantage of this strategy is that it can be used on the real time computation.

2.2.4 Modeling of Multi-Link Flexible Robots

The study of the multi-link flexible robots can falls into two fields: flexible multi-link robots and the distributed flexibility.

Modeling of Multi-Link Flexible Robots

For the multi-link flexible robots and manipulators, the assumed modes and FEM method lead to the more complicated derivations to get the dynamic motion equations due to the more complicated configurations.

In [Fuku 85], the author studied flexible robotic arms with two degrees of freedom and both the arm flexibility and joint elasticity. Each link was modeled independently by means of a body-fixed frame. The joint displacements were then used as constraints to derive the combined equations of motions in a manner similar to the component mode and substructure synthesis methods. But, the dimension of the Jacob transformation matrix turn to be very big due to the coupling between the links. This leads the investigations of the reduced order approach for the multi-link flexible robots. The experiment conclusion from [Kris 88] indicated that a controller designed for a reduced order model by *Hankel-Norm Minimization* method guarantees the effective vibration control of the flexible arm.

Distributed Flexibility

The more complicated problem is the distributed flexibility, which provides an strategy to average the performance and cost of the flexible robot systems.

In [Oakl 89], the authors built a modal expression model for the Stanford Multi-Link Flexible Manipulator configured with a rigid upper arm and a very flexible forearm. The model takes advantage of the assumed vibration modes method selecting the modes to let the low order model to be used effectively for the simulation and control purposes. The experiments verified this modeling strategy for this two-link flexible manipulator.

The other approach for the distributed flexibility problem can be found in [Bisw 88]. The complete dynamics of the robot was given in terms of a coupled system of ordinary and partial differential equations. A finite dimensional model is also developed from this model using the modal techniques. The author used a set of ordinary differential equations to represent the rigid body servomotor, and a set of partial differential equations to represent the flexible manipulator. The two sets of equations are dynamically coupled because of the presence of system variables, as well as centrifugal, Coriolis and Euler forces.

Symbolic Computations

The drawback of the existing formulating methods is the procedure is tedious and complex, the errors are almost inevitable. There is still a need for an efficient way of analysis flexible manipulator systems. To avoid the complication of manual calculation, the new systematic algorithm to symbolically derive the full nonlinear dynamic equations of multi-link flexible manipulators is presented in [Ceti 87]. Lagrangian's assumed modes is the basis of the new algorithm and adapted in the way suitable for symbolic operation by the digital computer.

Although there are many successful models of the flexible systems as mentioned before, the coupling between the rigid body motion and the elastic deformation stands as the main issue in the dynamic solutions of the flexible robots problems. In fact, the coupling between the rigid motion and the elastic deforma-

tion is not clearly described till now.

2.3 Control of the Flexible Robots and Manipulators

The research of the controller design for the flexible robots began about ten years ago. The successful control of the rigid robots brought the straightforward ideas for the flexible robots control until the *noncollocated problem* was introduced by Robert H. Cannon and Eric Schmitz in 1984. During the last 4 years, many control algorithms have been designed for the flexible robots and manipulators based on variety of control concepts and model formats. These researches provide rich in-depth knowledge of the flexible robots systems than ever. However, there still are many problems needed to be solved before the real world applications of the flexible robots and manipulators can be provided.

2.3.1 Classical Control

In [Cann 84], the author addressed that the flexibility introduced the *non-collocated problem* that make the well-defined classical control algorithm ineffective for the flexible robots and manipulators. The PD and PID control algorithm, which is effective for the rigid case, can reach the desired position for the flexible robots and manipulators, leaving vibrations and large errors at the end point of trajectory. As mentioned in [Cann 84], the collocated sensor is no long the effective method to achieve control satisfactorily for flexible robots.

More discuss about the effectiveness of the classic controller approach for the *noncollocated problem* can be found in [Shun 87]. The author used the Stanford Flexbot as the model and showed that the conventional PI controller can not stabilize the closed-loop system. The stable factoration approach for the controller design was explored to approximate original model with finite dimensional mode. Finally, the author concluded that the non-collocateness of the actuators and sensors is still a problem for the finite mode models.

2.3.2 Compute Torque Method

Confronted with the ineffectiveness of the classical controller, many researchers have investigated the possible approaches of *noncollocated* problem for years. The compute torque method, which is successful for the rigid arms, is the most straightforward idea for control of the flexible arms.

In [Luca 89], a general framework was given for computing the torque that would achieved the desired trajectory. The authors employed a dynamic generator system which is the full or reduced order inverse system associated to the arm dynamics and output in both the open and closed loop fashion. The simulation study of a nonlinear model of one-link flexible arm showed the effect of the system output choice on the closed-loop stability and on the overall tracking performance.

2.3.3 Adaptive Control

In resent years, the adaptive control has been introduced as the most promising method dealing with the flexible arms. The model reference adaptive control (MRAC) is the most used strategy of the adaptive control applications.

In [Yuh 87], the author addressed the feasibility of applying discrete-time MRAC techniques to the flexible link of robot mechanisms. The effect of the flexibility was treated as an internal disturbance torque acting on the rigid body motion of the system. An adaptive control system was determined by the equation of a rigid body motion with the disturbance term. The control algorithm is implemented for a collocated sensor and actuator system and for a noncollocated end-point sensor and actuator system. The other application of the MRAC can be found in [Sasi 88]. The author designed an successful controller for a distributed mass model of the flexible link by taking advantage of the merit of the adaptive control, which allow the less exact dynamic model to perform more effectively and overcome the nonlinearities. Finally, the author presented the parameter adjustment yielded more stable and robust system.

For the multi-link flexible robots control, the presentation can be found in [Yang 89]. This paper presented a digital adaptive control scheme for a manipulator with one rigid link and one flexible link. The adaptive control algorithm is indirect, and the control law at each sampling time is based on a prediction model of the plant whose time varying parameters are estimated adaptively. The prediction model is linear and of sufficient dimension to reflect some but not all of the elastic degrees of freedom in the plant.

The first application of the MRAC on the large space structure is [Donn 90]. Due to the complication of the large space structure, the model may not be known exactly or may change in time. The author presented the implementation of an adaptive PI control algorithm for a space structure *JPL/AFAL* of Jet Propulsion Laboratory with non-collocated sensor and actuators.

The summary of recent results in the development of optimal design of direct model reference adaptive controller can be found in [Baya 90]. Currently, two methods have been developed for direct model reference adaptive control: one employs an analytic averaging technique by solving a constrained nonlinear optimization problem yielding a close-form solution, the other method uses an numerical optimization approach with high-level learning capability. Additionally,

2.3.4. Perturbation Control

The perturbation control is the other promising strategy for the control of the flexible robots and manipulators. It can server as the tool to separate the flexible and rigid mode as the fast and slow subsystems.

The exhaustive investigation of the perturbation control is presented by the [Sici 88]. The dynamic model was derived on the basis of a Lagrangian assumed mode methods for RALF of the Flexible Automation Lab. at Georgia Institute of Technology. By the perturbation theory, the system model was modified into the reduced order model as: a slow subsystem which conveniently turns to be of

the same order as that of a rigid manipulator, and a fast subsystem in which the slow state variables play the role of parameters. A composite control strategy was adopted. The attractive feature of this strategy is that the slow control can be designed on the basis of well-established control schemes for the rigid manipulator. On the other hand, the fast control can be synthesized as a linear state feedback control with the slow state variables acting as parameter.

In [Khor 88], the resolution of separating the dynamics of flexible manipulators into rigid and flexible modes is considered. The decoupling is established on the single link case by the singular perturbation techniques. Furthermore, the flexible effects of the manipulator on its rigid body motion is included by appealing to the higher order terms in the asymptotic expansion. The model is used the *integro-partial differential equation* (IPDE) resulting from the Hamiltonian principle. Using this model rather than the FEM model yield more insights of the flexible manipulators and a compact way of obtaining the higher order terms that represent the coupling between the rigid and the flexible modes. It is showed that the rigid body mode can be decoupled from the flexible affects of the link. Further more the infinite-dimensional part of the dynamics which is similar to the dynamics of the Euler-Bernoulli beam is parameterlized by the slow variables. Currently these idea are being extended to the nonlinear model.

2.3.5 Optimal Control

The optimal control is belong to upper level control: trajectory planning. It provides the more feasible and economic performance of the flexible robots and manipulators. The objective of the optimal control may vary from the time to energy.

In [Shin 85], the author presented a method for obtaining trajectory for minimum time control of a mechanical arm given the desired geometric path and input torque constraints. Because the trajectory planning does not require much of the

dynamics, to remove at least partially this efficiency, this paper considered a solution to the problem of moving a manipulator in minimum time along a specificed geometric path subjest to the input torque/force constraints. First, the author described the manipulator dynamics using parametric functions which represent geometric path constraints to be honored for collision avoidance as well as task requirement. Second, constrains on the minimum time solution is deduced in an algorithm from using phase-plane technique. Finally, numerical example were presented to demonstrate the utility of the trajectory planning methods development.

The other discussion about the optimal control of flexible manipulators can be found in [Wang 87], the stable factoration approach was used to obtain the optimal step response of the system in the sense that the mean square tracking error is minimized over all stabilizing controller.

2.4 Parameter Identification

Some of the parameter of the model of the flexible robots and manipulators varies during the operations of the robots or may change with the configures of the flexible robots. These changes have the critical influences on the model pattern, control algorithms, exact vibration modes and controller computation.

System Identifications

Different from the popular frequence domain estimator, [Nels 86] provided the on-line estimator to provide periodic updates of load mass estimates to a parameteric optimal controller which then adjusts the control gains to maintain the desired arm response. The method appears to offer a promising means for achieving rapid smooth and accurate motion of flexible robot arms under varying load condition.

In [Yurk 89], Stphen Yurkovich and Fernando E. Pacheco presented the experimental results for the system identification and control of the single-link flexible

manipulator (ARMA) carrying an known varying payload. Various time-domain parameter estimation techniques were used to identify the ARMA model representation which was employed in the controller tuning scheme for the vibration compensation. Only the end-point acceleration measurement and a motor shaft measurement were utilized in the relatively simple PID control schemes. Additionally,

2.5 Stability Analysis

The stability of the controller is critical to the operations of the flexible robots and manipulators. The traditional analysis of the transfer function, which was addressed in [Wang 89], is no longer effective for the more complicated and nonlinear system. The *Lyapunov energy* analysis seems to be the only tool for the investigation of the stability of the complicated flexible robots systems. The application of the *Lyapunov Energy* analysis for the nonlinear model of one-link flexible manipulator can be found in [Wang 90]. Usually, this approach requires the heavy and even tedious computation effort.

The researches of the flexible robots and manipulators have gained the wide knowledge of the modeling and control strategies, and the insights of the flexible robots systems. The more applicable modeling and control methods are expected to be explored for the plant application. The next Chapter will present the whole derivations of four dynamic models of one-link flexible manipulators.

Chapter 3 Motion Equations of One-Link Flexible Manipulators

3.1 Problem Description

The flexibility of the one-link flexible manipulator is the elastic deformation along the beam length. This is the added degree of freedom second to the rotation of the hub. The main contribution resources of this deformation are the pure bending of the manipulator, rotatory inertia and shear deformation. The most common models of the flexible manipulators only claim the first deformation resource without mention the other two. In this chapter, all the resources will be discussed and the derivations will show the flexibility complicate the modeling procedure, especially when the tip mass is involved.

The considered manipulator is made of an actuator at the base with total (rotor and hub) inertia I_H, a flexible beam with length L, heigh H, width B, linear mass density ρ, rectangle transverse section area A, transverse section inertia I and a payload of mass M_p and its inertia J_p. Yang's modulus and shear modulus are E and G, respectively. The details of the stereotypical manipulator is shown in Fig. 1.

The reference frames X^0OY^0 in Figure 1. is the global reference frame fixed in horizontal plane, while the XOY is the coordinate reference frame fixed with the hub. The $AO'B$ is the tip mass reference frame which is fixed at and coincided with the end of the beam. The a_c and b_c are the coordinates of the tip mass center in the tip mass reference frame. The motion of the beam is described by the hub angular rotation $\theta(t)$ in the X^0OY^0, and the flexible deformation $w(x,t)$ due to the beam flexibility in the XOY.

To make the derivation more distinctly, the following differential notations is employed through all the derivations,

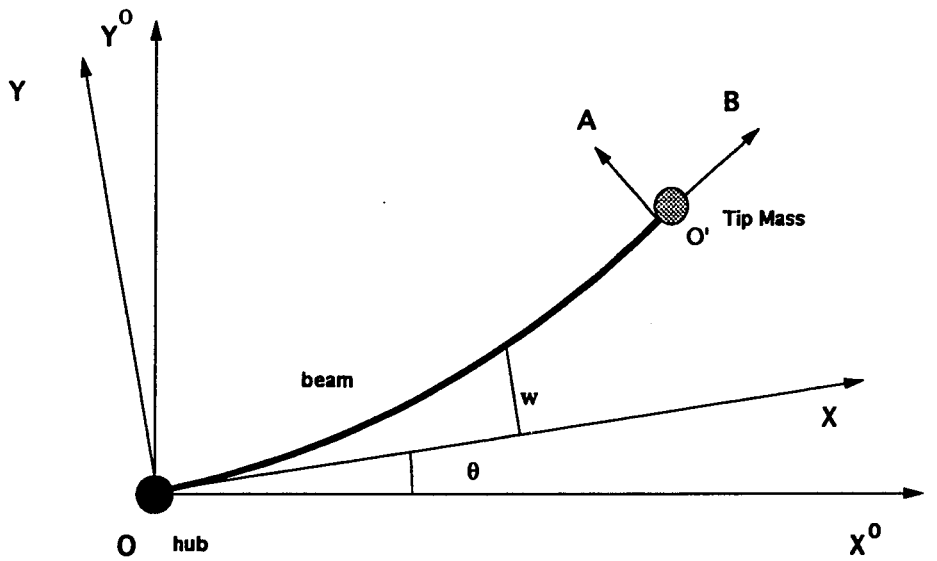

Figure 1: One-Link Flexible Manipulator

$$()' = \partial()/\partial x, \qquad \dot{()} = \partial()/\partial t$$

The motion of the transverse section of the beam is shown in the Fig. 2. The basic assumptions of the elastic theory about the motion of the transverse section is that the section is still a plane under the bending. The rotational angle of the transverse section in the X^0OY^0 is $\psi(x,t)$. Actually, the $\psi(x,t)$ includes two parts: the rotational angle due to the pure bending, $w'(x,t)$; and the rotational angle due to the shear deformation, $\beta(x,t)$. The discussion details of the motion of transverse section can be found in [Timo 49].

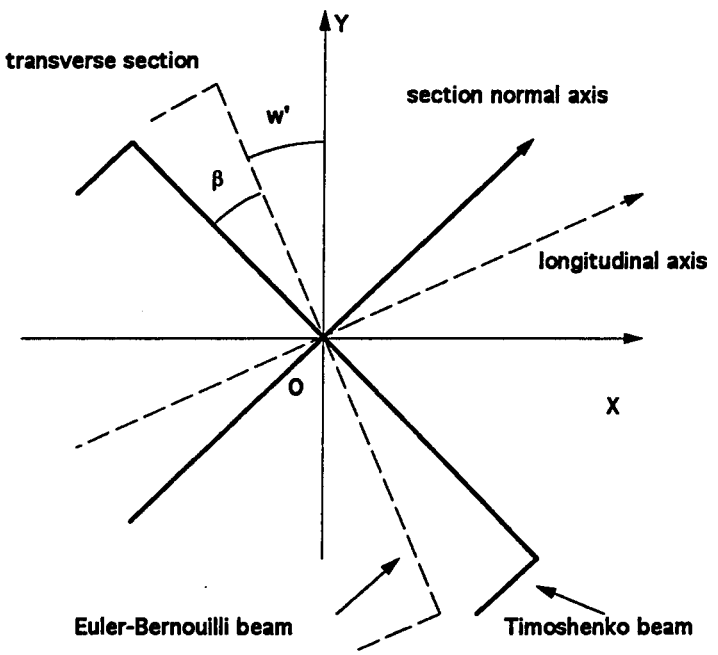

Figure 2: Motion of the Transverse Section

$$\psi(x,t) = w'(x,t) + \beta(x,t) \tag{1}$$

Obviously, after the deformation w, the coordinate, (x^0, y^0) of an arbitrary point in the transverse section of the beam with the distance x from the hub along the longitudinal axis and the distance ζ from the normal axis, is,

$$\begin{cases} x^0(x,\zeta,t) = x\cos\theta - w\sin\theta - \zeta\sin\psi \\ y^0(x,\zeta,t) = x\sin\theta + w\cos\theta + \zeta\cos\psi \end{cases} \tag{2}$$

Hence, the velocities of this point in global reference frame directions are,

$$\begin{cases} \dot{x^0} = -y^0\dot{\theta} - \dot{w}\sin\theta - \zeta\dot{\psi}\cos\psi \\ \dot{y^0} = x^0\dot{\theta} + \dot{w}\cos\theta - \zeta\dot{\psi}\sin\psi \end{cases}$$

Therefore, the square of Cartesian velocity of this specific point is:

$$
\begin{aligned}
v^2 &= \dot{x^0}^2 + \dot{y^0}^2 \\
&= ([x^0]^2 + [y^0]^2)\dot{\theta}^2 + \dot{w}^2 + 2\dot{\theta}\dot{w}(y\sin\theta + x\cos\theta) \\
&\quad +\zeta^2\dot{\psi}^2 + 2\zeta\dot{\psi}\cos\psi(y\dot{\theta} - \dot{w}\sin\theta) - 2\zeta\dot{\psi}\sin\psi(x\dot{\theta} + \dot{w}\cos\theta)
\end{aligned}
$$

The average square of the Cartesian velocity in this transverse section can be calculated as,

$$
\begin{aligned}
V^2 &= \frac{B}{A}\int_{-\frac{H}{2}}^{\frac{H}{2}} v^2 d\zeta \\
&= \Delta_x^2 + \Delta_y^2 + S\dot{\psi}^2 \qquad (3)
\end{aligned}
$$

where, the $S = I/A$, Δ_x and Δ_y are :

$$
\Delta_x = x\dot{\theta} + \dot{w}, \qquad \Delta_y = \dot{\theta}w \qquad (4)
$$

The above notations will be used through the derivation procedures in this chapter.

3.2 Basic Assumptions and Modeling Method

General Assumptions

The general assumptions are employed through all the following derivations to ensure the appropriate applications of the elastics theorys and the accuracy of the models. The assumptions which are employed as the general assumptions in modeling procedure of one-link flexible manipulators are as followings,

1. The link is uniform along its longitudinal direction, as well as its mass distribution and elastic properties.

2. The elastic deformation of the link is small enough, hence, all of the second or high order terms of the elastic deformation and their productions are negligible.

3. The transverse section is still a plane under the elastic deformations.

4. The vertical deformation of the link is negligible.

5. The neutral longitudinal axis of the beam coincides with the S-axis.

Assumptions of the Individual Models

In this chapter, there are four dynamic models developed. For each model, the assumptions of transverse section motion are different due to the accuracy considerations. The followings are the list of four models and the specific assumptions of the transverse section motions.

1. Euler-Bernoulli Dynamic Model

   The velocities of every point in the same transverse section are identical, and they are equal to the velocity of the neutral axis at that transverse section. Here, the rotatory inertia and shear deformation are negligible.

2. Euler-Bernoulli Dynamic Model with Rotatory

   The velocities of every point in the same transverse section are not identical due to the rotation of the transverse section. The rotation angle of the transverse section is the bending angle $w'(x,t)$. Here, the shear deformation is negligible.

3. Timoshenko Dynamic Model

   The velocities of every point in the same transverse section are not identical

due to the rotation of the transverse section. The rotation angle of the transverse section is the sum of the bending angle $w'(x,t)$ and shear angle $\beta(x,t)$. This is the most accurate assumption about the motion of the transverse section.

4. Euler-Bernoulli Dynamic Model with Tip Mass

   The assumptions are same as that of Euler-Bernoulli dynamic model.

Modeling Method

To gain more insights of the one-link flexible manipulators for the control purpose, the modal expansion method with *Hamilton Principle* is going to be employed for modeling. The typical vibration parameters, such as the resonant frequency and vibration modes, can be obtained through this method. The influences of rotatory inertia, and shear deformation and tip mass on the vibration behaviors can be investigated by the proposed method. The other reason not to use the FEM is that the modal expansion method is more direct for this one-link flexible manipulators problem.

3.3 Euler-Bernoulli Dynamic Model

The Euler-Bernoulli model doesn't consider the rotatory inertia and shear deformation. The only deformation that the transverse section has is the pure bending, and the transverse section still keep plane. Additionally, each point in the same transverse section moves at the same velocity. This is the typical model for the elastic beam for the engineering purpose. All the tip mass details are omitted in the following derivations.

3.3.1 Energy Calculations

Based on the above assumption, the average Cartesian velocity square of

arbitrary transverse section equation (3) become,

$$V^2 = \Delta_x^2 + \Delta_y^2 \tag{5}$$

So, Kinetic energy of the one-link flexible manipulator is,

$$T = \frac{1}{2} I_H \dot{\theta}^2 + \frac{1}{2} \int_0^L \rho V^2 dx \tag{6}$$

The Potential energy of the manipulator can be given by the Euler-Bernoulli beam theory,

$$P = \frac{1}{2} \int_0^L EI(w'')^2 dx \tag{7}$$

The work done by the input torque can be calculated as,

$$W = \tau\theta \tag{8}$$

3.3.2 Application of Hamilton Principle

Based on the *Hamilton Principle*, the *Hamilton Function* exhibits the property that the following is hold over arbitrary time period [t_0, t_1],

$$\delta \int_{t_0}^{t_1} (T + W - P) dt = 0 \tag{9}$$

Apply the variational operation to the *Hamilton Function*, and the variational operation result of the Kinetic energy is,

$$\delta \int_{t_0}^{t_1} \frac{1}{2} I_H \dot{\theta}^2 dt = - \int_{t_0}^{t_1} I_H \ddot{\theta} \delta\theta dt \tag{10}$$

$$\delta \int_{t_0}^{t_1} \frac{1}{2} \int_0^L \rho V^2 dx dt = -\int_{t_0}^{t_1} \int_0^L \overline{\dot{x\triangle_x + w\triangle_y}} \rho dx \delta\theta dt - \int_{t_0}^{t_1} \int_0^L (\dot{\triangle}_x - \dot{\theta}\triangle_y) \rho \delta w dx dt \quad (11)$$

The variational operation results of the Potential energy P of the flexible manipulator is,

$$\delta \int_{t_0}^{t_1} P dt = \int_{t_0}^{t_1} [EIw''\delta w' - (EIw'')'\delta w] \Big|_0^L dt + \int_{t_0}^{t_1} \int_0^L (EIw'')''\delta w dx dt \quad (12)$$

And, apply the variational operation to the work done by the input torque,

$$\delta \int_{t_0}^{t_1} W dt = \int_{t_0}^{t_1} \tau \delta\theta dt \quad (13)$$

According to the *Hamilton Principle* that all the coefficient of the δw and $\delta\theta$ must be zero, sum all the term of *Hamilton* functions and the two coefficients which corresponds to the $\delta\theta$ and δw, the variations of the hub motion and beam flexibility respectively, are;

$$\rho(\dot{\triangle}_x - \dot{\theta}\triangle_y) + (EIw'')'' = 0 \quad (14)$$

$$\tau - I_H\ddot{\theta} - \int_0^L \overline{\dot{x\triangle_x + w\triangle_y}} \rho dx = 0 \quad (15)$$

where the boundary conditions are,

when $x = 0$,

$$w(0,t) = 0; \qquad w'(0,t) = 0 \tag{16}$$

$$\tag{17}$$

when $x = L$,

$$w''(L,t) = 0; \qquad w'''(L,t) = 0 \tag{18}$$

Then apply the general assumption 2. hence, the $\triangle_y = 0$. The governing equations turn to be,

$$EIw'''' + \rho(x\ddot{\theta} + \ddot{w}) = 0 \tag{19}$$

$$\tau - I_H\ddot{\theta} - \frac{\partial}{\partial t}\int_0^L x(x\dot{\theta} + \dot{w})\rho dx = 0 \tag{20}$$

The integration term in the above equation can be reduced to the algebraic term through the integration of the equation (19) over the length of the manipulator,

$$\begin{aligned}
&\int_0^L x(EIw'''')dx + \int_0^L x\rho(x\ddot{\theta} + \ddot{w})dx \\
&= xEIw'''\Big|_0^L - EIw''\Big|_0^L + \int_0^L x\rho(x\ddot{\theta} + \ddot{w})dx \\
&= LEIw'''(L,t) - EIw''(L,t) + EIw''(0,t) + \int_0^L x\rho(x\ddot{\theta} + \ddot{w})dx \\
&= EIw''(0,t) + \int_0^L x\rho(x\ddot{\theta} + \ddot{w})dx = 0
\end{aligned} \tag{21}$$

Substitute the equation (21) into the (20) and define the new variable $v(x,t) = w(x,t) + x\theta(t)$ to reform the governing equations. In the section 3.6.2., the importance of this integration procedure will be discussed referring to the derivation of the exact vibration modes. The final PDE of the one-link flexible manipulator is,

A. Euler-Bernoulli Dynamic Model

$$EIv'''' + \rho\ddot{v} = 0 \tag{22}$$

$$\tau - I_H\ddot{\theta} + EIv''\Big|_{x=0} = 0 \tag{23}$$

while the boundary conditions are,

when $x = 0$;

$$v(0,t) = 0; \quad v'(0,t) = \theta \tag{24}$$

when $x = L$;

$$v''(L,t) = 0; \quad v'''(L,t) = 0 \tag{25}$$

3.4 Euler-Bernoulli Dynamic Model with Rotatory Inertia

The rotatory inertia has the certain influence on the vibration behavior of the rigid beam. When the beam has large flexibility, the influence of the effect of rotary increases. As presented in [Timo 57], the flexible beam performs not only a translatory motion but also transverse section rotation.

The physical explanation of the rotatory inertia is as following. During the operations of the flexible manipulator, the transverse section performs certain

rotation beside the translatory motion. The angle of rotation, which is equal to the slope of the deflection curve, is $\partial w/\partial x$, and the corresponding angular velocity and angular acceleration will be given by,

$$\frac{\partial^2 w}{\partial x \partial t}; \qquad \frac{\partial^3}{\partial x \partial t^2}$$

So, the inertial moment at the transverse section will be,

$$-\rho I \frac{\partial^3 w}{\partial x \partial t^2}$$

The total deformation become the sum of the pure bending and the additional deformation due to the inertia mement. However, currently, most of the models of the flexible manipulators do not mention the influence of the rotatory inertia.

3.4.1 Energy Calculations

Based on the transverse section assumptions of the Euler-Bernoulli dynamic model with rotatory inertia, the average Cartesian velocity square of the arbitrary transverse section equation (3) become,

$$V^2 = \Delta_x^2 + \Delta_y^2 + S(\dot{w}')^2 \tag{26}$$

The Kinetic energy of the flexible manipulator is ,

$$T = \frac{1}{2} I_H \dot{\theta}^2 + \frac{1}{2} \int_0^L \rho V^2 dx \tag{27}$$

The Potential energy of the flexible manipulator can be given by the Euler-Bernoulli beam theory, and is same as no rotatory inertia case.

The work done by the input torque can be calculated as,

$$W = \tau\theta \tag{28}$$

3.4.2 Application of the Hamilton Principle

Based on the *Hamilton Principle*, the *Hamilton Function* exhibits the property that the following is hold over arbitrary time period [t_0, t_1],

$$\delta \int_{t_0}^{t_1} (T + W - P)dt = 0 \tag{29}$$

Comparing to the Euler-Bernoulli dynamic model without rotatory inertia, the only difference of the variational operations of this *Hamilton Function* is the Kinetic energy of the beam,

$$\begin{aligned} \delta \int_{t_0}^{t_1} \frac{1}{2} \int_0^L \rho V^2 dx dt = & -\int_{t_0}^{t_1} \int_0^L \overline{\dot{x}\triangle_x + w\triangle_y} \rho dx \delta\theta dt \\ & -\int_{t_0}^{t_1} \int_0^L (\dot{\triangle}_x - \dot{\theta}\triangle_y)\rho\delta w dx dt \\ & -\int_0^L \rho\ddot{w}'\delta w \Big|_0^L dx + \int_{t_0}^{t_1} \int_0^L \rho\ddot{w}''\delta w dx dt \end{aligned} \tag{30}$$

So, the effect of the inertia rotary is related to the beam deformation w only. From the equation (30), the effect of inertia rotary introduces two terms to the linear PDE of Euler-Bernoulli model. The finial modified PDE turns to be,

B. Euler-Bernoulli Dynamic Model with Rotary Inertia

$$EIv'''' - \rho S\ddot{v}'' + \rho\ddot{v} = 0 \tag{31}$$

$$\tau - I_H\ddot{\theta} + EIv'' \Big|_{x=0} = 0 \tag{32}$$

where the boundary conditions,

when $x = 0$;

$$v(0,t) = 0; \quad v'(0,t) = \theta \tag{33}$$

when $x = L$;

$$v''(L,t) = 0; \quad EIv'''(L,t) = \rho S\ddot{v}'(L,t) \tag{34}$$

Where $S = I/A$, when $S \to 0$, the modified model reduces exactly to the linear PDE of Euler-Bernoulli model without rotatory inertia.

3.5 Timoshenko Dynamic Model

The more accurate dynamic model can be obtained if not only the rotary inertia but also the deflection due to shear is taken into account. The rotational angle of the transverse section depends not only on the slope of the deflection curve but also on the shear angle. Let ϑ denote the pure bending angle and β the shear angle at the neutral axis in the same transverse section. Then the total rotational angle of the transverse section (Fig. 2) is,

$$\psi(x,t) = \vartheta(x,t) + \beta(x,t)$$

The shear force can be calculated as ;

$$N = -k\beta AG = -k(\psi - \vartheta)AG \tag{35}$$

in which k is a numerical factor depending on the shape of the transverse section. So, the normal axis of the transverse section is no longer along the direction of w', and the difference is the shear angle β.

3.5.1 Energy Calculations

Based on the transverse section assumption of the Timoshenko dynamic model, the average Cartesian velocity square of the arbitrary transverse section equation (3) become,

$$V^2 = \Delta_x^2 + \Delta_y^2 + S(\dot{w}' + \dot{\beta})^2 \tag{36}$$

The Kinetic energy of the flexible manipulator become,

$$T = \frac{1}{2} I_H \dot{\theta}^2 + \frac{1}{2} \int_0^L \rho V^2 dx \tag{37}$$

And the expression of the Potential energy is given as,

$$P = \frac{1}{2} \int_0^L EI\psi'^2 dx \tag{38}$$

The work done by the input torque τ is,

$$W = \tau\theta \tag{39}$$

3.5.2 Application of Hamilton Principle

Based on the *Hamilton Principle*, the *Hamilton Function* exhibits the property that the following is hold over arbitrary period time [t_0, t_1],

$$\delta \int_{t_0}^{t_1} (T + W - P) dt = 0 \tag{40}$$

When introduce the new variable $\alpha(x,t) = \psi(x,t) + \theta(t)$, and apply the *Hamilton Principle* to this model. After the variational calculations, the resulting governing equations become,

$$EI\alpha'' + kGA(v' - \alpha) - \rho S\ddot{\alpha} = 0 \quad (41)$$

$$kGA(v'' - \alpha') - \rho\ddot{v} = 0 \quad (42)$$

$$\tau - I_H\ddot{\theta} + EI\alpha' \Big|_{x=0} = 0 \quad (43)$$

$$(44)$$

where, k is chosen as $10(1+\nu)/(12+11\nu)$ for rectangle section and ν is the Poisson's ratio. The boundary conditions are as followings,

when $x = 0$,

$$\alpha(0,t) = \theta(t); \qquad v(0,t) = 0 \quad (45)$$

when $x = L$,

$$\alpha'(L,t) = 0; \qquad v'(L,t) = \alpha(L,t) \quad (46)$$

The final PDE of the Timoshenko dynamic model can be expressed in the decoupled form as,

C. Timoshenko Dynamic Model

$$EI\phi'''' - \rho S(1+\mu)\ddot{\phi}'' + \rho\ddot{\phi} + \mu\frac{\rho^2 S}{EA}\frac{\partial^4\phi}{\partial t^4} = 0 \quad (47)$$

$$\tau - I_H\ddot{\theta} + EI\alpha' \Big|_{x=0} = 0 \quad (48)$$

$$\alpha = \phi'' - \rho\mu S\ddot{\phi}/EI, \qquad v = \phi' \quad (49)$$

where $\alpha = \theta + \psi$, $v = w + x\theta$, $\mu = E/kG$ and $\phi(x,t)$ is a defined function to decouple the PDE.

when $x = 0$,

$$\alpha(0,t) = \theta(t), \qquad v(0,t) = 0 \tag{50}$$

when $x = L$,

$$\alpha'(L,t) = 0; \qquad v'(L,t) = \alpha(L,t) \tag{51}$$

This PDE takes both the inertia rotary and shear deformation into account. When the shear deformation is ignored, the above PDE reduces exactly to the linear PDE of the Euler-Bernoulli dynamic model with rotatory inertia.

3.6 Euler-Bernoulli Dynamic Model with Tip Mass

This model is developed based on the derivations in section 3.3. The rotatory inertia and shear deformation are negligible. The only deformation that the transverse section has is the pure bending, and each point in the same transverse section moves at the same velocity. When the tip mass is considered, the calculations of the *Hamilton* function become a little complicated. All the details of the tip mass is showed in the Fig. 1.

3.6.1 Energy Calculations

Based on the transverse section assumptions of Euler-Bernoulli dynamic model, the average Cartesian velocity square of the arbitrary transverse section equation (3) become,

$$V^2 = \Delta_x^2 + \Delta_y^2 \tag{52}$$

If x_a and y_b are defined as coordinates of the arbitrary point in the tip mass domain S_p referring to the frame X^0OY^0, the a_c and b_c are the coordinates of the tip mass center in tip mass frame $AO'B$, the θ_p is the angular deformation of the tip end in XOY, and the ρ_p is the mass density of the tip mass. So, Kinetic energy of the whole flexible manipulator system can be found as:

$$T = \frac{1}{2}I_H\dot{\theta}^2 + \frac{1}{2}\int_0^L \rho V^2 dx + T_p \tag{53}$$

Where, the T_p is the Kinetic energy of the tip mass.

$$\begin{aligned} T_p &= \frac{1}{2}\int\int_{S_p} \rho_p(\dot{x}_a^2 + \dot{y}_b^2)dS \\ &= \frac{M_p}{2}\{V^2(L,t) + \frac{J_p}{M_p}\dot{\theta}_p^2 + 2\dot{\theta}_p[a_c\triangle_x(L,t) + b_c\triangle_y(L,t)]\cos(\theta_p - \theta) \\ &\quad +2\dot{\theta}_p[a_c\triangle_x(L,t) - b_c\triangle_y(L,t)]\sin(\theta_p - \theta)\} \\ &= \frac{M_p}{2}\{V^2(L,t) + \frac{J_p}{M_p}\dot{\theta}_p^2 + 2[G_x\cos(\theta_p - \theta) + G_y\sin(\theta_p - \theta)]\dot{\theta}_p\} \end{aligned} \tag{54}$$

And, the G_x and G_y are,

$$\begin{cases} G_x = a_c\triangle_x(L,t) + b_c\triangle_y(L,t) \\ G_y = a_c\triangle_y(L,t) - b_c\triangle_x(L,t) \end{cases} \tag{55}$$

The Potential energy of this flexible beam is still the same as the no-tip case:

$$P = \frac{1}{2}\int_0^L EI(w'')^2 dx \tag{56}$$

The work done by the input torque can be calculated as :

$$W = \tau\theta \tag{57}$$

3.6.2 Application of Hamilton Principle

The motion governing equations of this flexible manipulator can be obtained by applying the *Hamilton Principle*, which states that for any elastic system, the following equation must be hold over arbitrary time period [t_0, t_1]:

$$\delta \int_{t_0}^{t_1} (T + W - P) dt \;=\; 0 \tag{58}$$

The variational calculations are conducted to first and second term of (53) as,

$$\delta \int_{t_0}^{t_1} \frac{1}{2} I_H \dot{\theta}^2 dt \;=\; -\int_{t_0}^{t_1} I_H \ddot{\theta} \delta\theta dt \tag{59}$$

$$\begin{aligned} \delta \int_{t_0}^{t_1} \frac{1}{2} \int_0^L \rho V^2 dx dt \;&=\; -\int_{t_0}^{t_1} \int_0^L \dot{\overline{x\triangle_x + w\triangle_y}} \rho dx \delta\theta dt \\ &\quad -\int_{t_0}^{t_1} \int_0^L (\dot{\triangle}_x - \dot{\theta}\triangle_y) \rho \delta w dx dt \end{aligned} \tag{60}$$

The variational calculations of the first two terms of T_p in equation (54) are conducted by part integration,

$$\begin{aligned} &\delta \int_{t_0}^{t_1} \frac{M_P}{2} V^2 \Big|_{\,x = L} \; dt \\ =\; &-M_p \int_{t_0}^{t_1} \dot{\overline{x\triangle_x + w\triangle_y}} \Big|_{\,x = L} \; \delta\theta dt \\ &-M_p \int_{t_0}^{t_1} (\dot{\triangle}_x - \dot{\theta}\triangle_y) \Big|_{\,x = L} \; \delta w dt \end{aligned} \tag{61}$$

$$\begin{aligned} \delta \int_{t_0}^{t_1} \frac{J_p}{2} \dot{\theta}_p^2 dt \;&=\; -\int_{t_0}^{t_1} J_p \ddot{\theta}_p \delta\theta_p dt \\ &=\; -\int_{t_0}^{t_1} J_p \ddot{\theta}_p [\delta\theta + \cos^2(\theta_p - \theta)\delta w'] dt \end{aligned} \tag{62}$$

The remaining term of the tip mass Kinetic energy, T_p, is

$$\begin{aligned} H &= M_p\dot{\theta}_p[G_x\cos(\theta_p-\theta)+G_y\sin(\theta_p-\theta)] \\ &= M_p\dot{\theta}_p[H_x\triangle_x(L,t)+H_y\triangle_y(L,t)] \\ &= \dot{\theta}_p H_p \end{aligned} \tag{63}$$

$$H_x = a_c\cos(\theta_p-\theta)-b_c\sin(\theta_p-\theta) \tag{64}$$

$$H_y = b_c\cos(\theta_p-\theta)+a_c\sin(\theta_p-\theta) \tag{65}$$

$$H_p = M_p[H_x\triangle_x(L,t)+H_y\triangle_y(L,t)] \tag{66}$$

Then apply the variational operation to the equation (63):

$$\delta\int_{t_0}^{t_1} H dt = -\int_{t_0}^{t_1}\dot{H}_p\delta\theta_p dt+\int_{t_0}^{t_1}\dot{\theta}_p\delta H_p dt \tag{67}$$

and, apply the operation to the second terms of the above equation,

$$\begin{aligned} \int_{t_0}^{t_1}\dot{\theta}_p\delta H_p dt &= M_p\int_{t_0}^{t_1}\dot{\theta}_p[G_y\cos(\theta_p-\theta)-G_x\sin(\theta_p-\theta)]\delta(\theta_p-\theta)dt \\ &\quad +M_p\int_{t_0}^{t_1}\dot{\theta}_p[\delta G_x\cos(\theta_p-\theta)+\delta G_y\sin(\theta_p-\theta)]dt \end{aligned} \tag{68}$$

The second term of the above equation can be reformed as :

$$\begin{aligned} & M_p\int_{t_0}^{t_1}\dot{\theta}_p[\delta G_x\cos(\theta_p-\theta)+\delta G_y\sin(\theta_p-\theta)]dt \\ = \; & M_p\int_{t_0}^{t_1}\dot{\theta}_p[H_x\delta\triangle_x(L,t)+H_y\delta\triangle_y(L,t)]dt \\ = \; & M_p\int_{t_0}^{t_1}[H_y\dot{\theta}\dot{\theta}_p-\overline{\dot{H}_x\dot{\theta}_p}]\delta w-\overline{\dot{\theta}_p(LH_x+w(L,0)H_y)}\delta\theta dt \end{aligned} \tag{69}$$

Finally, the equation (67) is summaried as the following:

$$
\begin{aligned}
& \delta \int_{t_0}^{t_1} H dt \\
= & -\int_{t_0}^{t_1} \dot{H}_p \delta\theta_p dt \\
& + M_p \int_{t_0}^{t_1} \dot{\theta}_p [G_y \cos(\theta_p - \theta) - G_x \sin(\theta_p - \theta)] \cos^2(\theta_p - \theta) \delta w' dt \\
& + M_p \int_{t_0}^{t_1} [(H_y \dot{\theta}\dot{\theta}_p - \dot{\overline{H_x \dot{\theta}_p}}) \delta w - \dot{\overline{\dot{\theta}_p [L H_x + w(L,0) H_y]}} \delta\theta] dt \\
= & \int_{t_0}^{t_1} F_1 \delta\theta + F_2 \delta w + F_3 \delta w' dt
\end{aligned} \tag{70}
$$

where, the relative functions F_1, F_2 and F_3 are,

$$
F_1 = -\dot{H}_p - M_p \dot{\overline{\dot{\theta}_p [L H_x + w(L,0) H_y]}} \tag{71}
$$

$$
F_2 = M_p [H_y \dot{\theta}\dot{\theta}_p - \dot{\overline{H_x \dot{\theta}_p}}] \tag{72}
$$

$$
\begin{aligned}
F_3 = & M_p \dot{\theta}_p [G_y \cos(\theta_p - \theta) - G_x \sin(\theta_p - \theta)] \cos^2(\theta_p - \theta) \\
& - \dot{H}_p \cos^2(\theta_p - \theta)
\end{aligned} \tag{73}
$$

The variational operation result of the Potential energy P of the flexible manipulator is,

$$
\begin{aligned}
\delta \int_{t_0}^{t_1} P dt = & \int_{t_0}^{t_1} [EIw'' \delta w' - (EIw'')' \delta w] \Big|_0^L dt \\
& + \int_{t_0}^{t_1} \int_0^L (EIw'')'' \delta w dx dt
\end{aligned} \tag{74}
$$

And, the result of the variational operation to the work done by the input torque is,

$$
\delta \int_{t_0}^{t_1} W dt = \int_{t_0}^{t_1} \tau \delta\theta dt \tag{75}
$$

Sum all the terms of *Hamilton function* and the two coefficients which corresponds to the $\delta\theta$ and δw, the variations of hub motion and beam flexibility respectively, are,

$$\rho(\dot{\Delta}_x - \dot{\theta}\Delta_y) + (EIw'')'' = 0 \tag{76}$$

$$\tau - I_H\ddot{\theta} - \int_0^L \overline{\dot{x\Delta_x + w\Delta_y}}\rho dx - J_p\ddot{\theta}_p - M_p\overline{\dot{x\Delta_x + w\Delta_y}}\Big|_{x=L} + F_1 = 0 \tag{77}$$

The above equations are the governing *integro-partial differential equations* (IPDE) for the motion of this one-link flexible manipulator with tip mass. Also, the boundary conditions of the IPDE can be established by the *Hamilton Principle* and the motion constrains at the hub. Obviously, these boundary conditions guarantee the equilibrium conditions of the shear force and moment at the end of beam.

when $x = 0$,

$$w(0,t) = w'(0,t) = 0 \tag{78}$$

when $x = L$,

$$EIw'' - F_3 + J_p\ddot{\theta}_p\cos^2(\theta_p - \theta) = 0 \tag{79}$$

$$EIw''' + F_2 - M_p(\dot{\Delta}_x - \dot{\theta}\Delta_y)\Big|_{x=L} = 0 \tag{80}$$

Further, by substituting the Δ_x and Δ_y into the governing equations and conducting the integration by part, the governing equations become:

$$(EIw'')'' + \rho(x\ddot{\theta} + \ddot{w}) = 0 \tag{81}$$

$$\tau - I_H\ddot{\theta} - \frac{\partial}{\partial t}\int_0^L x(x\dot{\theta} + \dot{w})\rho dx - J_p[\ddot{\theta} + \ddot{w}'(L,t)] \\ -M_pL[L\ddot{\theta} + \ddot{w}(L,t)] + F_1 = 0 \quad (82)$$

where the boundary conditions are:

when $x = 0$;

$$w(0,t) = w'(0,t) = 0 \quad (83)$$

when $x = L$;

$$EIw'' = F_3 - J_p\ddot{\theta}_p \quad (84)$$

$$(EIw'')' = -F_2 + M_p[L\ddot{\theta} + \ddot{w}(L,t)] \quad (85)$$

The next section will discuss the simplification of this governing equations.

3.6.3 Linearization of Motion Equations

The linearization of the motion equation can be feasible and still guarantees the accuracy under the appropriate assumptions. Here, the assumption of the linearization (Assumption 2. in section 3.2) is that the bending deformation is small and its two or high order velocities and their productions are negligible. Based on the above assumption, the simplified notations can be described as the following;

$$\Delta_x = x\dot{\theta} + \dot{w}; \quad \Delta_y = 0; \quad \theta_P = \theta + w'(L,t) \quad (86)$$

$$H_x = a_c - b_c w'(L,t); \quad H_y = b_c + a_c w'(L,t) \quad (87)$$

$$G_x = a_c\Delta_x; \quad G_y = -b_c\Delta_x; \quad H_p = M_p a_c[L\dot{\theta} + \dot{w}(L,t)] \quad (88)$$

$$F_1 = -M_p a_c[L\ddot{\theta} + \ddot{w}(L,t) - L\ddot{\theta}_p] \quad (89)$$

$$F_2 = M_p[-a_c\ddot{\theta}_p] \quad (90)$$

$$F_3 = -M_p a_c[L\ddot{\theta}_p + \ddot{w}(L,t)] \quad (91)$$

When substitute the above relations into the IPDE, the governing equations turn to be,

$$EI(w'')'' + \rho(x\ddot{\theta} + \ddot{w}) = 0 \quad (92)$$

$$\begin{aligned} &\tau - I_H\ddot{\theta} - \frac{\partial}{\partial t}\int_0^L x(x\dot{\theta} + \dot{w})\rho dx \\ &-J_p\ddot{\theta}_p - M_pL^2[\ddot{\theta} + \frac{\ddot{w}(L,t)}{L}] - a_cM_pL[\ddot{\theta} + \frac{\ddot{w}(L,t)}{L} + \ddot{\theta}_p] = 0 \end{aligned} \quad (93)$$

where the boundary conditions:

$$w(0,t) = w'(0,t) = 0 \quad (94)$$

$$EIw''(L,t) = -M_pa_cL[\ddot{\theta} + \frac{\ddot{w}(L,t)}{L}] - J_p\ddot{\theta}_p \quad (95)$$

$$(EIw'')'(L,t) = M_pa_c\ddot{\theta}_p + M_pL[\ddot{\theta} + \frac{\ddot{w}(L,t)}{L}] \quad (96)$$

The integral term in the equation (93) can be reduced to the algebraic term through the integration of (92) over [$0, L$].

$$\begin{aligned} &\int_0^L x(EIw'')''dx + \int_0^L \rho x(x\ddot{\theta} + \ddot{w})dx \\ &= x(EIw'')'\Big|_0^L - EIw''\Big|_0^L + \int_0^L \rho x(x\ddot{\theta} + \ddot{w})dx \end{aligned}$$

$$
\begin{aligned}
&= L(EIw'')'(L,t) - EIw''(L,t) + EIw''(0) + \int_0^L \rho x(x\ddot{\theta} + \ddot{w})dx \\
&= J_p\ddot{\theta}_p + M_p a_c L[\ddot{\theta} + \frac{\ddot{w}(L,t)}{L}] + M_p a_c L\ddot{\theta}_p + M_p L^2[\ddot{\theta} + \frac{\ddot{w}(L,t)}{L}] \\
&\quad + EIw''(0) + \int_0^L \rho x(x\ddot{\theta} + \ddot{w})dx = 0 \qquad (97)
\end{aligned}
$$

Substitute the equation (97) into (93) and use the notation $v(x,t) = w(x,t) + x\theta(t)$, then the motion equations of Euler-Bernoulli dynamic model with tip mass are obtained,

D. Euler-Bernoulli Dynamic Model with Tip Mass

$$EIv'''' + \rho\ddot{v} = 0 \qquad (98)$$

$$\tau - I_H\ddot{\theta} + EIv''\Big|_{x=0} = 0 \qquad (99)$$

while the boundary conditions,

$$v(0,t) = 0; \quad v'(0,t) = \theta \qquad (100)$$

$$EIv''(L,t) = -J_p\ddot{v}'(L,t) - M_p a_c\ddot{v}(L,t) \qquad (101)$$

$$EIv'''(L,t) = M_p a_c\ddot{v}'(L,t) + M_p\ddot{v}(L,t) \qquad (102)$$

3.7 Summary

The influences of rotatory inertia, shear deformation and tip mass on the motion equations are presented in this chapter. The integration procedure to get the algebraic form of the second governing equation is a very important fact about the modeling of the one-link flexible manipulator. The second governing equation of the PDE, which are the equation (23), (32), (48) and (99), was treated as the

boundary conditions, which was derivated from the equilibrium conditions at the hub, in the early research work like [Cann 84]. Also, the boundary condition $w'(0) = 0$ was omitted in the same paper for the no tip mass case. In the practice of the modeling, *Hamilton Principle* has implicated the above necessary boundary condition $w'(0) = 0$. From the above derivation,

$$EI\frac{\partial^2}{\partial x^2}\delta\frac{\partial w}{\partial x}\Big|_{x=0} = 0$$

So, the either $\partial^2 w/\partial x^2 = 0$ or $\partial w/\partial x = 0$ to be ture at $x = 0$.

The Cannon's model are underconstrained because the absence of above two facts. Thus, the w and θ can not be solved simultaneously. Additionally, the exact vibration modes can not be derived through the underconstrained PDE, and leave the assumed mode shapes be the only tool of investigation. The following Chapter is going to show the four models developed in this Chapter provide the necessary conditions for derivations of the exact modal frequency equations and vibration modes.

Chapter 4 Frequency Equations and Vibration Modes

In the previous study of the flexible manipulators, most researchers used the assumed vibration modes to describe the motion of the flexible manipulators, obviously these assumed modes can not represent the exact physical insights of the flexible structures. Additionally, it rises the risk of controller ineffectiveness and even the unstability in the real world applications although the simulation study is acceptable. Conversely, the exact vibration modes provide more physical insights of the flexible systems and enhance the performance of controller with effectiveness and accuracy, even with fewer numbers of modes employed.

The derivations of the four models in the last chapter verify the existence of the second governing equation and boundary condition $w' = 0$. These two facts provide the well constrained PDE and the necessary conditions for the derivations of the modal frequency equations and exact vibration modes.

4.1 Introduction

The most common way to discretize the linearized partial equations is to conduct the eigenanalysis. The strategy is to separate the motion variables into two variables which are only the function of the time and position respectively. The motion can be determined by the production of vibration modes which only depend on the position variable, and modal amplitude functions that only depend on time. When the modes knowledge of the system is exhaustive and accurate, the control of modal amplitude function will guarantee the effective position control of the flexible manipulators. Obviously, this accuracy of the mode shapes takes the most parts of the differences between the dynamic simulation and real world application.

In this chapter, the frequency equations which determine the resonant frequency of the flexible manipulators are derivated through the Laplace transfor-

mations, while the vibration modes are derivated through the eigenanalysis. The verifications of the four models are conducted through the comparison of the numerical results and the experimental results. The influences of the rotatory inertia, shear deformation, hub inertia I_H and the tip mass on the vibration behaviors of the flexible manipulator are presented through the numerical analysis.

In the coming derivations of the frequency equations, it assumes the existence of the following Laplace transformations,

$$\begin{aligned} \Psi(x,s) = \mathcal{L}[\psi(x,t)], \quad \Lambda(x,s) &= \mathcal{L}[\alpha(x,t)], \quad \Phi(x,s) = \mathcal{L}[\phi(x,t)], \\ V(x,s) = \mathcal{L}[v(x,t)], &\qquad W(x,s) = \mathcal{L}[w(x,t)], \\ \Theta(s) = \mathcal{L}[\theta(t)], &\qquad T(s) = \mathcal{L}[\tau(t)] \end{aligned}$$

It is also assumed that Laplace transformations of derivatives of $v(x,t)$ and $\phi(x,t)$ upon to the fourth order with respect to x exist. In this case, it is easy to show that

$$V^{(n)}(x,s) = \mathcal{L}[v^{(n)}(x,t)]$$

4.2 Modal Frequency Equations and Vibration Modes of Euler-Bernoulli Dynamic Model

This derivations of modal frequencies and vibration modes of E-B model are the essential for the following three models. The results of the other three models are going to be compared with this one to investigate the influences of rotatory inertia, shear deformation and tip mass on the vibration behaviors, and also this model is the most usually studied by researchers.

4.2.1 Modal Frequency Equation

Apply Laplace transformation to governing motion equations of the Euler-Bernoulli dynamic model and the corresponding boundary conditions with homo-

geneous initial conditions, the following partial differential equations for Laplace transformations are obtained.

$$EIV'''' + \rho s^2 V = 0 \tag{103}$$

$$T - s^2 I_H \Theta + EIV'' \Big|_{x=0} = 0 \tag{104}$$

with boundary conditions,

$$V(0,s) = 0, \quad V'(0,s) = \Theta(s), \quad V''(L,s) = 0, \quad V'''(L,s) = 0 \tag{105}$$

Solving equations (103)-(105), the transfer functions are as,

$$\Theta(s) = H_{\theta\tau}(s)T(s), \quad H_{\theta\tau}(s) = \frac{1}{s^2 I_H + EIK_1(m)} \tag{106}$$

and

$$V(x,s) = H_{v\theta}(x,s)\Theta(s) = H_{v\tau}(x,s)T(s), \tag{107}$$

$$W(x,s) = H_{w\theta}(x,s)\Theta(s) = H_{w\tau}(x,s)T(s) \tag{108}$$

where

$$H_{v\theta}(x,s) = [\sin(mx) + \sinh(mL)\cos m(L-x) + \sin(mL)\cosh m(L-x) + \sinh(mx) - \cos(mL)\sinh m(L-x) - \cosh(mL)\sin m(L-x)]/2m\Sigma_1(m) \tag{109}$$

$$H_{w\theta}(x,s) = H_{v\theta}(x,s) - x \quad H_{v\tau}(x,s) = H_{v\theta}(x,s)H_{\theta\tau}(s) \quad H_{w\tau}(x,s) = H_{w\theta}(x,s)H_{\theta\tau}(s) \tag{110}$$

and,

$$K_1(m) = m[\sinh(mL)\cos(mL) - \cosh(mL)\sin(mL)]/\Sigma_1(m) \tag{111}$$

$$\Sigma_1(m) = 1 + \cos(mL)\cosh(mL), \quad m^4 = -\frac{\rho s^2}{EI}. \tag{112}$$

The poles of the flexible manipulator system, which correspond to the resonant frequency, are determined by following transendential equation,

Frequency Equation of the E-B Dynamic Model

$$m^4 \frac{I_H}{\rho} - K_1(m) = 0 \tag{113}$$

The countable infinite number of the solutions of the above equation correspond to the resonant frequencies, which are denoted as ω_n, $n = 1, 2, 3, 4, \cdots$

4.2.2 Exact Vibration Modes

Now, consider a sinusoidal torque $\tau = \tau_0 \sin(\omega)$ applied at the hub, the responses of the flexible manipulator are also perform periodically.

$$\begin{aligned} \theta(t) &= \theta_0 \sin(\omega t) \\ v(x,t) &= v_0(x) \sin(\omega t) \end{aligned}$$

Substitute these responses back to the Euler-Bernoulli dynamic model. After the trigonometric functions are deleted, result a four order ordinary differential equation,

$$EIv''''_0 - \rho\omega^2 v_0 = 0 \tag{114}$$

The general solution of this equation is,

$$v_0(x) = A\sin(kx) + B\sinh(kx) + C\cos(kx) + D\cosh(kx) \tag{115}$$

where the k is found by solving the characteristic function of the ordinary differential equation (114),

$$EIk^4 = \rho\omega^2$$

By substitute the expression $v(x,t) = v_0(x)sin(\omega t)$ into the boundary conditions of the Euler-Bernoulli dynamic model, the followings are obtained,

$$v_0(0) = 0; \quad v_0'(0) = \theta_0; \quad v_0''(L) = 0; \quad v_0'''(L) = 0$$

Then solve the above equations and the vibration modes are obtained,

Vibration Modes of B-E Dynamic Model

$$\psi_n(x) = A_n \sin(k_n x) + B_n \sinh(k_n x) + C_n \cos(k_n x) + D_n \cosh(k_n x) \quad (116)$$

where the C_n is chosed as the arbitrary constant and subscript n corresponds to the nth mode order. And,

$$A_n = \frac{R_A}{\Re} C_n; \quad B_n = \frac{R_B}{\Re} C_n; \quad D_n = -C_n$$

$$R_A = \sin(k_n L)\sinh(k_n L) + \cos(k_n L)\cosh(k_n L) + 1$$
$$R_B = \cos(k_n L)\cosh(k_n L) - \sin(k_n L)\sinh(k_n L) + 1$$
$$\Re = -\sin(k_n L)\cosh(k_n L) + \cos(k_n L)\sinh(k_n L); \quad k_n^4 = \frac{\rho\omega_n^2}{EI}$$

Beside the flexible modes, there is the rigid vibration mode which corresponds to resonant frequency $\omega_0 = 0$ represents the motion of the rigid body. The rigid vibration mode can be expressed as a linear function,

$$\psi_0(x) = cx \quad (117)$$

where, the c is constant.

4.3 Modal Frequency Equation and Vibration Modes of Euler-Bernoulli Dynamic Model with Rotatory Inertia

When take the influence of the rotary inertia into account, the more accurate model is obtained. The Derivations of the frequency equation and vibration modes of the E-B model with rotatory inertia are the same as the previous section except the rotatory inertia term.

4.3.1 Modal Frequency Equation

Similarly to the section 3.2.1, apply Laplace transformation to governing motion equations of the Euler-Bernoulli dynamic model with rotatory inertia and the corresponding boundary conditions with homogeneous initial conditions, the motion equations in frequency domain are given as,

$$EIV'''' - \rho s^2 SV'' + \rho s^2 V = 0 \tag{118}$$

$$T - s^2 I_H \Theta + EIV'' \Big|_{x=0} = 0 \tag{119}$$

with boundary conditions,

$$V(0,s) = 0, \quad V'(0,s) = \Theta(s); \qquad V''(L,s) = 0, \quad EIV'''(L,s) = \rho s^2 SV'(L,s). \tag{120}$$

Solving equations (118)-(120), the transfer functions are derivated as,

$$H_{\theta\tau}(s) = \frac{1}{s^2 I_H + EIK_2(m)}, \quad K_2(m) = C_1 m^2 \sqrt{4 + S^2 m^4} \tag{121}$$

and

$$\begin{aligned} H_{v\theta}(x,s) &= \sinh(m_1 x)/m_1 - C_1[\cosh(m_1 x) - \cos(m_2 x)] \\ &\quad -C_2[m_2 \sinh(m_1 x) - m_1 \sin(m_2 x)] \end{aligned} \tag{122}$$

where

$$\begin{aligned} 2m\Sigma_2(m)C_1 &= \beta_1^3 \sinh(m_1 L)\cos(m_2 L) - \beta_2^3 \cosh(m_1 L)\sin(m_2 L) \\ 2m^2\Sigma_2(m)C_2 &= 1 + \beta_1^2 \sinh(m_1 L)\sin(m_2 L) + \beta_2^4 \cosh(m_1 L)\cos(m_2 L) \end{aligned}$$

and,

$$m_i = m\beta_i, \quad \beta_i = \left[\frac{\sqrt{4+S^2m^4} + (-1)^i Sm^2}{2}\right]^{\frac{1}{2}} \tag{123}$$

$$\Sigma_2(m) = 1 + (1 + \frac{m^4S^2}{2})\cosh(m_1 L)\cos(m_2 L) - \frac{m^2 S}{2}\sinh(m_1 L)\sin(m_2 L) \tag{124}$$

The poles of manipulator system, which correspond to the resonant frequencies, are determined by following transendential equation,

Frequency Equation of the E-B Dynamic Model with RI

$$m^4\frac{I_H}{\rho} - K_2(m) = 0 \tag{125}$$

The countable infinite number of the solutions of the above equation correspond to the resonant frequencies, which are denoted as ω_n, $n = 1, 2, 3, 4, \cdots$ As expected, K_2 and Σ_2 reduce to K_1 and Σ_1 respectively, when S approaches zero (i.e., rotatory inertia becomes very small).

4.3.2 Exact Vibration Modes

After apply similar eigenanalysis by substituting the sinusoidal response $v(x,t) = v_0(x)\sin(\omega t)$ to the Euler-Bernoulli dynamic model with rotatory inertia, the resulting ordinary differential equation is,

$$EIv_0'''' + \rho S\omega^2 v_0'' - \rho\omega^2 v_0 = 0 \tag{126}$$

The general solution of the above equation is,

$$v_0(x) = A\sin(k_1 x) + B\sinh(k_0 x) + C\cos(k_1 x) + D\cosh(k_0 x) \quad (127)$$

where,

$$k_0 = \sqrt{-\sigma/2 + \sqrt{\sigma^2/4 + \sigma/S}}; \quad k_1 = \sqrt{k_0^2 + \sigma}; \quad \sigma = \frac{\rho S \omega^2}{EI} \quad (128)$$

By substituting the $v(x,t) = v_0 \sin(t)$ into the boundary conditions, the followings are obtained,

$$v_0(0) = 0; \quad v_0'(0) = \theta_0; \quad v_0''(L) = 0; \quad v_0'''(L) = -\sigma v_0'(L) \quad (129)$$

Solve the above equations, the vibration modes of the Euler-Bernoulli dynamic model with rotatory inertia can be given as,

Vibration Modes of E-B Dynamic Model with RI

$$\psi_n(x) = A_n\sin(k_1 x) + B_n\sinh(k_0 x) + C_n\cos(k_1 x) + D_n\cosh(k_0 x) \quad (130)$$

where the C_n is chosen as the arbitrary constant and subscript n corresponds to the nth mode order. And,

$$A_n = \frac{R_A}{\Re} C_n; \quad B_n = \frac{R_B}{\Re} C_n; \quad D_n = -C_n;$$

$$\begin{aligned} R_A &= k_1^3\cosh(k_0 L)\cos(k_1 L) + k_0^3\sinh(k_0 L)\sin(k_1 L) + k_0^2 k_1 \\ R_B &= k_0^3\cos(k_1 L)\cosh(k_0 L) - k_1^3\sin(k_1 L)\sinh(k_0 L) + k_1^2 k_0 \\ \Re &= -k_1^3\sin(k_1 L)\cosh(k_0 L) + k_0^3\sinh(k_0 L)\cos(k_1 L) \end{aligned}$$

$$k_0 = \sqrt{-\sigma/2 + \sqrt{\sigma^2/4 + \sigma/S}}; \quad k_1 = \sqrt{k_0^2 + \sigma}; \quad \sigma = \frac{\rho S \omega_n^2}{EI}$$

When the $S \rightarrow 0$, the above vibration modes reduce to the no rotatory inertia exactly. Beside the flexible modes, there is the rigid vibration mode which corresponds to resonant frequency $\omega_0 = 0$ represents the motion of the rigid body. The rigid vibration mode can be expressed as a linear function, which is the same as the no rotatory inertia case.

$$\psi_0(x) = cx \tag{131}$$

where, the c is constant,

4.4 Modal Frequency Equation and Vibration Modes of Timoshenko Dynamic Model

The derivations of the frequency equation and vibration modes of the Timoshenko dynamic model become more complicated due to the decoupled form. The decoupled variable $\phi(x,t)$ is used instead of the $v(x,t)$ in the motion equation, so the decoupled variable $\phi(x,t)$ need to be solved first before the expression of $v(x,t)$ can be obtained.

4.4.1 Modal Frequency Equation

The motion equations of the Timoshenko dynamic model in frequency domain can be derivated by applying Laplace transformation to governing motion equations of the Timoshenko dynamic model and the corresponding boundary conditions with homogeneous initial conditions.

$$EI\Phi'''' - \rho s^2 S(1+\mu)\Phi'' + \rho s^2 \Phi + \mu \frac{\rho^2 S}{EA} s^4 \Phi = 0 \tag{132}$$

$$\Lambda = \Phi'' - \rho\mu s^2 S\Phi/EI, \qquad V = \Phi' \tag{133}$$

$$T - s^2 I_H \Theta + EI\Lambda' \Big|_{x=0} = 0 \tag{134}$$

with boundary conditions:

$$\Lambda(0,s) = \Theta(s), \quad V(0,s) = 0; \qquad \Lambda'(L,s) = 0, \quad V'(L,s) = \Lambda(L,s) \tag{135}$$

After tedious algebraic manipulation, transfer functions are found to be,

$$H_{\theta\tau}(s) = \frac{1}{s^2 I_H + EIK_3(m)}, \quad K_3(m) = m_1 m_2 (m_1^2 + m_2^2) C_3 \tag{136}$$

and

$$\Psi(x,s) = H_{\psi\theta}(x,s)\Theta(s) = H_{\psi\tau}(x,s)T(s), \tag{137}$$

$$\Lambda(x,s) = H_{\alpha\theta}(x,s)\Theta(s) = H_{\alpha\tau}(x,s)T(s) \tag{138}$$

where

$$\begin{aligned} H_{\alpha\theta}(x,s) &= \cosh(m_1 x) + C_2(m_2^2 - \mu S m^4)[\cosh(m_1 x) - \cos(m_2 x)] \\ &\quad + C_3[m_2(m_1^2 + \mu S m^4)\sinh(m_1 x) + m_1(m_2^2 - \mu S m^4)\sin(m_2 x)] \\ H_{v\theta}(x,s) &= C_1 m_1 \sinh(m_1 x) - C_2 m_2 \sin(m_2 x) - m_1 m_2 C_3[\cosh(m_1 x) - \cos(m_2 x)] \end{aligned}$$

$$H_{\psi\theta}(x,s) = H_{\alpha\theta}(x,s) - 1; \quad H_{\alpha\tau}(x,s) = H_{\alpha\theta}(x,s)H_{\theta\tau}(s); \tag{139}$$

$$H_{\psi\tau}(x,s) = H_{\psi\theta}(x,s)H_{\theta\tau}(s) \tag{140}$$

The format of equation (113) is still held and Coefficients are,

$$\begin{aligned} 2m^6\Sigma_3(m)C_1 &= m_2[(m_2^2 - \mu S m^4)(m_1 - m_2\sinh(m_1 L)\sin(m_2 L)) + \\ &\quad m_1(m_1^2 + \mu S m^4)\cosh(m_1 L)\cos(m_2 L)] \\ 2m^6\Sigma_3(m)C_2 &= -m_1[(m_1^2 + \mu S m^4)(m_2 + m_1\sinh(m_1 L)\sin(m_2 L)] - \\ &\quad m_1 m_2(m_2^2 - \mu S m^4)\cosh(m_1 L)\cos(m_2 L) \\ 2m^6\Sigma_3(m)C_3 &= m_2(m_2^2 - \mu S m^4)\cosh(m_1 L)\sin(m_2 L) - \\ &\quad m_1(m_1^2 + \mu S m^4)\sinh(m_1 L)\cos(m_2 L) \end{aligned}$$

and,

$$m_i = m\beta_i, \quad \beta_i = \left[\frac{\sqrt{4 + S^2(1-\mu^2)m^4} + (-1)^i S(1+\mu)m^2}{2}\right]^{\frac{1}{2}} \tag{141}$$

$$\Sigma_3(m) = \beta_1\beta_2 + \beta_1\beta_2[1 + (1-\mu)^2\frac{m^4S^2}{2}]\cosh(m_1L)\cos(m_2L) \\ -(1+\mu)\frac{m^2S}{2}\sinh(m_1L)\sin(m_2L) \tag{142}$$

The poles of manipulator system, which correspond to the resonant frequency, are determined by the following transendential equation,

Frequency Equation of the Timoshenko Dynamic Model

$$m^4\frac{I_H}{\rho} - K_3(m) = 0 \tag{143}$$

The countable infinite number of the solutions of the above equation correspond to the resonant frequencies, which are denoted as ω_n, $n = 1, 2, 3, 4, \cdots$ When μ approaches to zero (i.e., shear effect becomes very small), β_i here will reduce to corresponding β_i in equation (125) and $\beta_1\beta_2$ will become 1. Therefore, K_3 and Σ_3 will reduce to K_2 and Σ_2 respectively.

4.4.2 Exact Vibration Modes

The eigenanalysis of the Timoshenko model turns to be complicated due to the decoupled format of the governing equations. First, let the output $\phi(x,t) = \phi_0(x)\sin(wt)$ corresponding to the input torque $\tau(t) = \tau_0\sin(wt)$. After substitute these expression into the governing equation, the ordinary differential equation is given as,

$$EI\phi''''_0 + \rho S(1+\mu)\omega^2\phi''_0 - (\omega^2\rho - \mu\frac{\rho^2S}{EA}\omega^4)\phi \;=\; 0 \tag{144}$$

The general solution of the above equation is,

$$\phi_0(x) = A\sin(k_1 x) + B\sinh(k_0 x) + C\cos(k_1 x) + D\cosh(k_0 x) \quad (145)$$

where,

$$k_0 = \sqrt{-\sigma/2 + \sqrt{\sigma^2/4 + \sigma_1/(\mu S) - \sigma_1^2/\mu}};$$
$$k_1 = \sqrt{\sigma + k_0^2}; \quad \sigma = \frac{\rho S(1+\mu)\omega^2}{EI}; \quad \sigma_1 = \frac{\rho\mu S\omega^2}{EI} \quad (146)$$

By substituting the $\phi(x,t) = \phi_0(x)\sin(t)$ into the the boundary conditions, the followings are obtained,

$$\phi_0'(0) = 0; \quad \phi_0'' + \sigma_1\phi_0 = \theta_0; \quad \phi_0(L) = 0; \quad \phi_0'''(L) + \sigma_1\phi_0'(L) = 0 \quad (147)$$

Solve the above equation, and the vibration modes of the Timoshenko dynamic model can be given as $v_0 = \phi_0'$,

Vibration Modes of Timoshenko Dynamic Model

$$\psi_n(x) = A_n\sin(k_1 x) + B_n\sinh(k_0 x) + C_n\cos(k_1 x) + D_n\cosh(k_0 x) \quad (148)$$

where the C_n is chosen as the arbitrary constant and the subscript n corresponds to the nth mode order. And,

$$A_n = \frac{R_A}{\Re}C_n; \quad B_n = \frac{R_B}{\Re}C_n; \quad D_n = -C_n$$

$$\begin{aligned} R_A &= (k_0^3 + \sigma_1 k_0)\sin(k_1 L)\sinh(k_0 L) + (k_1^3 - \sigma_1 k_1)\cos(k_1 L)\cosh(k_0 L) \\ &\quad +(k_1 k_0^2 + \sigma_1 k_1) \\ R_B &= (k_0^3 + \sigma_1 k_0)\cos(k_1 L)\cosh(k_0 L) - (k_1^3 - \sigma_1 k_1)\sin(k_1 L)\sinh(k_0 L) \\ &\quad +(k_1^2 k_0 - \sigma_1 k_0) \\ \Re &= -(k_1^3 - \sigma_1 k_1) + (k_0^3 + \sigma_1 k_0)\cos(k_1 L)\sinh(k_0 L)\sin(k_1 L)\cosh(k_0 L) \end{aligned}$$

$$k_0 = \sqrt{-\sigma/2 + \sqrt{\sigma^2/4 + \sigma_1/(\mu S) - \sigma_1^2/\mu}};$$
$$k_1 = \sqrt{\sigma + k_0^2}; \quad \sigma = \frac{\rho S(1+\mu)\omega^2}{EI}; \quad \sigma_1 = \frac{\rho\mu S\omega^2}{EI}$$

As expected, the above vibration modes reduced to that of Euler-Bernoulli model with rotatory inertia exactly when the shear effect is ignored. Beside the flexible modes, there is the rigid vibration mode which corresponds to resonant frequency $\omega_0 = 0$ represents the motion of the rigid body. The rigid vibration mode can be expressed as a linear function, which is the same as the no rotatory inertia case.

$$\psi_0(x) = cx \tag{149}$$

where, the c is constant,

4.5 Modal Frequency Equation and Vibration Modes of Euler-Bernoulli Dynamic Model with Tip Mass

The derivation of the frequency equation and the vibration modes of the Euler-Bernoulli dynamic model with the tip mass is similar with the no tip mass case, the only difference is the boundary conditions.

4.5.1 Modal Frequency Equation

Apply Laplace transformation to governing motion equations of the Euler-Bernoulli dynamic model with the tip mass and the corresponding boundary conditions with homogeneous initial conditions, the following partial differential equations for Laplace transformations can be derivated. epar

$$EIV'''' + \rho s^2 V = 0 \tag{150}$$
$$T - s^2 I_H \Theta + EIV'' \Big|_{x=0} = 0 \tag{151}$$

with boundary conditions,

$$V(0,s) = 0, \quad V'(0,s) = \Theta(s), \tag{152}$$

$$EIV''(L,s) = -J_p s^2 V'(L,s) - M_p a_c s^2 V(L,s), \tag{153}$$

$$EIV'''(x,s) = M_p a_c s^2 V'(L,s) + M_p s^2 V(L,s) \tag{154}$$

Solving equations (150)-(154), the transfer functions are as,

$$\Theta(s) = H_{\theta\tau}(s)T(s), \quad H_{\theta\tau}(s) = \frac{1}{s^2 I_H + EIK_4(m)} \tag{155}$$

and

$$V(x,s) = H_{v\theta}(x,s)\Theta(s) = H_{v\tau}(x,s)T(s), \tag{156}$$

$$W(x,s) = H_{w\theta}(x,s)\Theta(s) = H_{w\tau}(x,s)T(s) \tag{157}$$

where

$$\begin{aligned} H_{v\theta}(x,s) \;=\; & [(1+\delta_1)\sin(mx) + (1-\delta_2)\sinh(mL)\cos m(L-x) + \\ & (1-\delta_3)\sin(mL)\cosh m(L-x) + (1+\delta_1)\sinh(mx) - \\ & (1-\delta_2)\cos(mL)\sinh m(L-x) - (1-\delta_3)\cosh(mL)\sin m(L-x) - \\ & 2\xi_1 \sinh(mL)\sin(L-x) - 2\xi_3 \cosh(mL)\cos(L-x) + \\ & 2\xi_1 \sin(mL)\sinh(L-x) + 2\xi_3 \cos(mL)\cosh(L-x)]/2m\Sigma_4(m) \end{aligned} \tag{158}$$

where,

$$\delta_1 = -\xi_2^2 + \xi_1\xi_3; \quad \delta_2 = -\xi_2^2 + \xi_1\xi_3 + 2\xi_2; \quad \delta_3 = -\xi_2^2 + \xi_1\xi_3 - 2\xi_2; \tag{159}$$

$$\xi_1 = \frac{M_p m}{\rho}; \quad \xi_2 = \frac{M_p a_c m^2}{\rho}; \quad \xi_3 = \frac{J_p m^3}{\rho} \tag{160}$$

and,

$$H_{w\theta}(x,s) = H_{v\theta}(x,s) - x \quad H_{v\tau}(x,s) = H_{v\theta}(x,s)H_{\theta\tau}(s) \tag{161}$$

$$H_{w\tau}(x,s) = H_{w\theta}(x,s)H_{\theta\tau}(s) \tag{162}$$

and,

$$\begin{aligned} K_4(m) &= m\{(\xi_2^2 - \xi_1\xi_3 + 1)[\sinh(mL)\cos(mL) - \cosh(mL)\sin(mL)] \\ &\quad -2\xi_1 \sinh(mL)\sin(mL) - 2\xi_2[\sinh(mL)\cos(mL) \\ &\quad + \cosh(mL)\sin(mL)] - 2\xi_3 \cosh(mL)\cos(mL)\}/\Sigma_4(m) \end{aligned} \tag{163}$$

$$\begin{aligned} \Sigma_4(m) &= [1 + \cos(mL)\cosh(mL)] - \xi_1[\cosh(mL)\sin(mL) - \cos(mL)\sinh(mL)] \\ &\quad -2\xi_2[\sin(mL)\sinh(mL)] - \xi_3[\sinh(mL)\cos(mL) + \sin(mL)\cosh(mL)] \\ &\quad +(\xi_2^2 - \xi_1\xi_3)[\cosh(mL)\cos(mL) - 1] \end{aligned} \tag{164}$$

The poles of manipulator system, which correspond to the resonant frequency, are determined by transendential equation,

Frequency Equation of the E-B Dynamic Model with Tip Mass

$$m^4\frac{I_H}{\rho} - K_4(m) = 0 \tag{165}$$

The countable infinite number of the solutions of the above equation correspond to the resonant frequencies, which are denoted as ω_n, $n = 1, 2, 3, 4, \cdots$ As expected, the (165) reduce exactly to the no tip mass case, when the ξ_1, ξ_2 and ξ_3 approaches zero. (i.e., tip mass becomes very small).

4.5.2 Exact Vibration Modes

Same as the no tip mass case, the four order ordinary differential equation can be resulted by substituting $v(x,t) = v_0(x)\sin(\omega t)$ into the governing equation,

$$EIv_0'''' - \rho\omega^2 v_0 = 0 \tag{166}$$

The general solution of the above equation is,

$$v_0(x) = A\sin(kx) + B\sinh(kx) + C\cos(kx) + D\cosh(kx) \qquad (167)$$

where the k can be obtained through the characteristic function of the ordinary differential equation.

$$k^4 = \frac{\rho\omega^2}{EI} \qquad (168)$$

By substituting the $v_0(x)$ into the boundary conditions, the followings are obtained,

$$v_0(0) = 0; \quad v_0'(0) = \theta_0; \qquad (169)$$

$$EIv_0''(L) = J_p\omega^2 v_0'(L) + M_p a_c v_0(L); \quad EIv_0'''(L) = -M_p a_c v_0'(L) - M_p v_0(L)$$

Solve the above equation and the mode shape functions of the Euler-Bernoulli dynamic model with tip mass can be given as,

Vibration Modes of E-B Dynamic Model with Tip Mass

$$\psi_n(x) = A_n\sin(k_n x) + B_n\sinh(k_n x) + C_n\cos(k_n x) + D_n\cosh(k_n x) \quad (170)$$

where the C_n is chosen as the arbitrary constant and the subscript n corresponds to the nth mode order. And,

$$A_n = \frac{R_A}{\Re}C_n; \quad B_n = \frac{R_B}{\Re}C_n; \quad D_n = -C_n \qquad (171)$$

$$
\begin{aligned}
R_A &= [\sin(k_nL)\sinh(k_nL) + \cos(k_nL)\cosh(k_nL) + 1] + 2\eta_1 \sinh(k_nL)\cos(k_nL) \\
&\quad -2\eta_2[\sin(k_nL)\sinh(k_nL) - \cos(k_nL)\cosh(k_nL)] - 2\eta_3 \cosh(k_nL)\sin(k_nL) \\
&\quad -\eta_1\eta_3[\sinh(k_nL)\sin(k_nL) + \cosh(k_nL)\cos(k_nL) - 1] \\
&\quad -\eta_2^2[1 - \cosh(k_nL)\cos(k_nL) - \sinh(k_nL)\sin(k_nL)]
\end{aligned}
$$

$$
\begin{aligned}
R_B &= [1 - \sin(k_nL)\sinh(k_nL) + \cos(k_nL)\cosh(k_nL)] - 2\eta_1 \cosh(k_nL)\sin(k_nL) \\
&\quad -2\eta_2[\sin(k_nL)\sinh(k_nL) + \cos(k_nL)\cosh(k_nL)] - 2\eta_3 \cos(k_nL)\sinh(k_nL) \\
&\quad -\eta_1\eta_3[\cos(k_nL)\cosh(k_nL) - \sin(k_nL)\sinh(k_nL) - 1] \\
&\quad -\eta_2^2[\sin(k_nL)\sinh(k_nL) - \cos(k_nL)\cosh(k_nL) + 1]
\end{aligned}
$$

$$
\begin{aligned}
\Re &= [1 + \eta_2^2 - \eta_1\eta_3][-\sin(k_nL)\cosh(k_nL) + \sinh(k_nL)\cos(k_nL)] \\
&\quad -2\eta_1 \sin(k_nL)\sinh(k_nL) - 2\eta_3 \cos(k_nL)\cosh(k_nL) \\
&\quad -2\eta_2[\sin(k_nL)\cosh(k_nL) + \sinh(k_nL)\cos(k_nL)]
\end{aligned}
$$

$$
k_n^4 = \frac{\rho\omega_n^2}{EI}; \quad \eta_1 = \frac{M_p k}{\rho}; \quad \eta_2 = \frac{M_p a_c k^2}{\rho}; \quad \eta_3 = \frac{J_p k^3}{\rho}.
$$

It is easy to show the above vibration modes can be reduced to the no tip case exactly, when the η_1, η_2 and η_3 approach zero. Beside the flexible modes, the rigid vibration mode which corresponds to resonant frequency $\omega_0 = 0$ represents the motion of the rigid body. For the rigid body mode ($k_0 = 0$), the vibration mode can be expressed as a linear function,

$$
\psi_0(x) = cx \tag{172}
$$

where, the c is constant,

In contrast to the assumed vibration mode approach, there is *no* approximation in above exact modes derivation. The fewer number of the exact modes order can provides the more accuracy. This provides the effectiveness that the effective control of the modal amplitude function will insure the satisfied control of the flexible manipulator. These results will be utilized in Chapter. 5 for derivations of the exact dynamic solutions of Euler-Bernoulli model for step torque input.

4.6 Asymptotic Behaviors of Modal Frequencies and Vibration Modes

Since modal frequency equations and the vibration modes are transendential equation, they specify an infinite number (but countable) of natural modal frequencies and vibration modes for one-link flexible manipulator. Therefore it is very interesting to know analytically the properties of high order (or large) modal frequencies and the corresponding vibration modes. This is even more important for the purpose of numerical analysis, because as the order of vibration modes increases, the computation of exponential functions involved in the characteristic equations and expressions of vibration modes becomes extremely difficult, almost impossible to accomplish with a reasonable accuracy. In this section, the results of the asymptotic behaviors for high order vibrations of one-link flexible manipulators are presented.

A) Euler-Bernoulli Dynamic Model

The asymptotic expression for high order frequencies can be obtained by inspecting the characteristic equation (113). As m approaches to infinite, $K_1(m)$ approaches to $m\frac{\cos(mL)-\sin(mL)}{\cos(mL)}$. Therefore, in order to satisfy the characteristic equation, for large m, it must have,

$$\cos(mL) \longrightarrow 0$$

which leads to the following asymptotic expression for large modal frequencies,

$$\omega_n^1 = \left[\frac{(2n-1)\pi}{2L}\right]^2 \sqrt{\frac{EI}{\rho}} \qquad n \gg 1 \tag{173}$$

For the corresponding high order vibration modes, after the similar procedures, one can find the following simple asymptotic expression,

$$\psi_n^1(x) = -\sin(k_n x) + \cos(k_n x) \qquad 0 < x < L; \qquad k_n^4 = \frac{\rho\omega_n^2}{EI} \tag{174}$$

Note that the asymptotic expressions for high order vibration modes is not valid at the two ends of the manipulators, where the boundary conditions should be used.

B) Euler-Bernoulli Dynamic Model with Rotatory Inertia

Applying the same technique to the characteristic equation in this case, as m becomes larger, the following must be true,

$$\cos(m^2\sqrt{S}L) \longrightarrow 0$$

therefore, the asymptotic expression for high order frequencies becomes,

$$\omega_n^2 = \frac{(2n-1)\pi}{2L\sqrt{S}} \sqrt{\frac{EI}{\rho}} \qquad n \gg 1 \tag{175}$$

Similarly, for high order vibration modes,

$$\psi_n^2(x) = -\frac{k_2^3}{k_1^3}\sin(k_2 x) - \cos(k_2 x) \qquad 0 < x < L$$

$$k_1 = \sqrt{-\frac{\sigma}{2} + \sqrt{\frac{\sigma^2}{4} + \frac{\sigma}{S}}}; \quad k_2 = \sqrt{k_1^2 + \sigma}; \qquad \sigma = \frac{\rho S\omega_n^2}{EI} \tag{176}$$

C) Timoshenko Dynamic Model

For the Timoshenko dynamic model, the asymptotic expressions for high order modal frequencies and vibration modes can be obtained as,

$$\omega_n^3 = \frac{(2n-1)\pi}{2L\sqrt{S\mu}} \sqrt{\frac{EI}{\rho}} \qquad n \gg 1 \tag{177}$$

$$\psi_n^3(x) = -\frac{k_1^3 + \sigma_1 k_1}{k_2^3 - \sigma_1 k_2}\sin(k_2 x) - \cos(k_2 x) \qquad 0 < x < L$$

$$k_1 = \sqrt{-\frac{\sigma}{2} + \sqrt{\frac{\sigma^2}{4} + \frac{\sigma_1}{\mu S} - \frac{\sigma_1^2}{\mu}}}; \qquad k_2 = \sqrt{\sigma + k_1^2};$$

$$\sigma = \frac{\rho S(1+\mu)\omega_n^2}{EI}; \qquad \sigma_1 = \frac{\rho\mu S\omega_n^2}{EI} \tag{178}$$

ω_n^3 and ω_n^2 have the same magitude, and have a constant ratio $\frac{1}{\sqrt{\mu}}$.

D) Euler-Bernoulli Dynamic Model with Tip Load

In this case, the the asymptotic expression for high order frequencies becomes more involved. After some manipulations, it is shown that,

$$\omega_n^4 = \left[\frac{\arctan(\frac{1+\xi_1-\xi_3+\xi_2^2-\xi_1\xi_3}{\xi_1+2\xi_2+\xi_3})}{L} + \frac{(n-1)\pi}{L}\right]^2 \sqrt{\frac{EI}{\rho}} \qquad n \gg 1 \tag{179}$$

And, the corresponding vibration modes,

$$\psi_n^4(x) = -\sin(k_n x) + \cos(k_n x) \qquad 0 < x < L \tag{180}$$

which is the same as the high order vibration modes in model A. Therefore, tip load has no effect on the high order vibration modes, but it does affect the corresponding frequencies.

All these asymptotic expressions have been verified numerically and are utilized for high mode order in the simulation study conducted in Chapter 7. In most of cases, they give very accurate result for $n > 8$.

4.7 Experimental Results and Numerical Analysis

In the previous sections, the frequency equations and vibration modes of the four models are derivated. The influence of rotatory inertia, shear deformation and tip mass on the vibrational behaviors of the flexible manipulators are presented in the closed form. In this section, the four models are verified by the experimental

results and the numerical analysis and the influences of rotatory inertia, shear deformation, hub inertia and tip mass are presented.

4.7.1 Experimental Results and Modeling Verifications

The calculations of modal frequency and exact vibration modes are based on the physical model at the *NASA Center for Intelligent Robotic System for Space Exploration* (CIRSSE) at the Rensselaer Polytechnic Institute. The experimental results of the frequence for the no-tip case are also provided by the above center. The parameters of the one-link flexible manipulator are measured as the following,

	Variable Definition	*Variable Value*	
L	beam length	1.098	m
B	beam width	1.5875e-3	m
H	beam height	0.103	m
E	material Young's modulus	68950.0e6	N/m^2
γ	beam material density	2.713e3	$Kg/(m^3)$
I_H	hub inertia	0.007	$Kg.m^2$
ν	beam Poisson ratio	0.3	–
A	beam transverse area	1.6351e-4	m^2
I	beam transverse inertia	3.430e-11	$Kg.m^2$
ρ	beam mass unit length	0.4436	Kg/m
$Eadj$	E adjustment factor	0.88	–
$Iadj$	I adjustment factor	1.0	–
$Ihadj$	I_H adjustment factor	2.5	–
k	shape factor k	0.8497	–
S	$S = I/A$	2.1001e-7	m^2
μ	$\mu = E/kG$	3.06	–
λ_1 †	tip weight factor	0.150	%
λ_2 †	tip length factor	0.150	%
λ_3 †	tip inertia factor	0.150	%

†: This tip parameter is not from the experimental measures, just for the calculation of tip mass case.

Table 1 : Parameters of the CIRSSE One-Link Flexible Manipulator

The tip parameter λ_1, λ_2 and λ_3 are the percentages of beam weight, length and inertia, respectively. And they are defined as,

$$\lambda_1 = \frac{M_p}{\rho L}, \quad \lambda_2 = \frac{a_c}{L}, \quad \lambda_3 = \frac{J_p}{I} \tag{181}$$

The modal frequencies of the four models are calculated by the numerical methods with the *MATLAB*. The calculations for the 3-D graphic plotting were conducted on the *Convex/c240*. The first fifteen resonant frequences of the flexible manipulator are listed in the Table 2.

Mode	*No Tip Mass Case*				*Tip Mass Case*
Order	*EBDM*[a] *(Hz)*	*EBDMRI*[b] *(Hz)*	*TDM*[c] *(Hz)*	*Expe*[d] *(Hz)*	*EBDMTM*[e] *(Hz)*
0	0	0	0	0	0
1	2.9692	2.9692	2.9692	2.850	2.4470
2	7.2608	7.2608	7.2608	7.200	5.8448
3	17.977	17.977	17.977	18.42	14.716
4	34.752	34.751	34.751	35.65	30.807
5	57.277	57.276	57.273	58.70	53.572
6	85.482	85.480	85.472	88.00	82.266
7	119.35	119.34	119.33	126.3	116.58
8	158.87	158.86	158.84	166.6	156.47
9	204.04	204.03	203.98	214.4	201.94
10	254.86	254.84	254.77	N/A	252.99
11	311.33	311.30	311.20	N/A	309.64
12	373.45	373.41	373.27	N/A	371.92
13	441.22	441.16	440.97	N/A	439.82
14	514.63	514.55	514.29	N/A	513.34
15	593.69	593.58	593.24	N/A	592.50

[a]Euler-Bernoulli Dynamic Model
[b]Euler-Bernoulli Dynamic Model with Rotatory Inertia
[c]Timoshenko Dynamic Model
[d]Experimental Results of CIRSSE Model
[e]Euler-Bernoulli Dynamic Model with Tip Mass

Table 2 : Modal Frequency of CIRSSE Model

The above table shows that the experimental results agree with analytic prediction within ±5% for the no tip mass case. The declines of the frequency are very small when the rotatory inertia and shear deformation are taken into account. The reason is that the beam width has been designed very small against the height to decrease theses influences of the rotatory inertia and shear deformations for the experimental purposes. Although this decline is small, it is excepted that the shear deformation has more contribution due to its including the influence of the rotatory inertia. It is very reasonable that the modal frequency declines when the tip mass is added. The influences of the tip mass on the low order are more obvious than on the high order.

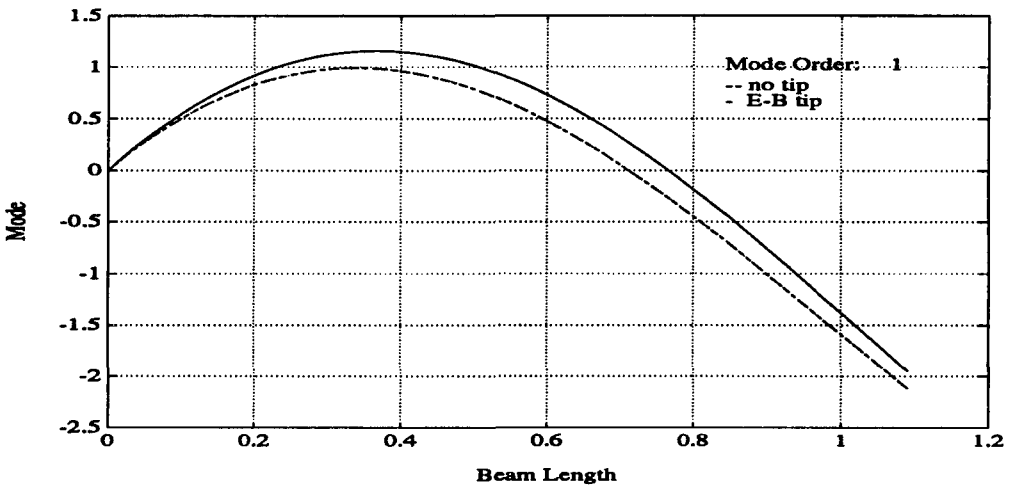

Figure 3: First Order Vibration Mode

The selected mode orders of the vibration modes of the four models are presented in the Fig. 3 - 5. Because of the limited differences between the vibration modes of the first three dynamic models, they are plotted identically as the no tip case in the figures. For this specific flexible manipulator, the influences of the

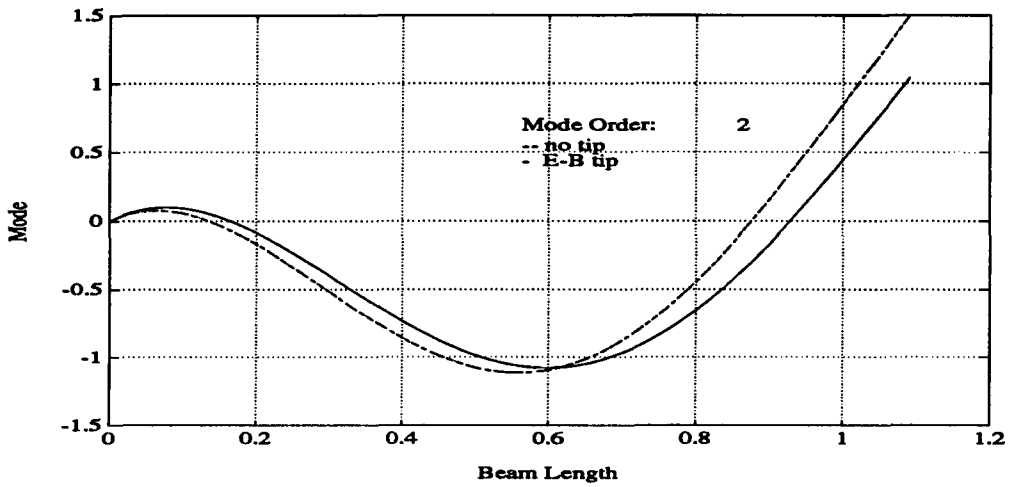

Figure 4: Second Order Vibration Mode

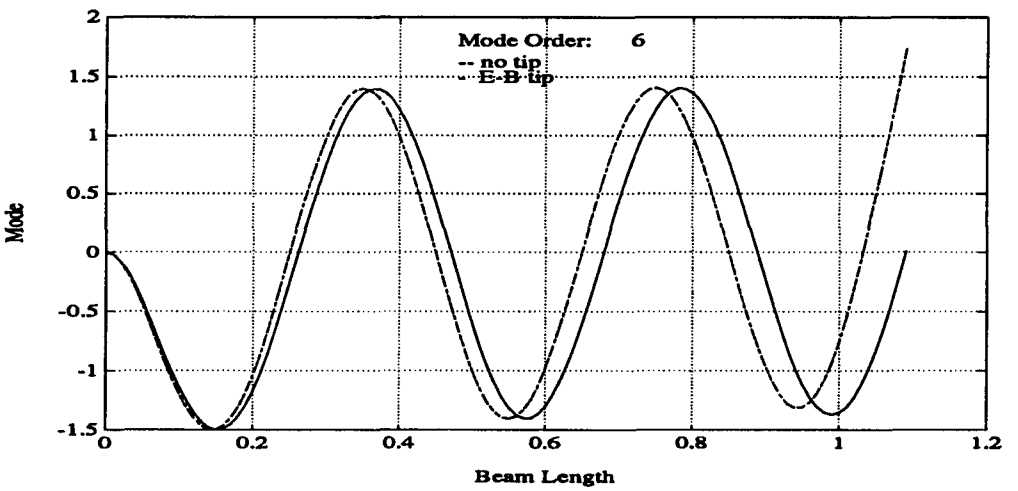

Figure 5: Sixth Order Vibration Mode

rotatory inertia and shear deformation on the vibration modes can be negligible. The influences of the tip mass on the vibration modes are more obvious for the low order than the high order. Also, the similar results are presented for the modal frequency in section 4.7.5.

The above numerical results and the analysis of the resonant frequency and vibration modes have verified the accuracy of the four models.

4.7.2 Influence of Rotatory Inertia

The influence of the rotatory inertia introduces two terms into the PDE equations, one in the governing equation, while the other in the tip end boundary condition. The measure of this influence can be given as the S, in fact, it is the $B^2/12$. Actually, it reflects the ratio of the beam heigh H to the beam width B. Figure 6-8 show influence of rotatory inertia on the first, second and sixth order modal frequency with Poisson ratio $\nu = 0.3$, as $\frac{B}{H}$ from zero to one. Here, the calculations are conducted by fixing the beam height and increasing the beam width by times.

Generally, the resonant frequency decreases when the rotatory inertia is taken into account, but the amount of the decrease is within 10%. As shown in the figures, the influence of the rotatory inertia on the frequency of flexible manipulator increases with the beam width height ratio and the mode order. And the results also indicate that for the lower vibration order modes, the effect of rotatory inertia is not very significant and generally can be ignored. For high order vibration modes, however, as will be indicated later in the following subsection, the shear effect is indeed significant.

4.7.3 Influence of Shear Deformation

When the shear deformation is taken into account, it already includes the influence of the rotatory inertia. The measure of the influence of the shear defor-

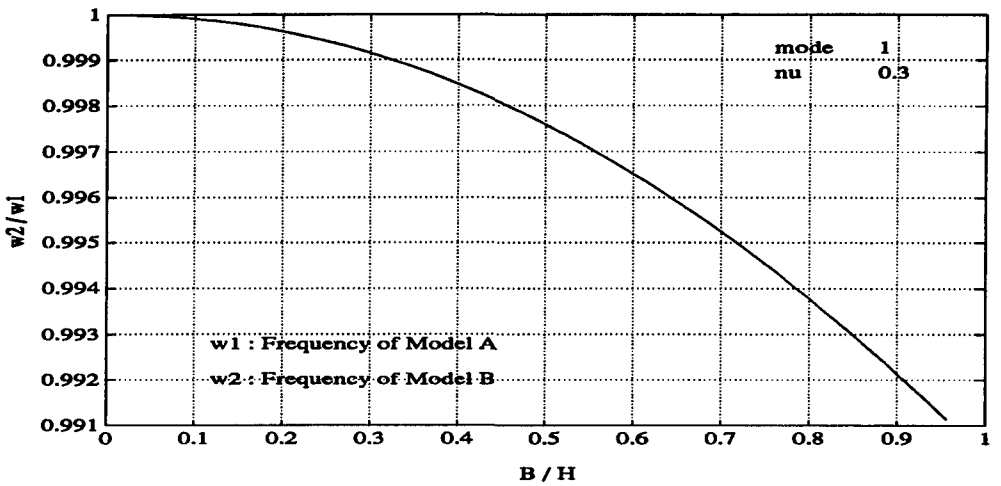

Figure 6: Influence of Rotatory Inertia: First Order

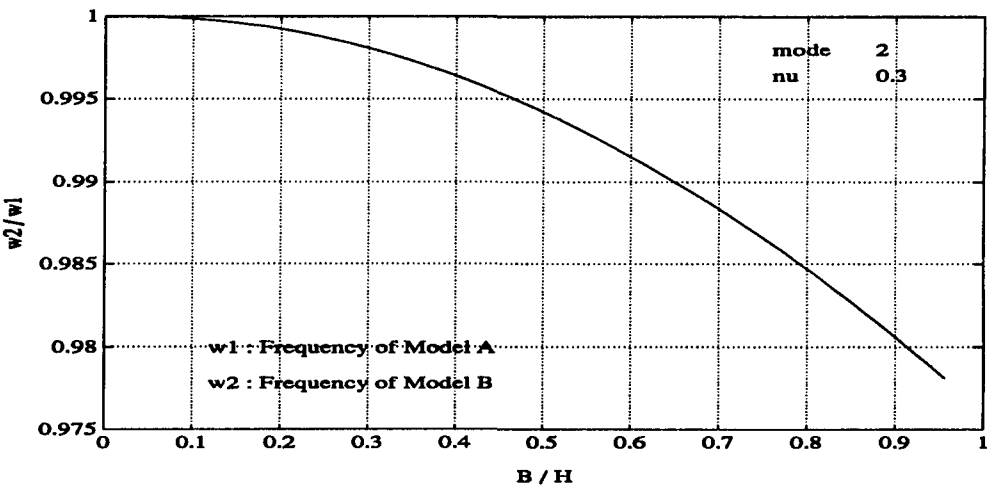

Figure 7: Influence of Rotatory Inertia: Second Order

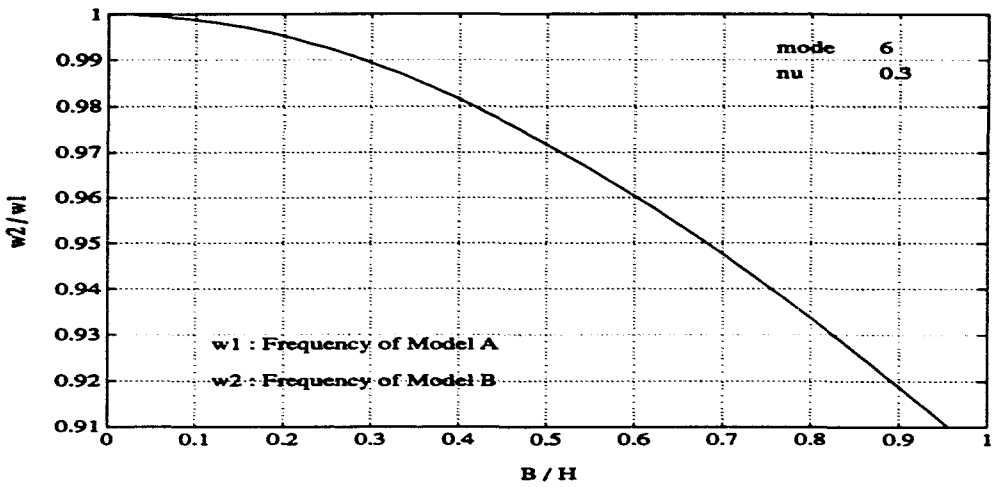

Figure 8: Influence of Rotatory Inertia: Sixth Order

mation are material Poisson ratio ν and S. Figure 9-11 show the influence of shear deformation on the first, second and sixth order modal frequencies with Poisson ratio $\nu = 0.3$, as $\frac{B}{H}$ increases from zero to one.

Similar to the case of totatory inertia, the results show that frequencies calculated become smaller when shear deformation is included. For the six order frequency, the difference is already more than $\pm 26\%$, therefore the effect of shear deformation generally can not be ignored. The results also demonstrate that the effect of shear deformation is much more significant than that of rotatory inertia, a conclusion which should be expected since rotatory inertia has already been considered in shear deformation.

Fig. 12 illustrates different modal frequencies calculated from Euler-Bernoulli, Euler-Bernoulli with rotatory inertia, and Timoshenko models respectively, in terms of $\frac{4\omega L}{(n+1)\pi}\sqrt{\frac{\rho}{EI}}$ versus $\frac{n+1}{2L}$. It indicates clearly the effect of rotatory

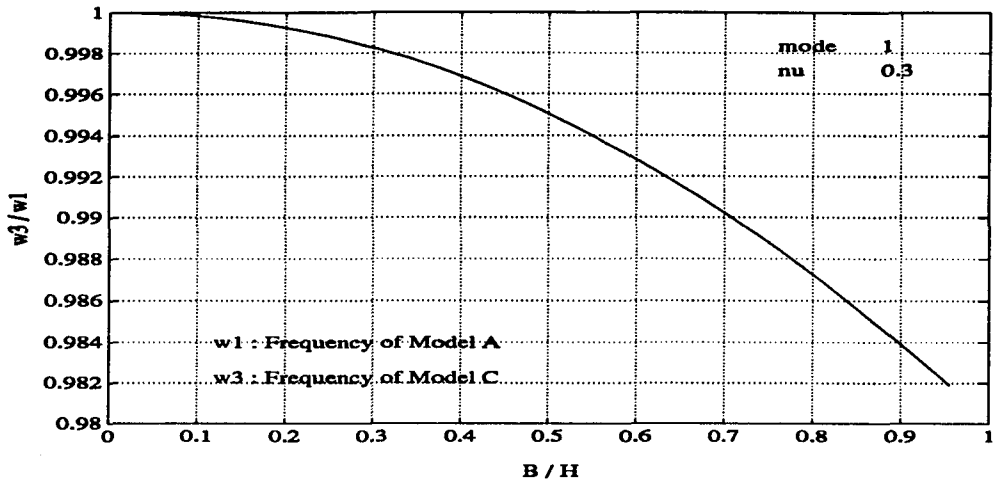

Figure 9: Influence of Shear Deformation: First Order

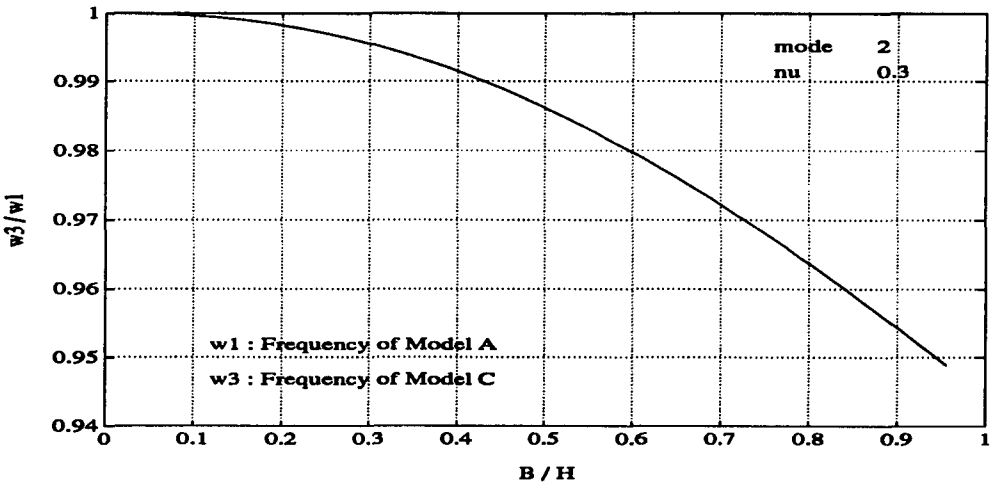

Figure 10: Influence of Shear Deformation: Second Order

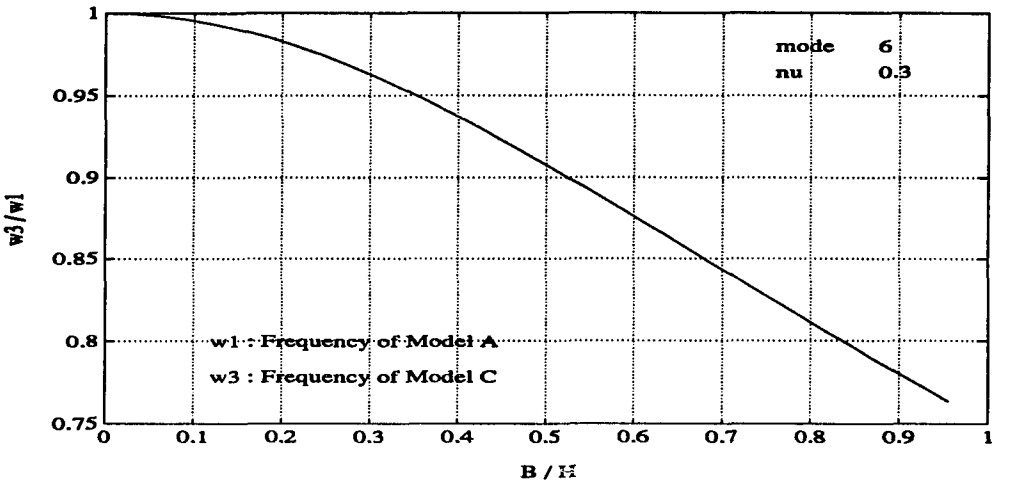

Figure 11: Influence of Shear Deformation: Sixth Order

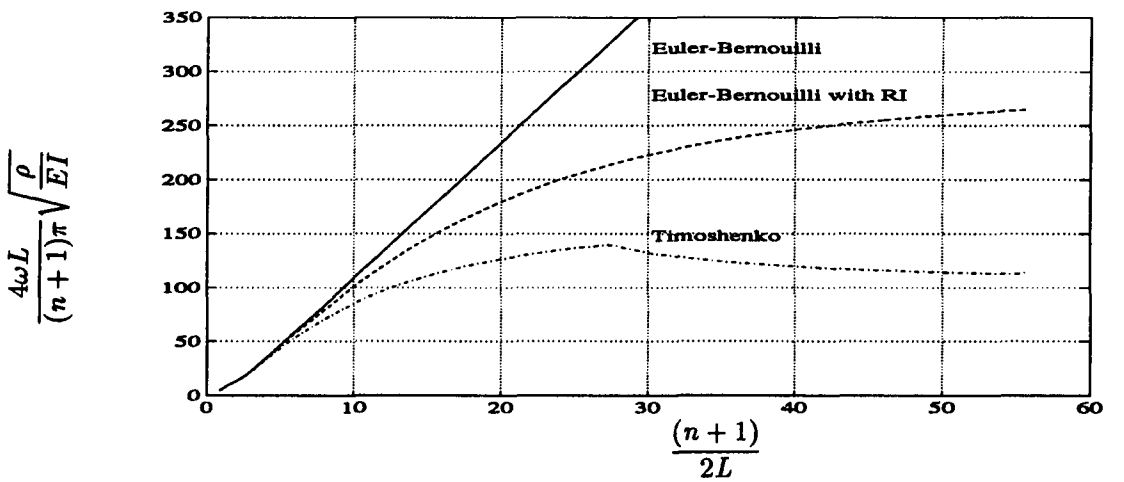

Figure 12: Influence of Rotatory Inertia and Shear Deformation

inertia and shear deformation is profound for high order vibration modes. This figure is very similar to the classical results obtained in theory of elasticity on the influence of rotatory inertia and shear deformation on vibrations of beams and plates [Davi 48].

4.7.4 Influence of Hub Inertia

In the established models, the hub (includes the motor) is treated as the part of the flexible manipulator. Obviously, its inertia has the influence on the vibration behavior of the flexible manipulator. Usually, the hub inertia is huge comparing with the flexible beam inertia to insure the stability and to minimize the deformation of the hub for the accuracy purpose. Figure 13-15 show the influence of the hub inertia on the first, second and sixth order mode frequency.

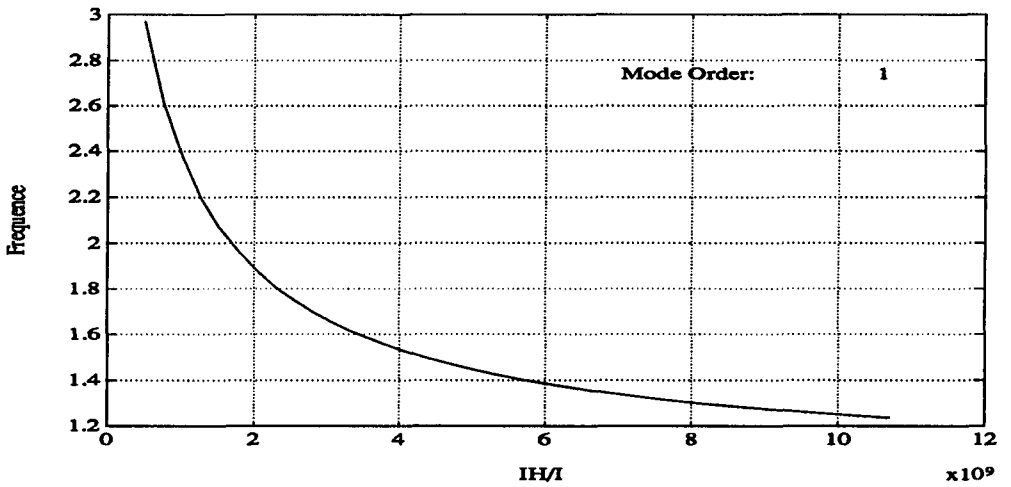

Figure 13: Influence of Hub Inertia : First Order

As showed in the figures, the hub inertia only have the obvious influence

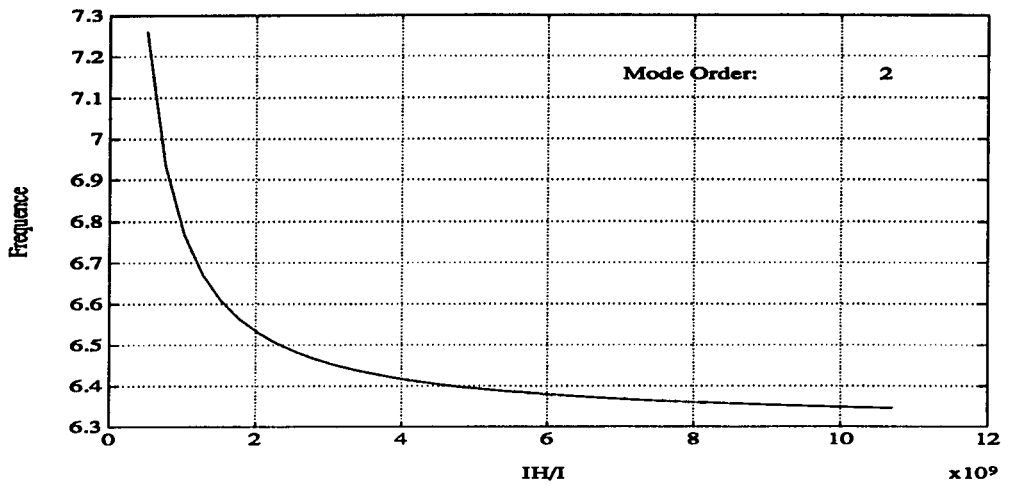

Figure 14: Influence of Hub Inertia : Second Order

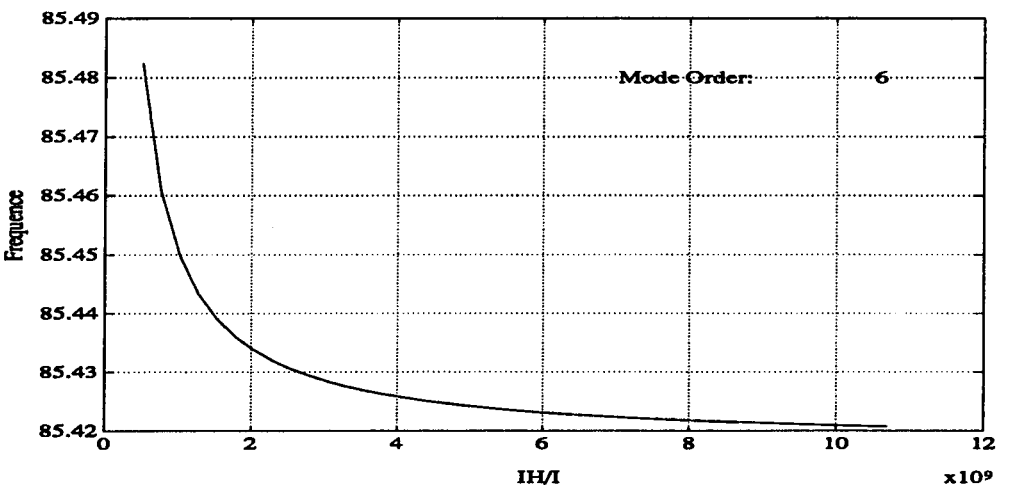

Figure 15: Influence of Hub Inertia : Sixth Order

on the lower order frequency. For the sixth order frequency, the change of the frequency are very small along the range of I_H/I. And influence of hub inertia decreases with the ratio I_H/I, the dramatic decreases are expected for the first order when the I_H/I under $4.0e+9$.

4.7.5 Influence of Tip Mass

The most impressing influence resource on the vibration behavior is the tip mass. The tip mass will drive the resonant frequency down as it is showed in the Table 2.. But all these three the tip mass factors, λ_1, λ_2 and λ_3, have the different weight on the vibration behavior of the manipulator. The different weights among these three tip mass factor are the major knowledge for the identification of the model and the choice of the control patterns when the tip mass is subjected to change during the robot operations. Figure 16-25 show the influences of these three tip mass factors on the first, second and sixth order modal frequencies.

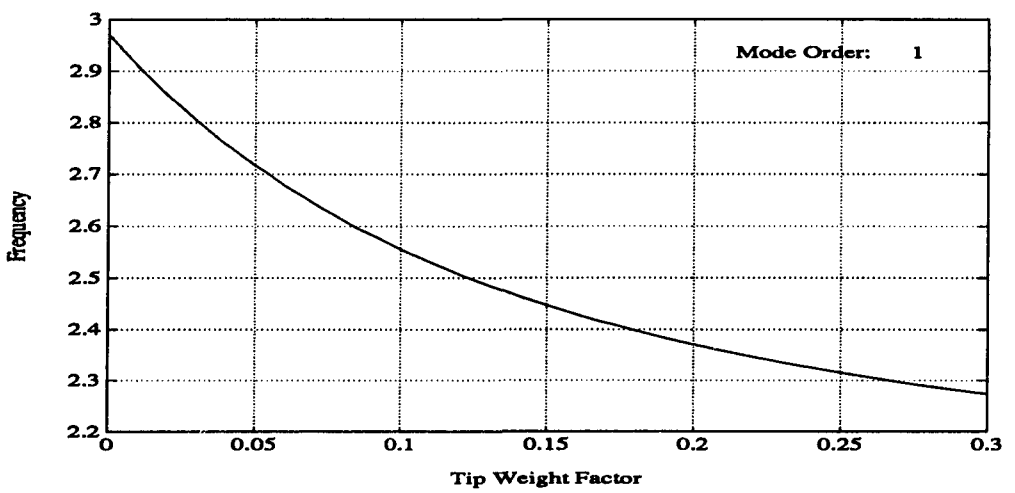

Figure 16: Influence of Tip Mass: First Order

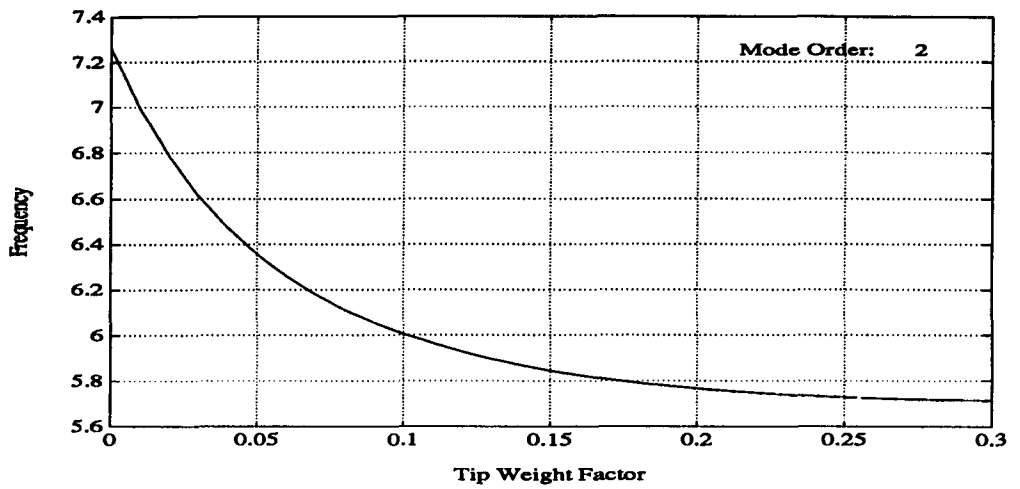

Figure 17: Influence of Tip Mass: Second Order

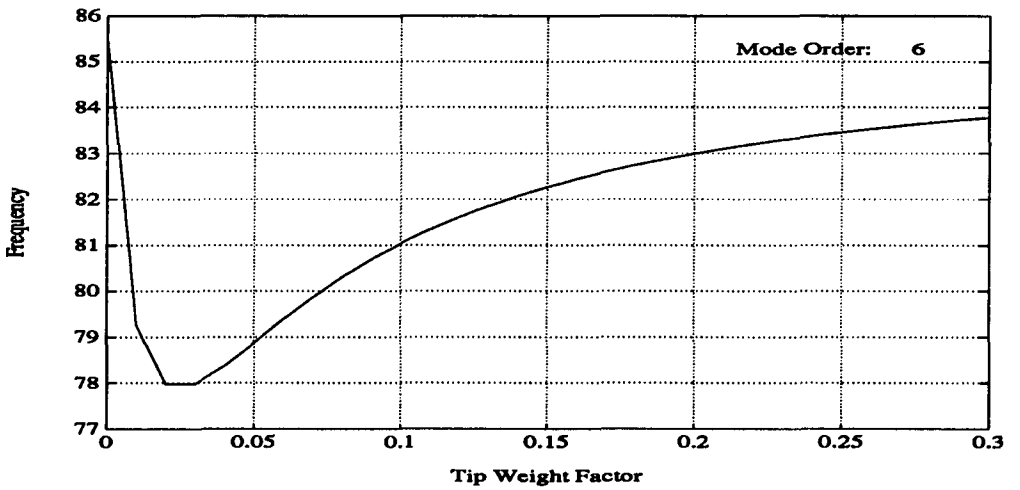

Figure 18: Influence of Tip Mass: Sixth Order

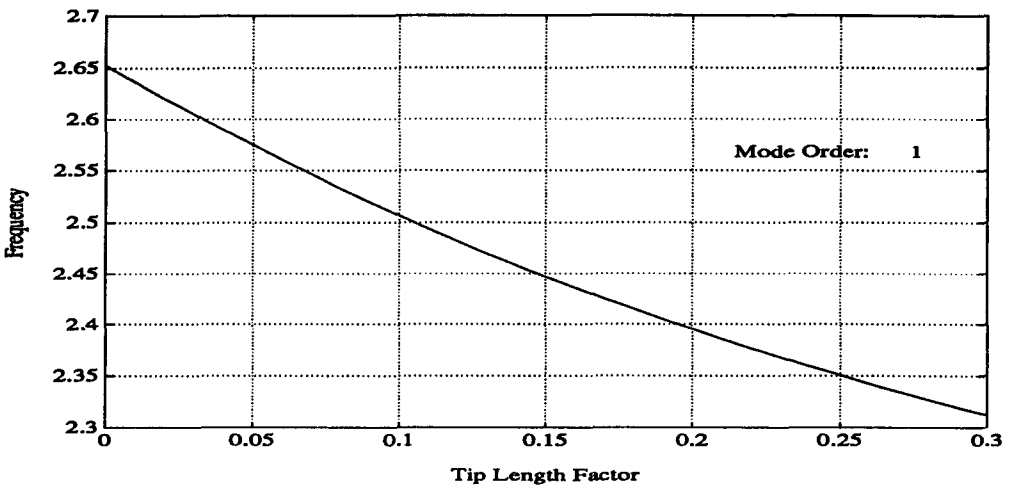

Figure 19: Influence of Tip Length: First Order

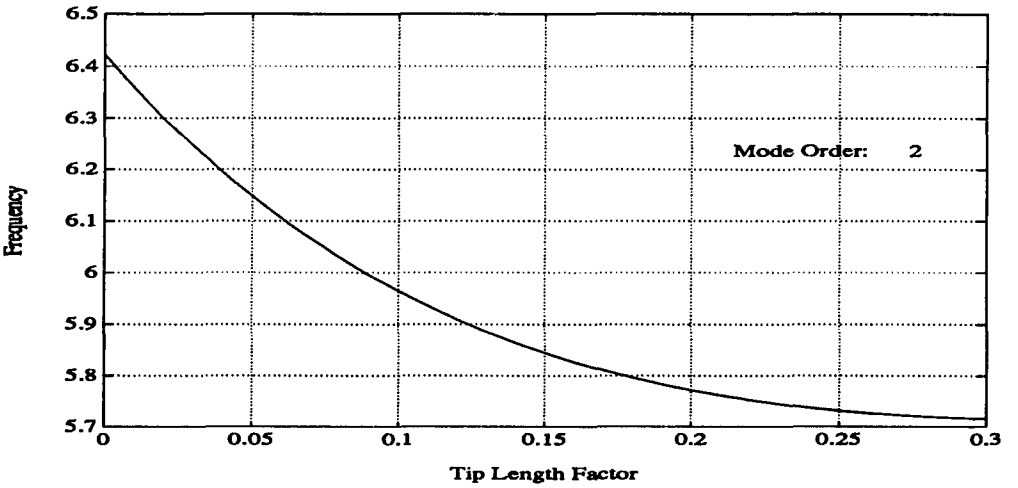

Figure 20: Influence of Tip Length: Second Order

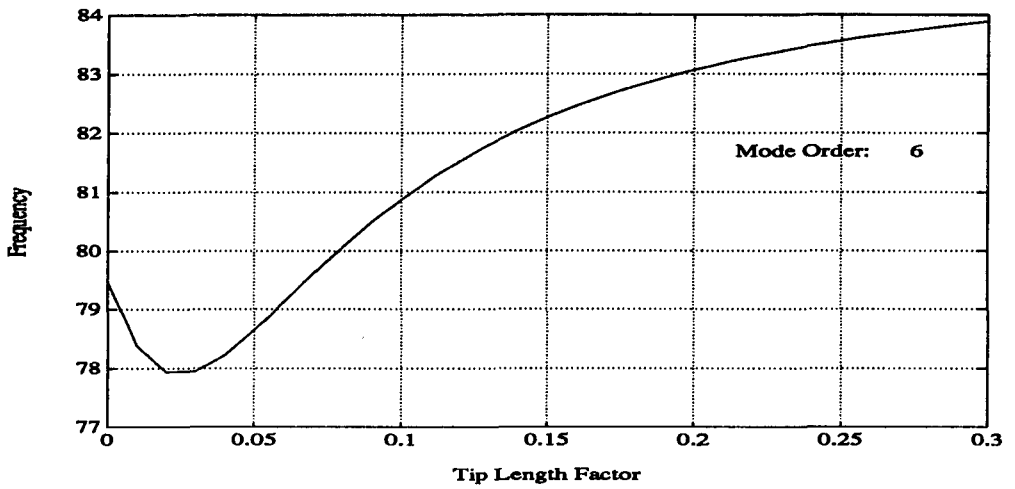

Figure 21: Influence of Tip Length: Sixth Order

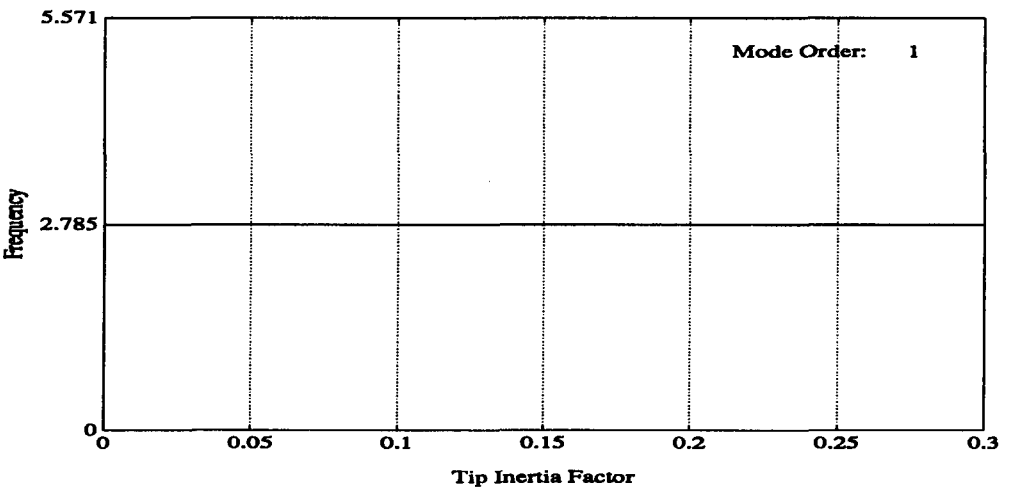

Figure 22: Influence of Tip Inertia: First Order

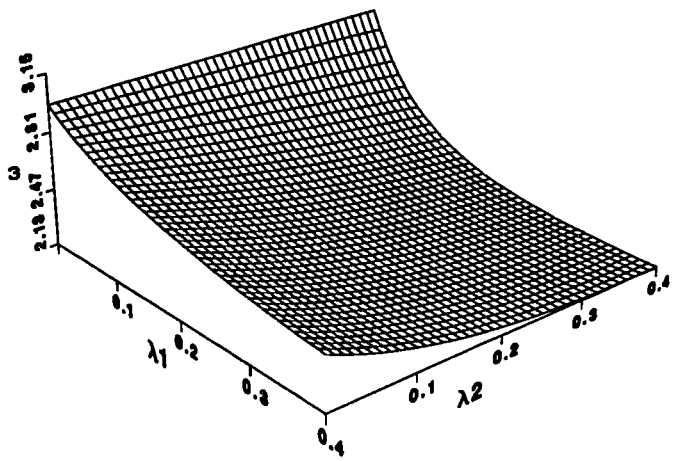

Figure 23: First Order Frequency .vs. λ_1 and λ_2

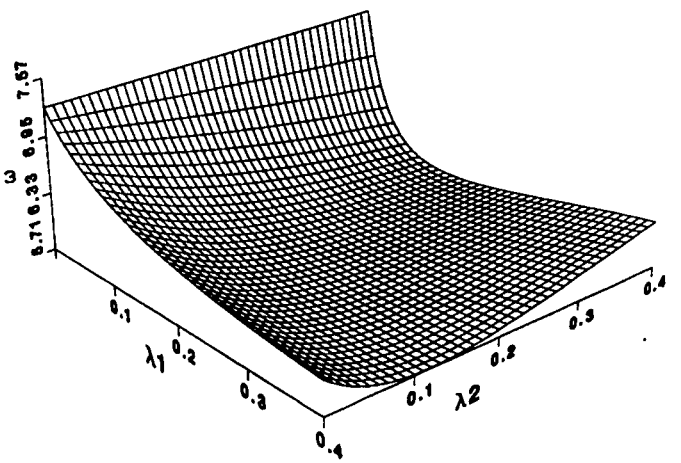

Figure 24: Second Order Frequency .vs. λ_1 and λ_2

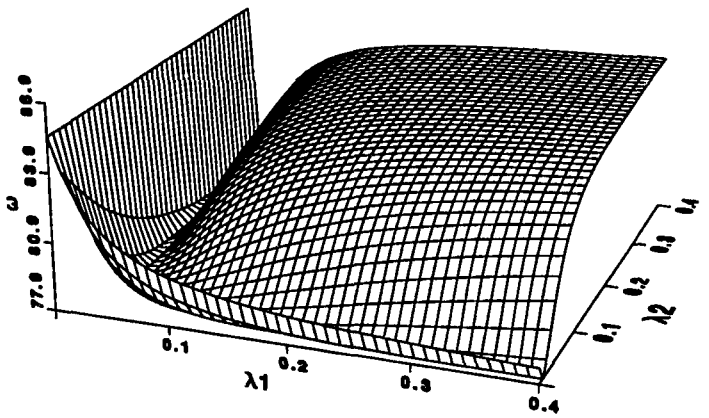

Figure 25: Sixth Order Frequency .vs. λ_1 and λ_2

In these figures, all parameters except the varying one take the values specified in Table 1. The results indicate that the mass of tip load is the most significant factor for the effect of tip load on vibration. For example, it drives the first order frequency down by 10% when the mass of tip load is 5% of the beam mass, and down by 25% when it is 30%. Therefore, when a load with large mass is grasped by a flexible manipulator, the dynamics of the manipulator will be changed dramatically. If the controller of the manipulator can not predicate this change in dynamics, its performance would degenerate. This observation is important since, in civil construction and space applications, a flexible manipulator is usually expected to deal with loads of relatively large mass comparing to its own one. The length of tip load affects the modal frequencies in a similar fashion but the variation of frequencies is generally more gentle than that induced by the change of tip mass. To our surprise, the inertia moment of tip load is the least significant factor of the three, and has almost no influence on the lower order vibration modes (see Fig. 22).

The most surprising result is the influence of tip mass and length on the

higher order vibration modes (see Fig. 18, 21, and 25). First of all, for vibration modes with order higher than six, their frequencies vary dramatically with the change of tip mass and length. The unexpected result, however, is that when the tip mass or length passing over certain values (e.g., for the six order vibration mode, $\lambda_1 > 0.02$ or $\lambda_2 > 0.02$), modal frequencies increase with the tip mass or length, instead of decreasing as it is expected intuitively. A careful inspection into the numerical results indicates that this phenomenon is caused by the increased distance between modal frequencies of two vibration modes. In other words, the distribution of modal frequencies has been changed when the tip mass or length becomes large. More specifically, within a given frequency range, one can find more vibration modes for very small tip mass or length, but fewer for large tip mass or length.

4.8 Summary

The derivations and numerical analysis of the modal frequency and vibration modes have verified the established four dynamic models for the one-link flexible manipulators. The numerical results indicate that the influence of rotatory inertia and shear deformation on the vibration behaviors of the flexible manipulators are focused on the high mode order, however, the tip mass weight more influence on the lower mode order. The hub inertia also rise the dramatic influence at low order, especially the first order. Additionally, the numerical results provide the valuable knowledge for the identification of the flexible robot systems.

The next Chapter will present the derivations of the exact dynamic solutions of the Euler-Bernoulli model for step torque input, which lead to the design of the dynamics simulator for the one-link flexible manipulators.

Chapter 5 Exact Dynamic Solutions of Euler-Bernoulli Model for Step Torque Input

5.1 Introduction

The research of the flexible manipulators has been restrained to utilize the assumed modes and finite element methods due to the lack of the physical insights of the flexible manipulators. In the previous chapters, the derivations and the numerical analysis demonstrate that the rich knowledge of the one-link flexible manipulators have been gained. With the exact modal frequency function and vibration modes, the derivations of the exact dynamic solutions of the Euler-Bernoulli model for step torque input become feasible. These exact solutions consummate our knowledge about the one-link flexible manipulators, and the direct applications presented in this thesis ia the design of the dynamics simulator. The motivation for the design such a simulator is to facilitate the design and evaluation of feedback control algorithms without invoking the computation-intensive numerical methods such as finite element method (FEM) or the expensive physical set-uos.

In this chapter, the exact dynamic solutions of Euler-Bernoulli model for step torque input are derivated. And the verifications of the β's are discussed in section 3. Last, the response of Euler-Bernoulli dynamic model to the pulse and impulse torque are presented in the section 4.

5.2 Exact Dynamic Solution of Euler-Bernoulli Model for Step Torque Input

In this section, the exact dynamic solutions of the Euler-Bernoulli dynamic model for step torque input are presented. The solution is represented in terms of expression of eigenfunctions or vibration modes and provides the foundation for the design of dynamics simulator in next chapter. The first step toward the dynamic

solution is to rearrange the motion equations of Euler-Bernoulli model (22) to (25). Mathematically, the boundary condition $\theta(t) = v'(0,t)$ can be considerated as the definition of hub rotation. And replace this condition with equation (23). This will lead to the following governing equations, boundary conditions and initial conditions for $v(x,t)$,

$$EIv'''' + \rho\ddot{v} = 0 \tag{182}$$

$$v(0,t) = 0; \qquad \tau_0 = I_H\ddot{v}'(0,t) - EIv''(0,t) \tag{183}$$

$$v''(L,t) = 0, \quad v'''(L,t) = 0, \qquad v(x,t_0) = v_0(x), \quad v'(x,t_0) = v_0'(x) \tag{184}$$

For a step torque input τ, the decomposed $v(x,t)$ can be given as,

$$v(x,t) = u(x,t) + v_p(x,t); \quad v_p(x,t) = w_p(x) + x\theta_p(t) \tag{185}$$

where the $v_p(x,t)$ is the particular solution of equation (182)-(184), and $w_p(x,t)$ and θ_p can be solved as,

$$w_p(x,t) = -\frac{\rho L^5\tau_0}{6EII_E}\left(\frac{x}{L}\right)^2\left[\frac{1}{20}\left(\frac{x}{L}\right)^3 - \frac{1}{2}\left(\frac{x}{L}\right) + 1\right] \tag{186}$$

$$= -\gamma\tau_0\left(\frac{x}{L}\right)^2\left[\frac{1}{20}\left(\frac{x}{L}\right)^3 - \frac{1}{2}\left(\frac{x}{L}\right) + 1\right]; \tag{187}$$

$$\theta_p(x,t) = \frac{3\tau_0}{3I_H + \rho L^3}\frac{(t-t_0)^2}{2} = \frac{\tau_0}{I_E}\frac{(t-t_0)^2}{2} \tag{188}$$

$$\gamma = \frac{\rho L^5}{6EII_E}; \quad I_E = I_H + \frac{\rho L^3}{3} \tag{189}$$

And, $u(x,t)$ satisfies the following homogeneous equations,

$$EIu'''' + \rho\ddot{u} = 0 \tag{190}$$

$$u(0,t) = 0; \qquad I_H\ddot{u}'(0,t) = EIu''(0,t); \tag{191}$$

$$u''(L,t) = 0; \quad u'''(L,t) = 0; \qquad u(x,t_0) = u_0(x); \quad \dot{u}(x,t_0) = \dot{u}_0(x) \tag{192}$$

The solution of the above equation can be expressed as the following series,

$$u(x,t) = \sum_{n=0}^{\infty} U_n(x) T_n(t) \tag{193}$$

where, U_n is the nth vibration mode of the Euler-Bernoulli dynamic model, in which C_n is chosen as 1. Additionally, define the $U_0 = x$. The U_n's satisfy the boundary conditions at the hub,

$$U_n'(0) = \frac{2\rho}{I_H k_n^2}; \quad U''_n(0) = -2k_n^2 \tag{194}$$

The $T_n(t)$ can be defined as,

$$T_n(t) = u_n \cos\omega_n(t-t_0) + \frac{\dot{u}_n}{\omega_n} \sin\omega_n(t-t_0) \tag{195}$$

$$T_0(t) = \lim_{\omega_n \to 0} T_n(t) = u_0 + \dot{u}_0 t \tag{196}$$

where the u_n and u_n' are specified by the initial conditions,

$$u(x,t_0) = u_0(x) = \sum_{n=0}^{\infty} u_n U_n(x); \quad \dot{u}(x,t_0) = \dot{u}_0(x) = \sum_{k=0}^{\infty} \dot{u}_n U_n(x) \tag{197}$$

Therefore, once u_n and $\dot{u}_n$ are known, the dynamic solution of equations (182)-(184) will be determined. To find u_n and $\dot{u}_n$, expand w_p and initial conditions into the series forms,

$$w_p(x) = \sum_{n=0}^{\infty} \beta_n U_n(x) \tag{198}$$

$$v_0(x) = w_0(x) + x\theta_0 = \sum_{n=0}^{\infty} v_n U_n \tag{199}$$

$$\dot{v}_0(x) = \dot{w}_0(x) + x\dot{\theta}_0 = \sum_{n=0}^{\infty} \dot{v}_n U_n \tag{200}$$

$$w_0(x) = \sum_{n=0}^{\infty} w_n U_n(x); \quad \dot{w}_0(x) = \sum_{n=0}^{\infty} \dot{w}_n U_n(x) \tag{201}$$

The calculation of coefficients β_n are given in next section. It is very easy to note that from the boundary conditions and equation (193), the following conditions

must be hold,

$$w_0 + \frac{2\rho}{I_H}\sum_{n=1}^{\infty}\frac{\omega_n}{k_n^2} = 0; \quad \dot{w}_0 + \frac{2\rho}{I_H}\sum_{n=1}^{\infty}\frac{\dot{w}_n}{k_n^2} = 0 \tag{202}$$

Now, u_n and $\dot{u}_n$ can be found as,

$$u_0 = w_0 + \theta_0 + \gamma\tau\beta_n; \qquad \dot{u}_0 = \dot{w}_0 + \dot{\theta}_0 \tag{203}$$

$$u_n = w_n + \gamma\tau\beta_n, \qquad \dot{u}_n = \dot{w}_n, \qquad n > 0 \tag{204}$$

Substitute $u(x,t)$ into (185) and use equations (201) for simplification, the final expression of $v(x,t)$ can be reached as the following,

$$\begin{aligned} v(x,t) &= x\left[\theta_0 + \dot{\theta}_0(t-t_0) + \frac{\tau}{2I_E}(t-t_0)^2\right] + \\ &\sum_{n=0}^{\infty} U_n(x)\left\{w_n\cos\omega_n(t-t_0) + \frac{\dot{w}_n}{\omega_n}\sin\omega_n(t-t_0) + \gamma\tau\beta_n[\cos\omega_n(t-t_0)-1]\right\} \end{aligned} \tag{205}$$

Correspondingly, the rotation $\theta(t)$ and flexible displacement $w(x,t)$ are determined as,

$$\begin{aligned} \theta(t) &= v'(0,t) = \theta_0 + \dot{\theta}_0(t-t_0) + \frac{\tau}{2I_E}(t-t_0)^2 + w_0 + \dot{w}_0(t-t_0) + \\ &\frac{2\rho}{I_H}\sum_{n=1}^{\infty} k_n^{-2}\{w_n\cos\omega^n(t-t_0) + \frac{\dot{w}_n}{\omega_n}\sin\omega_n(t-t_0) + \gamma\tau\beta_n[\cos\omega_n(t-t_0)-1]\} \end{aligned} \tag{206}$$

$$\begin{aligned} w(x,t) &= v(x,t) - x\theta(t) \\ &= \sum_{n=1}^{\infty}[U_n(x) - \frac{2\rho}{I_H k_n^2}x]\{w_n\cos\omega_n(t-t_0) + \frac{\dot{w}_n}{\omega_n}\sin\omega_n(t-t_0) + \\ &\gamma\tau\beta_n[\cos\omega_n(t-t_0)-1]\} \end{aligned} \tag{207}$$

The above are the exact dynamic solutions of Euler-Bernoulli model for step torque input. Equations (205)-(207) are key formulas to be used in the design of the dynamic simulator for one-link flexible manipulator. The calculation accuracy

of β_n's is the most critical in the application of these exact dynamic solutions. The next section will discuss the details about the calculations of β_n's.

5.3 Calculation of β_n's

The accuracy of the β_n's determine the effectiveness of the applications of the exact dynamic solution s of Euler-Bernoulli dynamic model for the step torque input. The closed form of the exact solution, which is developed in the previous section, bases on the consistence of the series form of w_g. The β_n can be determined by the following equation w_g,

$$w_g(x) = (\frac{x}{L})^2 \left[\frac{1}{20}(\frac{x}{L})^3 - \frac{1}{2}(\frac{x}{L}) + 1\right] = \sum_{n=0}^{\infty} \beta_n U_n(x) \tag{208}$$

The close form of the β_n's can be obtained through the orthogonal condition of the vibration modes. The next subsection presents the derivation details of the orthogonal condition of vibration modes.

5.3.1 Orthogonal Condition of Vibration Modes

Recall the exact vibration modes (116) of Euler-Bernoulli model, it is easy to show,

$$\psi''''_n = k_n^4 \psi_n \tag{209}$$

Then take the integration of equation (115) along the [0,L] with the innerproduction with ψ_m,

$$k_n{}^4 \int_0^L \psi_m \psi_n \, dx = k_n^4 \langle \psi_n, \psi_m \rangle \tag{210}$$

where,

$$\langle \psi_n, \psi_m \rangle = \int_0^L \psi_m \psi_n dx$$

By the integration by parts, the innerproduction $\langle \psi_n, \psi_m \rangle$ become

$$\begin{aligned} {k_n}^4 \langle \psi_n, \psi_m \rangle &= \int_0^L \psi_m \, d{\psi'''}_n \\ &= \psi_m {\psi'''}_n \Big|_0^L - \int_0^L {\psi'''}_n \, d\psi_m \\ &= \psi_m(L) {\psi'''}_n(L) - \int_0^L \psi'_m \, d{\psi''}_n \\ &= \psi_m(L) {\psi'''}_n(L) - \psi'_m {\psi''}_n \Big|_0^L + \int_0^L {\psi''}_n {\psi''}_m \, dx \end{aligned} \tag{211}$$

Again, do the innerproduction with the reverse ψ_m and ψ_n order.

$${k_m}^4 \langle \psi_m, \psi_n \rangle = \psi_n(L) {\psi'''}_m(L) - \psi'_n {\psi''}_m \Big|_0^L + \int_0^L {\psi''}_m {\psi''}_n \, dx \tag{212}$$

Combine the equation (211) and (212) by the boundary conditions of the vibration modes, one can get the follow orthogonal conditions for the vibration modes,

$$\langle U_n, U_m \rangle + \frac{I_H}{\rho} U'_n(0) U'_m(0) = a \delta_{nm} \tag{213}$$

where a is a constant depending on C_n and δ_{nm} is the Kronecker notation. And U_n and U_m are denoted as the vibration modes ψ_n and ψ_m,

$$\langle U_n, U_m \rangle = \int_0^L U_n U_m dx \tag{214}$$

5.3.2 Calculation of β_n's

To derivate the β_n's, the following assumption (215) is required. That means the fourth order derivative of (208) is still hold, and the numerical verification of (215) can be found in the section 7.2.1.

$${w'_g}'''' = \sum_{n=1}^{\infty} \beta_n {U''''}_n \tag{215}$$

If the above equation is hold, then it must be true for the second order derivative. Applying the integration of the second order derivative of (208) with U''_n and using the orthogonal condition, the closed form of β's are obtained.

$$\beta_n = \frac{\langle U''_n, w_g'' \rangle}{\langle U_n'', U_n'' \rangle}; \qquad n > 0 \tag{216}$$

From the boundary conditions of equations (182)-(184), the β's also satifies the following,

$$\beta_0 + \frac{2\rho}{I_H} \sum_{n=1}^{\infty} \frac{\beta_n}{k_n^2} = 0; \qquad \sum_{n=1}^{\infty} \beta_n k_n^2 = -\frac{1}{L^2}; \tag{217}$$

therefore, the β_0 can be determined as,

$$\beta_0 = -\frac{2\rho}{I_H} \sum_{n=1}^{\infty} \frac{\beta_n}{k_n^2} \tag{218}$$

The closed form of β_n should not be used for high order mode due to the difficulty in computing hyperbotic functions. In the chapter 4, the asymptotic behaviors of modal frequencies and vibration mode have been discussed, these results are going to be used for the high order calculation of β_n. The simulation examples in chapter 7 are going to show that the reasonable number of vibration modes used for β_0 is 12 for CIRSSE model. The asymptotic expressions of vibration modes has been used for the modes with order higher than 10.

5.4 Pulse Response of Euler-Bernoulli Dynamic Model

As a aspect of vibration behavior, the pulse response of the Euler-Bernoulli dynamic model is investigated in this section. The follow derivations are based on the exact dynamic solution in section 5.2. The input torque in this case is specified as,

$$\tau_i = \tau_0, \quad 0 \le i \le D, \qquad \tau_i = 0, \quad i > D \tag{219}$$

where D is the pulse duration.

It is easy to show that the pulse response can be obtained as,

$$\begin{aligned} v(x,t) &= \frac{\tau_0 x}{2I_E}D^2 + \gamma\tau_0 \sum_{n=0}^{\infty}\beta_n[\cos\omega_n(t-t_0)-1]U_n(x); \qquad t_0 \le t \le t_D \\ v(x,t) &= \frac{\tau_0 x}{I_E}(t-\frac{t_D+t_0}{2}) + \gamma\tau_0\beta_n[\cos\omega_n(t-t_0)-\cos\omega_n(t-t_D)]U_n(x) \\ & \qquad\qquad t_D < t < \infty \end{aligned} \tag{220}$$

When $t_D \to t_0$, the pulse response approaches the impulse response, which has been given in the following for the sake of completeness.

$$h(x,t) = \lim_{\Delta t\to 0} v(x,t) = \frac{x(t-t_0)}{I_E} - \gamma\sum_{n=1}^{\infty}\omega_n\beta_n U_n(x)\sin\omega_n(t-t_0) \tag{221}$$

$$\theta_h(t) = h'(0,t) = \frac{t-t_0}{I_E} - \frac{2\gamma\rho}{I_H C_\rho^2}\sum_{n=1}^{\infty}\beta_n\sin\omega_n(t-t_0); \quad C_p^4 = \frac{\rho}{EI} \tag{222}$$

$$w_h(x,t) = h(x,t) - x\theta_h(t) = 2\sum_{n=1}^{\infty}[\frac{2\rho}{I_H C_\rho^2}x - \omega_n U_n(x)]\beta_n\sin\omega_n(t-t_0) \tag{223}$$

and the velocity jumps of hub rotation and beam displacement are,

$$\dot\theta_h(0) = \frac{1}{I_H} - \frac{2\gamma\rho}{I_H C_\rho^2}\sum_{n=1}^{\infty}\beta_n\omega_n = \frac{1}{I_E} + \frac{2\gamma\rho}{I_h C_\rho^4 L^2} = \frac{1}{I_H} + \frac{2\gamma EI}{I_H L^2} = \frac{1}{I_H} \tag{224}$$

$$\begin{aligned} \dot w_h(x,0) &= \gamma\sum_{n=1}^{\infty}[\frac{2\rho}{I_H C_\rho^2}x - \omega_n U_n]\beta_n\omega_n = \frac{I_H - I_E}{I_H I_E}x - \gamma\sum_{n=1}^{\infty}\beta_n\omega_n^2 U_n(x) \\ &= (\frac{1}{I_E} - \frac{1}{I_H})x - \gamma\sum_{n=0}^{\infty}\beta_n\omega_n^2 U_n(x) = -\frac{x}{I_H} \end{aligned} \tag{225}$$

The study of pulse response of the Euler-Bernoulli dynamic model can provide more physical insights of the flexible manipulator, meanwhile, it also provides a mean to verify the effectiveness of the exact dynamic solution of the Euler-Bernoulli model for

5.5 Summary

In this chapter, the exact dynamic solution of the Euler-Bernoulli model for the step torque input is presented. These solutions are the direct results from the previous derivations of the exact modal frequencies and vibration mode, as well as their asymptotic behavior of high mode order. The solutions provided in this chapter are the foundation for the following design of the dynamics simulator, which can provide multi-pattern outputs for specified control algorithms and also provide the unique tool for controller evaluation without the physical set-ups.

Chapter 6 Design of Dynamics Simulator for One-Link Flexible Manipulators

The design of dynamics simulator of one-link flexible manipulators is based on the exact dynamic solutions for step torque input presented in the previous chapter and the actual implementation of digital feedback control systems. The design motivation of such a simulator is to facilitate the design and evaluation of feedback control algorithms without invoking the computation-intensive numerical methods such as finite element method (FEM) or the expensive physical set-ups. Additionally, the design of the dynamics simulator provides the tool for the verification of the exact dynamic solutions. In following sections, the principle of design and procedure of simulation are illustrated, and then the four sensory models are discussed to provide multi-pattern output data sets for the specific control algorithms.

6.1 Design Principle

Fig. 26 presents the block diagram of a digital feedback control system for flexible manipulators with two sample-and-hold devices for control signal and feedback signal respectively. For all the signals involved with the system, only the states at the sampling instants $t_i = t_0 + iT$, $i = 0, 1, 2, 3, \cdots$, are needed to be investigated, where t_0 is the initial time and T is the sampling period. To simulate the dynamics of the flexible manipulators, the following information at each sampling instant is necessary,

$$r(t_i), \qquad \Phi_i = \left\{\theta(t_i), \dot{\theta}(t_i), w(x,t_i), \dot{w}(x,t_i)\right\} \tag{226}$$

$$\tau(t_{i+1}) = \tau(r(t_i), \Phi_i), \qquad i = 0, 1, 2, 3, \cdots \tag{227}$$

where $r(t)$ is the reference signal representing motion control command, and $\tau[r(t_i), \Phi_i]$ is some feedback control law.

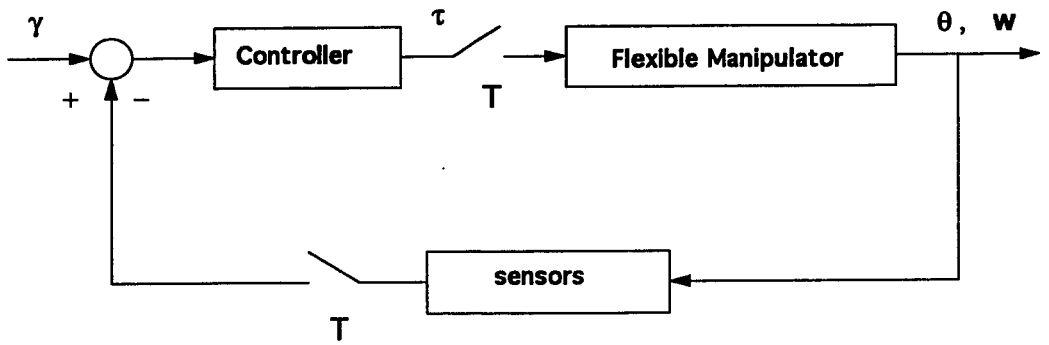

Figure 26: Digital Feedback Control System

Since input torque is held constant during each sampling period, the dynamics of one-link flexible manipulators can be simulated by the following algorithm,

BEGIN
INPUT *Initial state*
$\Phi_0 = \left\{\theta(t_0), \dot{\theta}(t_0), w(x,t_0), \dot{w}(x,t_0)\right\}$
and the simulation period M.
FOR $i = 1$ *to M DO*
1. *Calculate the current input torque*
$\tau_i = \tau[r(t_{i-1}), \Phi_{i-1}]$
by using the feedback control law;
2. *Update the state*
$\Phi_i = \left\{\theta(t_i), \dot{\theta}(t_i), w(x,t_i), \dot{w}(x,t_i)\right\}$
by using the step response given in the previous section with torque τ_i *and initial state* Φ_{i-1}.

CONTINUE
END

The feedback control algorithms could be the input of this dynamics simu-

lator for effectiveness evaluation. The state updating procedure of this flexible manipulator, Φ_i,can be determined by the exact dynamic solutions of Euler-Bernoulli model.

6.2 Simulation Procedure

To specify the procedure for updating the state Φ_i in detail, the following equations for ith sampling instant are utilized through the derivations.

$$w(x,t_i) = \sum_{n=0}^{\infty} w_n^i U_n(x), \qquad \dot{w}(x,t_i) = \sum_{n=0}^{\infty} \dot{w}_n^i U_n(x) \tag{228}$$

$$\theta(t_i) = \theta^i; \qquad \dot{\theta}(t_i) = \dot{\theta}^i; \qquad i = 0,1,2,3,\cdots \tag{229}$$

Using the above notations, the followings can be easily obtained.

$$T_n^i = w_n^i \cos\omega_n T + \frac{\dot{w}_n^i}{\omega_n} \sin\omega_n T + \gamma\tau_{i+1}\beta_n(\cos\omega_n T - 1) \tag{230}$$

$$\dot{T}_n^i = \dot{w}_n^i \cos\omega_n T - \omega_n(w_n^i + \gamma\tau_{i+1}\beta_n)\sin\omega_n T \tag{231}$$

and, when first N vibration modes are used for approximation, the following notations can be introduced,

$$S^i(N) \approx \frac{2\rho}{I_H}\sum_{n=1}^{N}\frac{T_n^i}{k_n^2}, \qquad \dot{S}^i(N) \approx \frac{2\rho}{I_H}\sum_{n=1}^{N}\frac{\dot{T}_n^i}{k_n^2} \tag{232}$$

Then the new state can be updated by the following procedures, which can be derivated through the step response of the Euler-Bernoulli model. Here, the state includes the beam displacement (flexibility) and the hub rotation (rigid motion).

1. Beam Displacement

$$w_n^{i+1} \longleftarrow T_n^i, \qquad \dot{w}_n^{i+1} \longleftarrow \dot{T}_n^i, \qquad n > 0 \tag{233}$$

$$w_0^{i+1} \longleftarrow -S^i(N), \qquad \dot{w}_0^{i+1} \longleftarrow -\dot{S}^i(N) \tag{234}$$

$$w(x,t_{i+1}) = \sum_{n=0}^{N} w_n^{i+1} U_n(x), \qquad \dot{w}(x,t_{i+1}) = \sum_{n=0}^{N} \dot{w}_n^{i+1} U_n(x) \tag{235}$$

(236)

2. Hub Rotation

$$\theta^{i+1} \longleftarrow \theta^i + \dot{\theta}^i T + \frac{\tau_{i+1}}{2I_E} T^2 + w_0^i + \dot{w}_0^i T - w_0^{i+1} \tag{237}$$

$$\dot{\theta}^{i+1} \longleftarrow \dot{\theta}^i + \frac{\tau_{i+1}}{2I_E} T + \dot{w}_0^i - \dot{w}_0^{i+1} \tag{238}$$

The choose of N is based on the fitting of equation (215). Several simulation examples indicates that $N = 12$ would give very accurate result for CIRSSE model, and the details can be found in the section 7.2.1.

6.3 Specification of Sensor Models

Different feedback control algorithms may require different types of sensory data. The most commonly used sensors in the control of flexible manipulators are potentiometer and tachometer for rigid rotation, and photodiode optical sensor and strain gage for the flexible displacement. Therefore, the following sensory information may be available from a flexible manipulator control system.

- $\theta(t)$ and $\dot{\theta}(t)$ for hub rotation
- $w(x,t)$, $\dot{w}(x,t)$, $w''(x,t)$ and $\dot{w}''(x,t)$ for beam displacement

Based on those sensors used in the existing control algorithms, four types of sensors models are implemented in the designed dynamics simulator,

S1 Simulator outputs :

$$S1 = [\theta(t_i), \dot{\theta}(t_i)] \tag{239}$$

S2 Simulator outputs :

$$S2 = [\theta(t_i), \dot{\theta}(t_i), W(X), \dot{W}(X)] \tag{240}$$

S3 Simulator outputs :

$$S3 = [\theta(t_i), \dot{\theta}(t_i), W''(X), \dot{W}''(X)] \tag{241}$$

S4 Simulator outputs :

$$S4 = [\theta(t_i), \dot{\theta}(t_i), W(X), \dot{W}(X), W''(X), \dot{W}''(X)] \tag{242}$$

where $X = (x_1, ...x_n)$ is the coordinator of the segment point on the beam for the strain gage and n is the number of strain gages. And, the displacement vectors are defined as the followings,

$$W(X) = [w(x_1, t_0), ...w(x_n, t_i)], \qquad \dot{W}(X) = [\dot{w}(x_1, t_i), ...\dot{w}(x_n, t_i)] \tag{243}$$

$$W'' = [w''(x_1, t_i), ...w''(x_n, t_i)]; \qquad \dot{W}'' = [\dot{w}''(x_1, t_i), ...\dot{w}''(x_n, t_i)] \tag{244}$$

Note that the location vector X is not required to be the same in $W(X)$, $\dot{W}(X)$, $W''(X)$ and $\dot{W}''(X)$. Other types of sensor models, which are required by the specific control algorithms, can be added into the dynamic simulator easily, The expressions of the commonly used outputs $w(L,t)$, $\dot{w}(L,t)$, $w''(0,t)$ and $\dot{w}''(0,t)$ are listed as,

$$w(L, t_i) = \sum_{n=0}^{N} [U_n(L) - \frac{2\rho L}{I_H k_n^2}] T_n^{i-1}, \qquad \dot{w}(L, t_i) = \sum_{n=0}^{N} [U_n(L) - \frac{2\rho L}{I_H k_n^2}] \dot{T}_n^{i-1} \tag{245}$$

$$w''(0, t_i) = -2 \sum_{n=0}^{N} k_n^2 T_n^{i-1}, \qquad \dot{w}''(0, t_i) = -2 \sum_{n=0}^{N} k_n^2 \dot{T}_n^{i-1} \tag{246}$$

where T_n^{i-1} and $\dot{T}_n^{i-1}$ are given by equations (230)-(231).

6.4 Summary

In this Chapter, the design of the dynamics simulator is presented. This simulator provides multi-pattern outputs sensory data sets for the specific control algorithms through the designed sensor models, and it can serve as the testbed for the control algorithms, especially for the initial controller design for the one-link flexible manipulators. The Chapter will present a simulation study of the CIRSSE model to verify the design of this dynamics simulator and three simple control algorithms are been evaluated.

Charper 7 Simulation Study

7.1 Introduction

To verify the exact dynamic solution of Euler-Bernoulli model and the design of the dynamics simulator, to demonstrate the usage of the dynamic simulator designed, the Chapter conducts a series simulation studies of CIRSSE model: verification of β_n's, the pulse responses of the Euler-Bernoulli model and the evaluations of three simple control algorithms. All the parameters of the flexible manipulator used in this section are listed in Table 1 and are taken from the physical model of one-link very flexible manipulator built at the NASA Center for Intelligent Robotic Systems for Space Exploration (CIRSSE) at the Rensselaer Polytechnic Institute. Note that in order to reduce the effect of rotatory inertia and shear deformation, this manipulator has been constructed with a long beam of small width/height ratio. As indicated in [Wang 91b], the influence of rotatory inertia and shear deformation can be ignored in this case.

7.2 Verification of Designed Dynamics Simulator

As shown through the derivations of the exact dynamic solutions of the Euler-Bernoulli model in section 5.2 and 5.3, the accuracy of the β_n's is critical for the numerical analysis due to the assumption (215). Any numerical analysis can not be conducted until the accuracy of the β_n's is verified. In this section, the the verification of the designed dynamics simulator is conducted by the verifications of β_n's and the pulse response of the Euler-Bernoulli model.

7.2.1 Verification of β

The first task toward the verification of the β_n's is the choose of the numer of the involved vibration modes, N. Also, the start vibration mode, at which

the asymptotic expressions are going to used. need to be determined to assure the accuracy. Finally, the numerical analysis indicates that the following choose gives excellent accuracy in terms of computation efforts: N=12 and the asymptotic expression is used for mode order higher than 9. The Table 3 presents the coefficient β_n's of the CIRSSE model. Additionally, Figure 27 and 28 show the fitting of equation (208) and (215), respectively. As the figures shown, the fitting of the equation (208) is perfect. Note that the differences at the hub and tip end in Figure 28 are due to the utilization of the asymptotic expressions of vibration modes, which violate the boundary conditions.

β_n's	Value of CIRSSE Model
β_0	0.3941
β_1	-0.0620
β_2	-0.0117
β_3	-6.549e-4
β_4	-8.517e-5
β_5	-1.8613e-5
β_6	-5.5447e-6
β_7	-2.0283e-6
β_8	-8.5824e-7
β_9	-4.0476e-7
β_{10}	-2.0716e-7
β_{11}	-1.1192e-7
β_{12}	-7.5532e-8

Table 3 : Coefficient β_n's of the CIRSSE One-Link Flexible Manipulator

The second equation in (217), which is required as the boundary condition, is also verified by the β_n's in Table 3. The above analysis indicates that the β_n's set in Table 3. guarantee the effective derivations of the exact dynamic solutions and the design of the dynamics simulator.

7.2.2 Pulse Response

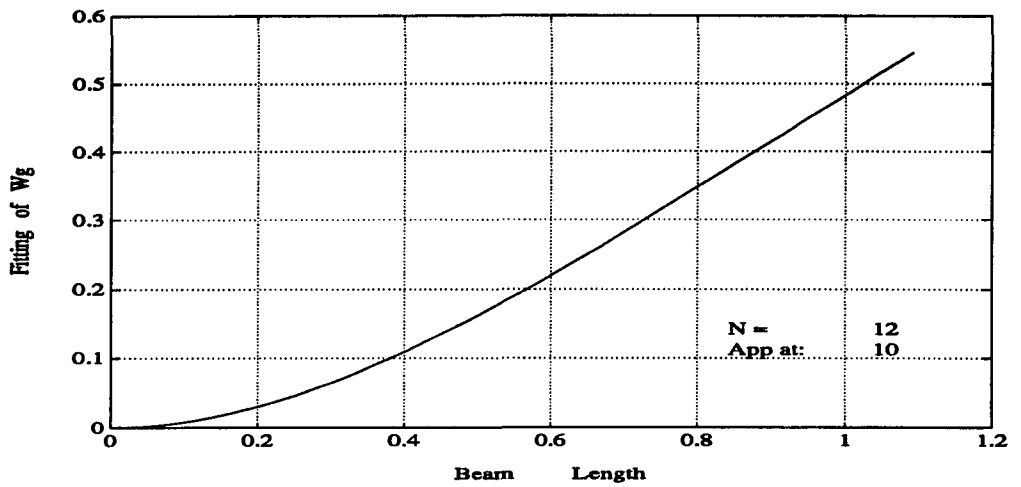

Figure 27: Fitting of Equation w_g

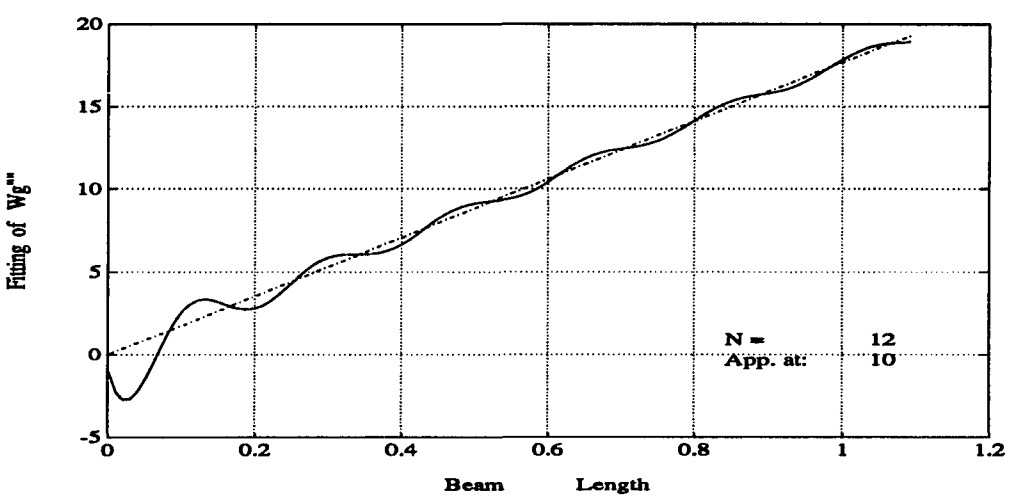

Figure 28: Fitting of Equation w_g'''

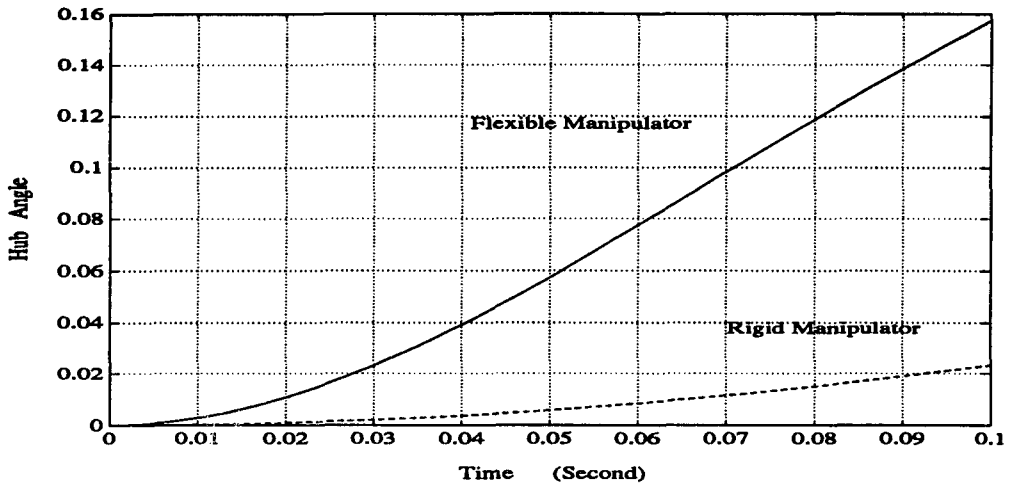

Figure 29: Hub Rotation Response of Pulse Torque $(t_0 \leq t \leq t_D)$

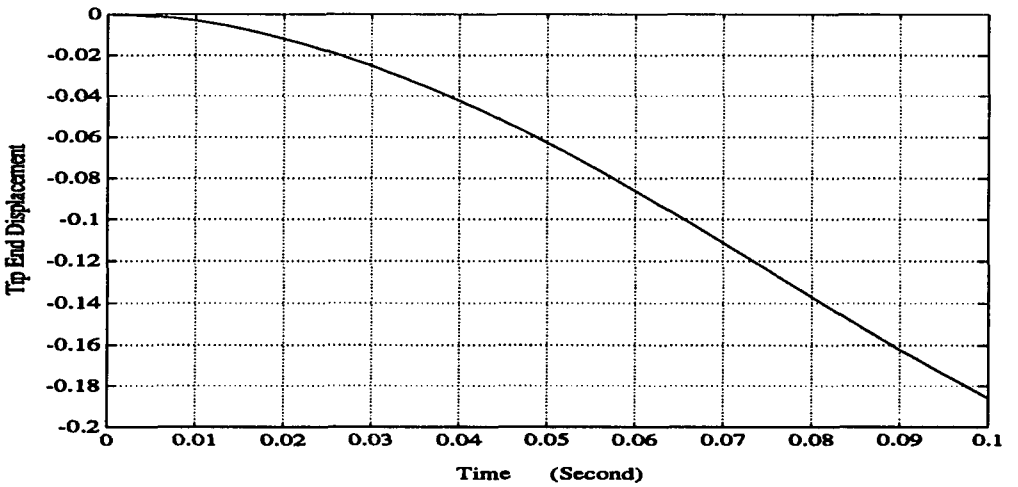

Figure 30: Tip End Displacement Response of Pulse Torque $(t_0 \leq t \leq t_D)$

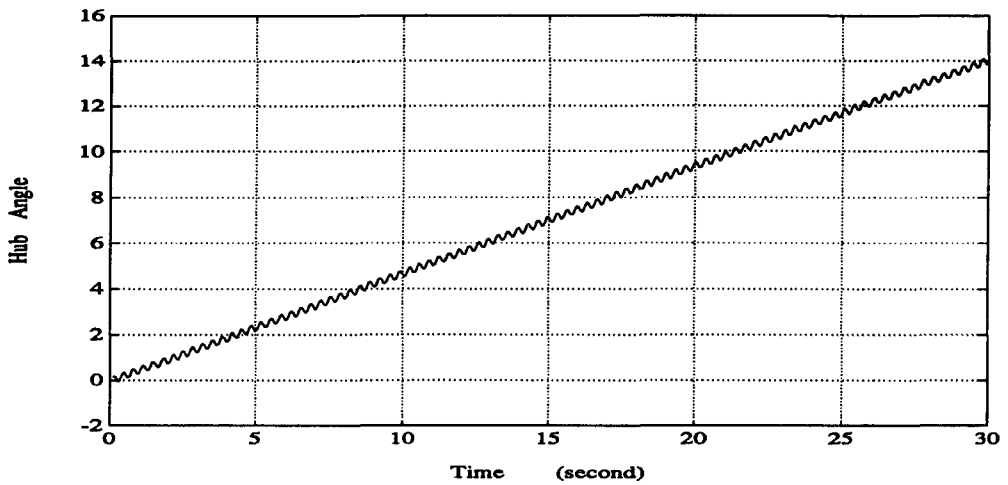

Figure 31: Hub Rotation Response of Pulse Torque $(t_D < t \leq 30)$

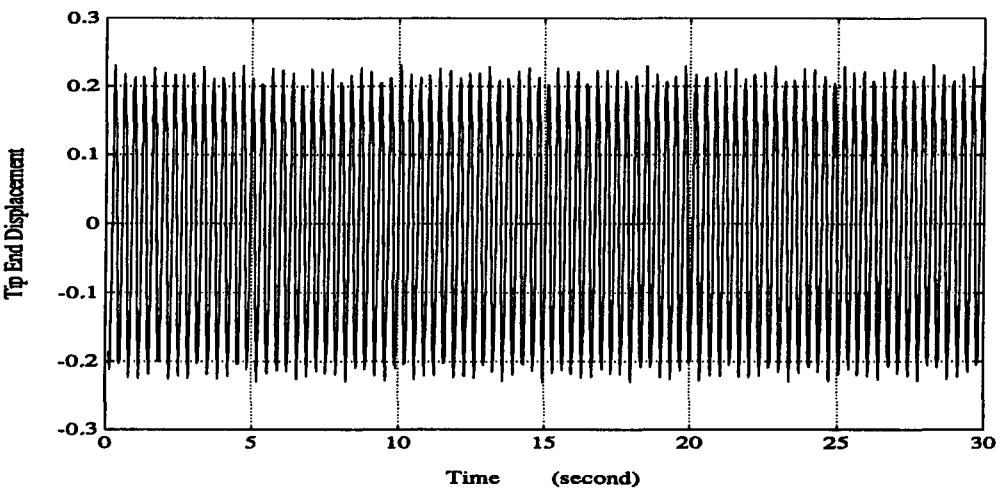

Figure 32: Tip End Displacement Response of Pulse Torque $(t_D < t \leq 30)$

Recall the pulse response analysis in the section 5.4, when the inout is specified as,

$$\tau_i = \tau_0, \quad 0 \le i \le D, \qquad \tau_i = 0, \quad i > D \tag{247}$$

where D is the pulse duration.

It is easy to show that the pulse response can be obtained as,

$$\begin{aligned} v(x,t) &= \frac{\tau_0 x}{2I_E} D^2 + \gamma\tau_0 \sum_{n=0}^{\infty} \beta_n [\cos\omega_n(t-t_0) - 1] U_n(x); \qquad t_0 \le t \le t_D \\ v(x,t) &= \frac{\tau_0 x}{I_E}(t - \frac{t_D + t_0}{2}) + \gamma\tau_0\beta_n[\cos\omega_n(t-t_0) - \cos\omega_n(t-t_D)]U_n(x) \\ & \qquad\qquad t_D < t < \infty \end{aligned} \tag{248}$$

Figure 29 illustrates the pulse response of the hub rotation during $[t_0, t_D]$ for $\Delta t = t_D - t_0 = 0.1$, and $\tau_0 = 1.0N/m$. The hub rotation of the corresponding rigid manipulator with inertia moment I_E is also presented in the same figure. As expected, it indicates that the flexible manipulator rotates much fast than the rigid one does. Figure 30 shows the motion of the manipulator tip end ($x = L$) over the pulse duration. Figure 31 and 32 give the rotation of hub and the vibration of tip end during the first 30 seconds. Note that since frictions of the flexible manipulator system has not been considered in the simulator, both the hub rotation and beam vibration would continue forever.

The above numerical analysis has verified the effectiveness of the exact dynamic solutions of Euler-Bernoulli model and the design of the dynamics simulator for this CIRSSE model. The evaluations of the control algorithms in the next section are conducted under the above parameters.

7.3 Evaluation of Control Algorithms

The performance of three simple PD feedback controllers with different sensor models has been evaluated by using the dynamic simulator. Three control algorithms are specified in the sequel,

A) PD Control with Sensor Model S1

$$\tau = K_p e + K_v \dot{e} + I_E \ddot{\theta}_d = \tau_A \tag{249}$$

$$e = \theta_d - \theta; \qquad \dot{e} = \dot{\theta}_d - \dot{\theta} \tag{250}$$

where $(\theta_d, \dot{\theta}_d, \ddot{\theta}_d)$ is the desired trajectory, and K_p and K_v are joint position and velocity error feedback gains, respectively. Note this is the PD feedback control for rigid rotation only, and the link flexibi

B) PD Control with Sensor Model S2

$$\tau = \tau_A - K_{wp} w(L,t) - K_{wv} \dot{w}(L,t) \tag{251}$$

where K_{wp} and K_{wv} are tip displacement and velocity feedback gains, respectively,

C) PD Control with Sensor Model S3

$$\tau = \tau_A - K_{sp} w''(0,t) - K_{sv} \dot{w}''(0,t) \tag{252}$$

where K_{sp} and K_{sv} are strain and strain rate feedback gains, respectively.

The performance evaluation is conducted with the following desired position and feedback gains,

$$\theta_d = \tfrac{\pi}{2}; \quad K_p = 2.40, \quad K_v = 1.19; \tag{253}$$

$$K_{wp} = 4.10, \quad K_{wv} = 0.03; \quad K_{sp} = 1.72, \quad K_{sv} = 0.0006. \tag{254}$$

Figure 33 to 35 illustrate the performances of three controllers on this simple motion task. The results confirm that those controllers with deformation feedback perform better than the without deformation feedback. Since all three controllers here are simply specified, the improvements are not significant at all.

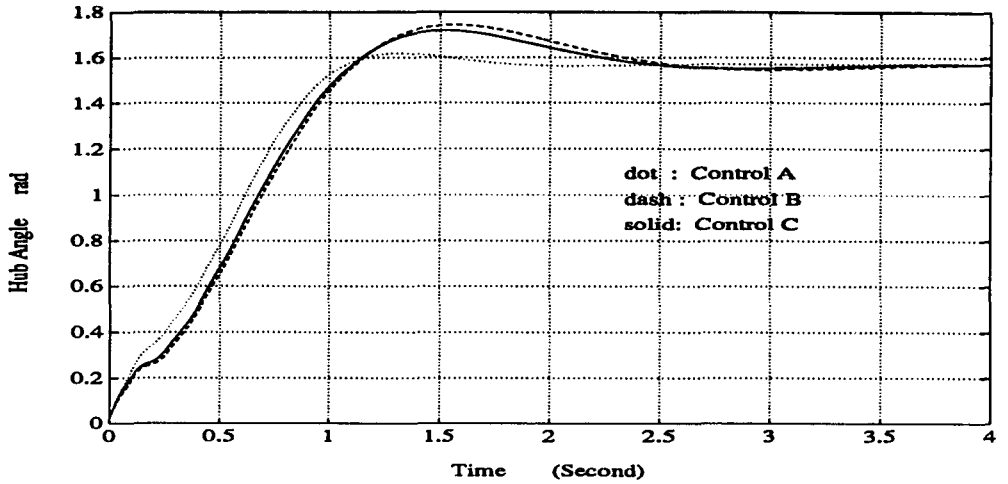

Figure 33: Hub Rotation Responses of Three Controllers

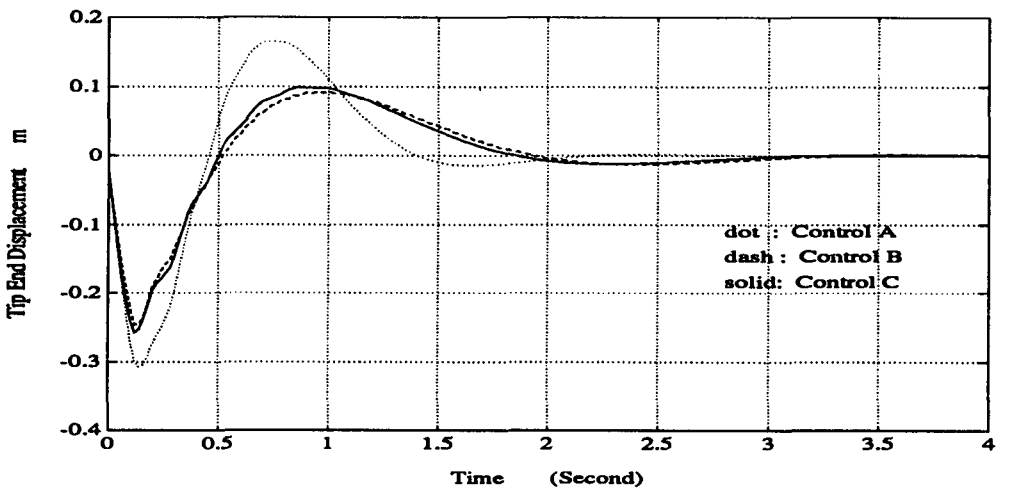

Figure 34: Tip End Displacement Responses of Three Controllers

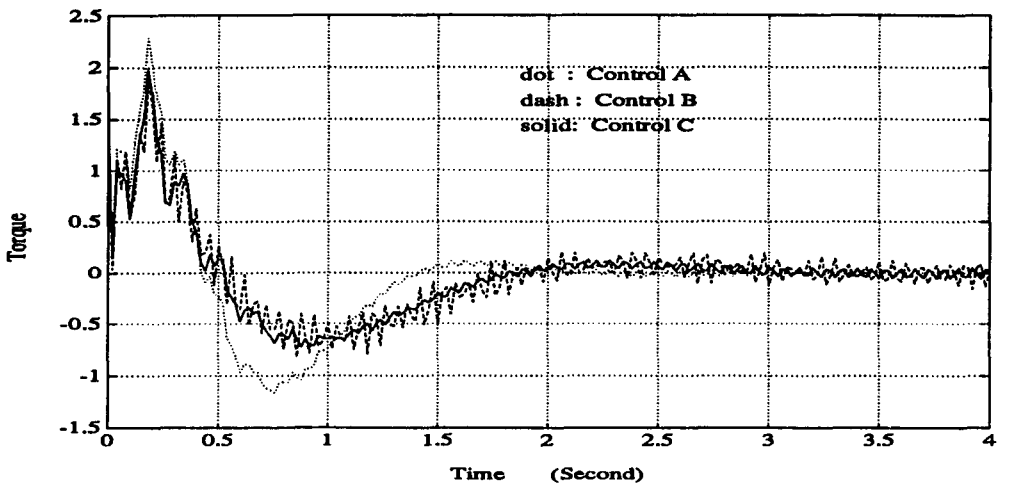

Figure 35: Torques Responses of Three Controllers

7.4 Summary

The results of simulation have verified the derivations of the exact dynamic solution of Euler-Bernoulli model and the design of dynamics simulator. By using the simulator have indicated that flexible manipulators as a kind of mechanisms can indeed offer fast motion and better energy consumption. The evaluations of three simple control algorithms have demonstrated that the dynamics simulator provides an ideal tool for evaluation of control algorithms by computer simulation. This is especially useful in designing or selecting control algorithms for flexible manipulators. Before such simulator is available, the test or evaluation of feedback controllers in early design stage can only be conducted with finite-element-methods or with physical set-ups, which is usually expensive and time-consuming. Certainly, the test of controller with physical manipulator is still necessary and should be performed at least at the final design stage.

Chapter 8 Conclusions

The conclusions drawn from this thesis can fall into two parts:

First, based on the four dynamic models for one-link flexible manipulators, a comprehensive study on the influence of rotatory inertia, shear deformation, and tip load on the vibration behaviors of one-link flexible manipulators has been conducted in this thesis. The modal frequency equations and exact vibration modes, as well as their asymptotic expressions, are derivated for the four well-constrained models. The excellent agreement between the analytic prediction and the experimental results has verified the accuracy of these equations. From the results of numerical analysis, the following three main conclusions can be made about the influence of different factors on the vibration behaviors of one-link manipulators:

1. For not very high vibration modes, the influence of rotatory inertia can be ignored for low beam width-to-height ratio $\frac{B}{H}$, and even for large $\frac{B}{H}$, the influence is not very significant. For vibration modes with very high order, however, the influence can not be neglected.

2. In general, the influence of shear deformation is more significant than that of rotatory inertia. It can be ignored only for low $\frac{B}{H}$ in the case of low order vibration modes. For high $\frac{B}{H}$ or high vibration modes, the influence of shear deformation should be taken into account.

3. The tip load generally has significant effect on the vibration, and thereof on the dynamics of flexible manipulators. Even the first order modal frequency decreases dramatically with the tip mass or tip length. More significantly, the tip mass or length also changes the distribution of modal frequencies. As not expected initially, the influence of the tip inertia moment is very small and

can be ignored. The results obtained here suggest strongly that for better performance, adaptive control approach should be used to control flexible manipulator systems.

Second, The exact dynamic solutions of Euler-Bernoulli model for step torque input are derivated in terms of the modal frequency and exact vibration modes. Based on solutions, a dynamics simulator for one-link flexible manipulators has been designed in this thesis. Four different types of sensor models have been included in the dynamics simulator to generate various sensory information which may be required for feedback control purpose. The results of simulation by using the simulator have indicated that flexible manipulators as a kind of mechanisms can indeed offer fast motion and better energy consumption.

The dynamics simulator provides an ideal tool for evaluation of control algorithms by computer simulation. This is especially useful in designing or selecting control algorithms for flexible manipulators. Before such simulator is available, the test or evaluation of feedback controllers in early design stage can only be conducted with finite-element-methods or with physical set-ups, which is usually expensive and time-consuming. Certainly, the test of controller with physical manipulator is still necessary and should be performed at least at the final design stage.

References

[Barb 88] E. Barbieri and ÜOzgüner, Unconstrained and constrained model expansion for a flexible slewing link, *ASME Journal of Dynamic Systems, Measure and Control*, Volume 110, Dec. 1988

[Baya 90] D. S. Bayard, C. H. C. Ih, S. J. Wang, Z. Gao, J. Ott, and P. J. Antsaklis, Adaptive Control System Optimization for Vibration Control of Flexible Structures, *IEEE 19990 International Conference on Robotics and Automation*, Volume 1, 1990 pp.745-747

[Bayo 88] E. Bayo, Computed Torque for the Position Control of Open-Chain Flexible Robots, *IEEE 1988 International Conference on Robotics and Automation*, Volume 1, 1988

[Bayo 89] E. Bayo and H. Moulin, An efficient Computation of the Inverse Dynamics of Flexible Manipulators in the Time Domain, *IEEE 1989 International Conference on Robotics and Automation*, Volume 2, 1989. pp.710-715

[Bell 90] F. Bellezze, L. Lanari and G. Ulivi, Exact Modeling of the Flexible Slewing Link, *IEEE 1990 International Conference on Robotics and Automation*, Volume 2, 1990. pp.734-739

[Bisw 88] S. K. Biswas and R. D. Klafter, Dynamic Modeling and Optimal Control of Flexible Robotic Manipulators, *IEEE 1988 International Conference on Robotics and Automation*, Volume 1, 1988

[Book 82] W. J. Book, Recursive Lagrangian Dynamics of Flexible Manipulator Arms Via Transmission Matrices, *Proc. Second IFAC Symposium on CAD of Multivariable Technological Systems*, West Lafayette, IN., Sept. 1982. pp.5-17

[Book 83] W. J. Book and M. Majette, Controller Design for Flexible, Distributed Parameter Mechanical Arms Via Combined State Space and Frequency Domain Techniques, *Journal of Dynamic System, Measurement and Control*, Volume 105, No.4, Dec. 1983

[Brem 87] H. Bremer, On the Dynamics of Flexible Manipulators, *IEEE 1987 International Conference on Robotics and Automation*, Volume 3, 1987

[Cann 84] R. H. Cannon, Jr. and Schmitz, E., Precise Control of Flexible Manipulators, *Robotics Research: The First International Symposium,* (MIT Press, Cambridge, MA 1984) pp.841-861.

[Ceti 87] George Cetinkunt and Wayne J. Book, Symbolic Modeling of Flexible Manipulators, *IEEE 1987 International Conference on Robotics and Automation*, Volume 2, 1987

[Dado 86] M. Dado and A. H. Soni, A Generalized Approach for Forward and Inverse Dynamic of Elastic Manipulators, *IEEE 1986 International Conference on Robotics and Automation*, Volume 1, 1986

[Davi 48] R. M. Davies, A Critical Study of Hopkins Pressure Bar, *Philosophical Transactions of Royal Society*, Serial A. 240, 1948 pp.454-461

[Donn 90] J. Donne, K. Ossman, and A. Ahmed, MTS, Adaptive Control of a Flexible Structure with Non-Collocated Sensors and Actuators, *IEEE 1990 Transaction*, Volume 2, 1990

[Eppi 88] Eppinger, S. D. and Seering, W. P., Modeling Robot Flexibility for Endpoint Force Control, *IEEE 1988 International Conference on Robotics and Automation*, Volume 1, 1988. pp.165-170

[Fuku 85] Fukuda, T., Flexibility Control of Elastic Robotic Arms, *Journal of Robotic Systems*, Volume 2, 1985. pp.73-88

[Hast 86] Gordon G. Hastings and Wayne J. Book, Verification of a Linear Dynamic Model for Flexible Robotic Manipulators, *IEEE 1986 International Conference on Robotics And Automation*, Volume 2, 1986

[Khor 88] Farshad Khorrami and Ümit Özgöner, Perturbation Method in Control of Flexible Link Manipulators, *IEEE 1988 International Conference on Robotics and Automation*, Volume 1, 1988

[Kris 88] H. Krishnan and M. Vidyasagar, Control of a Single-Link Flexible Beam Using a Hankel-Norm-Based Reduced Order Model, *IEEE 1988 International Conference on Robotics and Automation*, Volume 1, 1988

[Luca 89] A. De Luca, P. Lucibello and G. Ulivi, Inversion Techniques for Trajectory Control of Flexible Robot Arms, *Journal of Robotic Systems*, Volume 6, No.4, Aug. 1989

[Nels 86] W. L. Nelson and D. Mitra, Load Estimation and Load-Adaptive Optimal Control for a Flexible Robot Arm, *IEEE 1986 International Conference on Robotics and Automation*, Volume 1, 1986

[Oakl 89] Oakley, C. M. and R. H. Cannon, Jr., End-Point Control of a Two-Link Manipulator with a Very Flexible Forearm: Issues and Experiments, *Proc. 1989 American Control Conference*, Pittsburgh, PA, June 1989, 1381-1388.

[Park 90] Jahag-Hyon Park and Haruhiko Asada, Design and Control of Minimum-Phase Flexible Arms with Torque Transmission Mechanisms, *IEEE 1990 International Conference on Robotics and Automation*, Volume 3, 1990. pp.1790-1795

[Rovn 87] D. M. Rovner and R. H. Cannon, Jr., Experiments toward On-Line Identification and Control of a Very Flexible One-Link Manipulator, *The*

International Journal of Robotics Research, Volume 6, No.4, Winter 1987

[Sasi 88] Jerzy Z. Sasiadek and Ramesh Srinivasan, Dynamic Modeling and Adaptive Control of A Single-Link Flexible Manipulator, *Journal of Guidance, Control and Dynamics*, Volume 12, No.6, Nov.-Dec. 1988

[Shin 85] Kang G. Shin and Neil D. Mclay, Minimum-Time Control of Robotic Manipulators with Geometric Path Constrains, *IEEE Transaction on Automatic Control*, Volume AC-30, No.6, 1985

[Shun 87] I. Y. Shung and M. Vidyasagar, Control of a Flexible Robot Arm with Bounded Input: Optimum Step Responses, *IEEE 1987 International Conference on Robotics and Automation*, Volume 2, 1987

[Sici 88] Bruno Siciliano and Wayne J. Book, A Singular Perturbation Approach to Control of Lightweight Flexible Manipulators, *The International Journal of Robotics Research*, Volume 7, No.4, August 1988

[Timo 49] S. Timoshenko and G. H. MacCullough, *Elements of Strength of Materials*, Third Edition. (D. Van Nostrand Company, Inc., New York, 1949).

[Timo 57] S. Timoshenko, D. H. Young, and W. Weaver, Jr., *Vibration Problems in Engineering*, Third Edition. (D. Van Nostrand Company, Inc., New York, 1957).

[Wang 87] David Wang and M. Vidyasagar, Control of a Flexible Beam for Optimum Step Response, *IEEE 1987 International Conference on Robotics and Automation*, Volume 3, 1987

[Wang 89] David Wang and M. Vidyasagar, Transfer Function for A Flexible Link, *IEEE 1989 International Conference on Robotics and Automation*, Volume 2, 1989

[Wang 90] F. Y. Wang and John T. Wen, Nonlinear Dynamical Model and Control for a Flexible beam, Rensselaer Polytechnic Inst. Electrical, computer, and System Engineering, Cirsse Report # 75, Nov, 1990

[Wang 91a] Fei-Yue Wang, Exact Dynamic Solutions of One-Link Flexible Manipulators with Different Dynamic Models, SIE working paper, Dept. of System and Industrial Engineering, University of Arizona, July 1991

[Wang 91b] Fei-Yue Wang and Guoguang Guan, Influence of Rotatory Inertia, Shear and Loading on Vibrations of Flexible Manipulators, SIE working paper 91-036, Dept. System and Industrial Engineering, University of Arizona, September 1991

[Wang 91c] Fei-Yue Wang and Guoguang Guan, Design of a Dynamics Simulator for One-Link Flexible Manipulators, SIE working paper 91-035, System and Industrial Engineering, University of Arizona, September 1991

[Yang 89] Y. P. Yang and J. S. Gibson, Adaptive Control of A Manipulator with A Flexible Link, *Journal of Robotic Systems*, Volume 6, No.3, June 1989

[Yuh 87] J. Yuh, Application of Discrete-Time Model Reference Adaptive Control of A Flexible Single-Link Robot, *Journal of Robotic Systems*, Volume 4, No.5, Oct. 1987

[Yurk 89] Stephen Yurkovich and Fornando E. Pacheco, On Controller Tuning for a Flexible-Link Manipulator with Varying Payload, *Journal of Robotics Systems*, 6(3), 1989 pp.233-254